



SCHOOL of
GRADUATE STUDIES
EAST TENNESSEE STATE UNIVERSITY

East Tennessee State University
Digital Commons @ East
Tennessee State University

Electronic Theses and Dissertations

Student Works


8-2014

Characterization Of A Putative SIR2 Like Deacetylase And Its Role In SABP2 Dependent Salicylic Acid Mediated Pathways In Plant

Md I. Haq

East Tennessee State University

Follow this and additional works at: <https://dc.etsu.edu/etd>

 Part of the [Biochemistry Commons](#), and the [Molecular Biology Commons](#)

Recommended Citation

Haq, Md I., "Characterization Of A Putative SIR2 Like Deacetylase And Its Role In SABP2 Dependent Salicylic Acid Mediated Pathways In Plant" (2014). *Electronic Theses and Dissertations*. Paper 2394. <https://dc.etsu.edu/etd/2394>

This Thesis - Open Access is brought to you for free and open access by the Student Works at Digital Commons @ East Tennessee State University. It has been accepted for inclusion in Electronic Theses and Dissertations by an authorized administrator of Digital Commons @ East Tennessee State University. For more information, please contact digilib@etsu.edu.

Characterization Of A Putative SIR2 Like Deacetylase And Its Role In SABP2 Dependent
Salicylic Acid Mediated Pathways In Plant

A thesis
presented to
the faculty of the Department of Biological Sciences
East Tennessee State University

In partial fulfilment
of the requirement for the degree
Master of Science in Biology

by
Md Imdadul Haq
August 2014

Dhirendra Kumar, PhD Chair

Aruna Kilaru, PhD

Christopher Pritchett, PhD

Keywords: Plant defense, Salicylic Acid, SABP2, SBIP-428, SIR2 deacetylase, Acetylation.

ABSTRACT

Characterization Of A Putative SIR2 Like Deacetylase And Its Role In SABP2 Dependent Salicylic Acid Mediated Pathways In Plant

by

MD Imdadul Haq

Salicylic Acid Binding Protein2 (SABP2) is an enzyme known to play an important role in the SA mediated pathway. SBIP-428 (SABP2 InteractingProtein-428), an SIR2 like deacetylase, has been found to interact with SABP2. We demonstrate that SBIP-428 functions as a Sirtuin deacetylase and that SBIP-428 itself is lysine acetylated. Interactions of SBIP-428 with SABP2 also increased the possibility of SABP2 itself being lysine acetylated. Both recombinant purified SABP2 and native partially purified SABP2 displayed no acetylation. In response to TMV infection, expression of *SBIP-428* was down regulated at 48 hpi. Additionally, *SBIP-428* was up regulated in plants known to accumulate less SA. This evidence suggests that the expression of SBIP-428 is negatively correlated to levels of SA in plants. The *AtSRT2* plants exhibit no altered growth phenotype but exhibit higher resistance to bacterial pathogens. Our results indicate that SBIP-428 is an important regulator in the plant defense pathway.

ACKNOWLEDGEMENTS

I would like to thank my committee members, Dr. Aruna Kilaru and Dr. Christopher Pritchett, for their guidance throughout this thesis project with constructive criticism and advice. I owe my deepest gratitude to my mentor, Dr. Dharendra Kumar, whose encouragement, guidance, and support from initial to the final level helped me develop a good understanding of this project. I would also like to thank my lab members for their constant help. I would like to thank all the staff members of Biological Sciences for their support. I would like to thank the ETSU Graduate School for the graduate assistantship, the selection committee for awarding “Marcia Davis Research Award for graduate research”, ETSU for RDC grant (14-021M to DK), and NSF grant (MCB 1022077 to DK) to support this project. I am also thankful to my family members and friends for their support and love.

TABLE OF CONTENTS

	Page
ABSTRACT.....	2
ACKNOWLEDGEMENTS.....	3
LIST OF TABLES.....	7
LIST OF FIGURES.....	8
Chapter	
1. INTRODUCTION.....	10
Plant Immune System.....	10
Domain Structure of Pattern-Recognition Receptors (PRR) and Resistance (R) Proteins	11
Signaling Pathways and Cross Talk Between JA, ET, and SA.....	12
Systemic Acquired Resistance	12
Induced Systemic Resistance	14
Salicylic Acid Synthesis Pathway.....	15
Salicylic Acid Binding Protein2 (SABP2).....	16
SABP2 Interacting Proteins	17
Silent Information Regulator2 (SIR2).....	17
SIR2 in Plants	19
Non-Histone Protein Acetylation and Metabolic Enzymes	20
Hypotheses	21
2. MATERIALS AND METHODS.....	22
Materials.....	22
Plant Materials.....	22
Chemicals and Reagents.....	22
Other Materials	23
Methods.....	24
Biochemical Characterization (Hypothesis I).....	24
Bioinformatics Analysis	24
Expression and Purification of SBIP-428.....	24
Deacetylase Activity of SBIP-428.....	27

Lysine Acetylation of SBIP-428.....	29
SABP2 Acetylation (Hypothesis II).....	29
Purification of Recombinant SABP2 Expressed in <i>E. coli</i>	29
Purification of Native SABP2 from Tobacco.....	30
Purification of Native SABP2 form Tobacco upon TMV Infection	31
SBIP-428 is SA Mediate Defense Pathway (Hypothesis III).....	32
Effect of SA on the Deacetylase Activity in Tobacco Transgenic Plants	32
Expression of <i>SBIP-428</i> in Tobacco Transgenic Plants	32
Expression of <i>SBIP-428</i> in Tobacco upon TMV Infection	32
Complementation Experiment.....	33
Confirmation of T-DNA Insertion.....	33
Growth Phenotype Analysis of Mutant	35
Bacterial Growth Assay.....	35
Protocols for RT-PCR (Reverse Transcriptase Polymerase Chain Reaction) and Western Blot	37
Isolation of Total RNA for Leaves	37
cDNA Synthesis	37
Reverse Transcriptase-Polymerase Chain Reaction (RT-PCR)	38
Agarose Gel Electrophoresis	38
SDS-PAGE	38
Western Blot Analysis for SABP2 and His-Tagged Protein.....	39
Western Blot Analysis for Lysine Acetylated Proteins	39
Spin Column.....	40
3. RESULTS.....	41
Section I: Biochemical Characterization of SBIP-428.....	41
Bioinformatics Analysis of SBIP-428	41
Expression and Purification of SBIP-428.....	47
Deacetylase Enzyme Activity of SBIP-428.....	51
Lysine Acetylation of SBIP-428.....	56
Section II: Acetylation of Internal Lysine Residues of SABP2	60
SABP2 Acetylation.....	60

Section III: SBIP-428 in SA Mediated Defense Mechanism.....	66
Effect of SA on the Deacetylase Activity in Tobacco Transgenic Plants	66
Effect of SA in Expression of <i>SBIP-428</i>	67
<i>SBIP-428</i> Expression upon TMV Infection.....	68
Complementation Assay.....	69
Growth Phenotype of <i>Arabidopsis SRT2</i> Mutant (SALK_131994C)	73
Pathogen Growth Assay	76
4. DISCUSSION	82
Biochemical Characterization of SBIP-428	83
Acetylation of SABP2.....	85
SBIP-428 in Plant Defense.....	86
Future Direction	89
REFERENCES	90
APPENDICES	100
Appendix A – Abbreviations.....	100
Appendix B – Buffers and Reagents.....	103
VITA.....	107

LIST OF TABLES

Table	Page
1. Details Of SBIP-428 Enzyme Assay Work Flow	27
2. Details Of <i>Arabidopsis SRT2</i> Mutant.	33
3. Primer Details Of <i>Arabidopsis SRT2</i> Mutants	34
4. Primer Details Of <i>Arabidopsis SRT2</i> And <i>Histone Deacetylase</i>	35
5. Luminescence Reading Of SBIP-428 Deacetylase Activity And Statistical Analysis.	53
6. Luminescence Reading Of SBIP-428 Deacetylase Activity And Statistical Analysis.	55
7. Predicted Internal Lysine Residues In SBIP-428.....	57
8. Predicted Internal Lysine Residues In SABP2	60
9. Bacterial Population (<i>Pst</i> Dc3000 And <i>Pst</i> Dc3000 <i>AvrRpt2</i>) In Col-0 And <i>SRT2</i> Mutant At 4 dpi	79

LIST OF FIGURES

Figure	Page
1. Activation Of Systemic Acquired Resistance In Plant System.	14
2. Synthesis Of Sa From Phenylalanine Or Chorismate In Plant.	16
3. SBIP-428 Dna Sequence Obtained From Y2h.....	41
4. Corresponding Amino Acid Sequence Of SBIP-428.....	42
5. Protein Blast Of SBIP-428.....	43
6. Sequence Alignment Of SBIP-428 AtSRT2, and Human SIR2.....	44
7. Protein Model Of SBIP-428 And AtSRT2..	45
8. Protein Model Of Human SIR2 Deacetylase..	46
9. Predicted Subcellular Localization Of SBIP-428..	47
10. Purification Of SBIP-428 Using Ni-NTA Affinity Column.....	48
11. Chromatography Profile Of Protein In Mono Q Column.	49
12. Purification Of SBIP-428 In Mono Q Column.....	49
13. Dialyzed SBIP-428 After Mono-Q Purification.	50
14. Deacetylase Activity Assay Of SBIP-428.	52
15. Determination Of Linear Range Of SBIP-428 Enzyme Activity..	54
16. Determination Of Linear Range Of SBIP-428 Deacetylase.	56
17. Western Blot Analysis Of Mono Q Purified SBIP-428.....	58
18. Acetylation Of SBIP-428.....	59
19. Acetylation Of Recombinant SABP2..	62
20. Acetylation Of Native SABP2.....	64
21. SABP2 Acetylation Upon TMV Infection.....	66

22. RT-PCR Amplification Of <i>PR1</i> Gene.....	66
23. Effect Of SA On Lysine Acetylated Protein Profile.....	67
24. <i>SBIP-428</i> Gene Expression In XNN, NahG, C3, And 1-2 Plants.....	68
25. <i>SBIP-428</i> Gene Expression In XNN Plant Upon TMV Infection.	69
26. T-DNA Insertion Confirmation Analysis Of <i>SRT2</i> Mutation In <i>Arabidopsis thaliana</i>	70
27. T-DNA Insertion Confirmation Analysis Of <i>Arabidopsis SRT2</i> Mutant.....	71
28. RT-PCR Amplification Of <i>EF1α</i> Gene In <i>Arabidopsis</i>	72
29. RT-PCR Amplification Of <i>SRT2</i> And <i>Histone Deacetylase</i> Gene In <i>Arabidopsis</i> Mutants..	72
30. <i>ATSRT2</i> Gene Analysis In <i>SRT2</i> Mutant.	73
31. Growth Phenotype Of <i>Arabidopsis SRT2</i> Mutant.....	74
32. Growth Phenotype Of <i>Arabidopsis Thaliana</i> Col-0 And <i>SRT2</i> Mutant..	75
33. Growth Phenotype Of <i>Arabidopsis SRT2</i> Mutant In 1/2 MS Media..	77
34. Disease Phenotype Of <i>Arabidopsis thaliana</i> At 2 dpi And 4 dpi..	79
35. Bacterial Population Of <i>Pst</i> DC3000.....	80
36. Bacterial Population Of <i>Pst</i> DC3000 <i>AvrRpt2</i>	80
37. A Comparison Graph Between <i>Pst</i> Dc3000 And <i>Pst</i> Dc3000 <i>AvrRpt2</i> Growth.	81

CHAPTER 1

INTRODUCTION

From archaea to eukaryotic cells, all biotic living organism use plants as their primary source of food. Some microorganisms, parasitic insects, nematodes, and even parasitic plants use plants to complete their life cycle. Extensive range of organisms attack plants for various reasons. In agriculture pathogen and herbivores attack can cause serious damage to the quality and yield of crops. Plants have evolved mechanisms to organize and assemble their own defense mechanism to deal with attacks by diverse organisms. In this study we have tried to understand the defense signaling mechanism of plants.

Plant Immune System

Pattern-triggered immunity (PTI) and effector-triggered immunity (ETI) are 2 distinguished models of plant immunity defined by recognition of different types of molecules by plants that are affected by pathogen attack (Jones and Dangl 2006). PTI occurs in plant cell membrane by recognition of microbe-associated molecular patterns (MAMPs) or damage-associated molecular patterns (DAMPs) by plant pattern-recognition receptors (PRR) (Boller and Felix 2009). ETI is triggered upon recognition of pathogen effectors by plant resistance (R) proteins that are normally localized inside the cell (Jones and Dangl 2006).

PTI and ETI have both have strengths and weaknesses; ETI signaling evolved to be strong response against pathogen effector because of high recognition specificity; however, some pathogen can often escape ETI by eluding such specific recognition. PTI can provide immunity against potential pathogens that are not well adapted but is not very effective against well adopted pathogens (Tsuda et al. 2009). However, how an effector trigger's immune response in

plants, coordinates resistance to a broad range of pathogens and their corresponding effector is a question yet to be answered (Chisholm et al. 2006).

Domain Structure of Pattern-Recognition Receptors (PRR) and Resistance (R) Proteins

'PRR' and 'R' proteins are the 2 major types of proteins involved plant resistance mechanisms. PRRs are associated with or contain interleukin-1 receptor-associated kinase (IRAK) family that is a member of monophyletic group that includes *Arabidopsis* Flagellin Sensitive2 (FLS2), rice XA21 (*Xanthomonas* resistance 21), human interleukin-1 receptor-associated kinase (IRKs) and *Drosophila* Pelle. Pathogen recognition at the surface of cell is carried out by Receptor-Like Proteins (RLPs) and serine-threonine receptor kinases that are known class of PRRs. Receptor kinases XA21 and FLS2 and the RLPs, Cf-9, and XA21D are the best-studied plant PRRs in recent years (Dardick and Ronald, 2006).

Two major classes of protein encoded by resistance (*R*) genes are; NB-LRR class and eLRR (extracellular Leucine Rich Repeat). They are named after their characteristics nucleotide binding (NB) and leucine rich repeat (LRR), and extracellular leucine rich repeat (eLRR) domains. The length of LRR is usually 20-30 amino acid and the motifs have been identified in proteins with wide range from viruses to eukaryotes. These proteins are involved in various processes from plant development to disease resistance. The subclasses of NB-LRR are coiled-coil (CC) NB-LRR and Toll-interleukin-1 receptor (TIR) NB-LRR. They are divided based on their N-terminal domain. The best characterized member of NB-LRR proteins are RPS2, RPM1, and RPS5. These *Arabidopsis* R proteins specify resistance to *Pseudomonas syringae* carrying the bacterial effectors AvrRpt2, AvrRpm1/AvrB, and AvrPphB, respectively (Chisholm et al. 2006). NB-LRR proteins determine the resistance to viral, bacterial, oomycete, and fungal pathogens (Dangl and Jones 2001). eLRR proteins can be further divided according to their

domain structure (Fritz-Laylin et al. 2005). RLP (receptor-like proteins; extracellular LRR and transmembrane [TM] domain), RLK (extracellular LRR, TM domain and cytoplasmic kinase) and PGIP (polygalacturonase-inhibiting protein; cell wall LRR) are the 3 subdivisions of eLRR, which is based on their domain structures (Fritz-Laylin et al. 2005).

Signaling Pathways and Cross Talk Between JA, ET, and SA.

Jasmonate (JA), ethylene (ET), salicylate (SA), and PAD4, which are termed as ‘signaling sectors’ of a network rather than “pathways”, synthesized with the help of *DDE2*, *EIN2*, *SID2*, and *PAD4* genes, respectively. The product of these genes function as hubs that interact with each other. The fragment of bacterial flagellin, flg22 (flg22-PTI) and *Pseudomonas syringae* effector, AvrRpt2 trigger the PTI and ETI, respectively. The interaction between 4 sectors and flg22-PTI was synergistic, whereas, AvrRpt2-ETI and 4 sectors were compensatory; this difference is not because of the nature of signaling machinery they use but because of how common signaling machinery they use (Tsuda and Katagiri 2010). Major parts of the networks are not different; the speed of the responses affects which immune responses deliver effective immunity (Tsuda et al. 2009). For example, AvrRpm1-ETI responses are markedly faster comparing with AvrRpt2-ETI (Ritter and Dangl 1996; Tao et al. 2003). The signal of pathogen attack branches into multiple signal flows and that multiple signals enter from different points of the common network, which suggests that plants use an integrated signaling network for various modes of immunity but use the common network differently for different modes (Katagiri and Tsuda 2010).

Systemic Acquired Resistance

Systemic acquired resistance (SAR) is a mechanism in which resistance spreads away from the site of primary infection to the uninfected parts of the plant. In this mechanism plants

induce resistance that confers long-lasting defense against a wide spectrum of pathogens (Durrant and Dong 2004) (Figure 1). Increased level of SA is associated with activation of SAR. SAR is characterized by coordinate expression of a set of *Pathogenesis-Related (PR)* genes, many of which encode PR protein with antimicrobial activity (Van Loon et al. 2006). There are several reports using transgenic or mutant plants to verify the hypothesis that the perception or production of SA has a key role in SAR? (Loake and Grant 2007; Volt et al. 2009). NPR1, a regulatory protein, which plays a vital role as transducer of the SA signal, is activated by SA and acts as coactivator of *PR* gene expression (Dong and Durrant 2004). SA, JA, and ET also play roles in inducing SAR. There are several reports that suggested that SAR is not activated in *sgt1b*, *oopr3*, *jar*, *eds8*, and *coil* *Arabidopsis* mutants that are known JA signaling mutants (Pieterse et al. 1998; Ton et al. 2002a; Cui et al. 2005; Truman et al. 2007; Attaran et al. 2009). Verberne et al. (2003) reported that ethylene had a role in SA-dependent SAR induction against tobacco mosaic virus (TMV). However, the exact role of JA and ET needs to be further studied. Liu et al. (2011) proposed that interaction of 2 mobile signals: MeSA and a complex of lipid transfer protein DIR1 and a glycerolipid, control SAR. SAR induction by MeSA is determined by light period; MeSA and its metabolizing enzymes showed influential effect on SAR during late in day when plants are expected to receive little light in hours after infection (Liu et al. 2009).

Recently, scientist started to look into long-lasting impact on gene expression and plant immunity by analyzing epigenic regulatory mechanism, such as chromatin remodeling and DNA methylation (Bruce et al. 2007; Van Den Burg and Takken 2009; Alvarez et al. 2010).

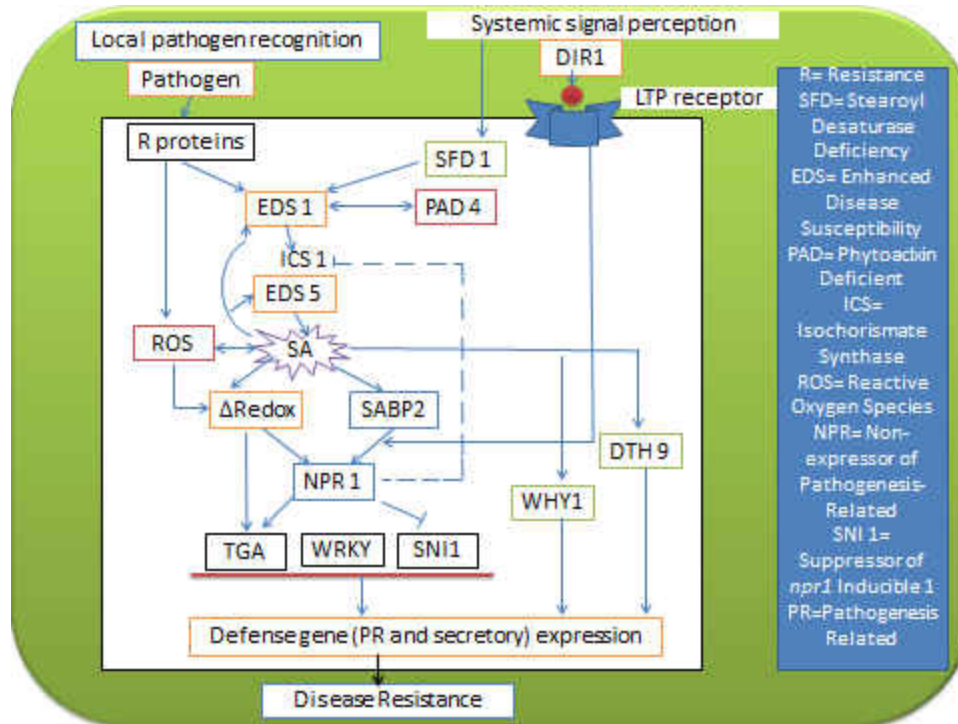


Figure 1: Activation of Systemic Acquired Resistance in Plant System (Re-drawn with permission from Durrant and Dong 2004). Resistance (R) proteins activate Enhanced Disease Susceptibility 1 (EDS1) and Reactive Oxygen Species (ROS) which activate SA and downstream cascades.

Induced Systemic Resistance

Both pathogenic and nonpathogenic microbes can elevate the disease resistance level in plants. Van loon et al. (1998) first reported that colonization of plant roots by PGPR (plant growth-promoting rhizobacteria) were shown to defend above ground plant tissue against pathogenic microbes. Many nonpathogenic *Pseudomonas* spp and *Bacillus* spp have been documented to be responsible for induced systemic resistance in many plants (Kloepper et al. 2004; Van Loon and Bakker 2006).

Salicylic Acid Synthesis Pathway

SA has been studied for more than 200 years in medicine for humans, but in plants its role is documented only in past ~30 years (Vlot et al. 2009). Wide varieties of role is played by SA in plants, particularly, influencing seed germination, seedling establishment, cell growth, respiration, senescence-associated gene expression, stomata closure, abiotic stress responses, basal thermo-tolerance, nodule formation in legumes, and fruit yield.

Two distinct enzymatic pathways are known to generate SA in plants. Salicylic acid can be produced from chorismate via isochorismate catalyzed by isochorismate synthase (ICS) and isochorismate pyruvate lyase (IPL) (Verberne et al. 2000; Wildermuth et al. 2001; Strawn et al. 2007). On the other hand, SA also can be generated via phenylalanine, cinnamic acid, and benzoate intermediates or coumaric acid (Figure 2). SA glucosyltransferase (SAGT) catalyzes the conversion of SA into SA O- β -glucoside (SAG), or salicyloyl glucose ester (SGE) but how SA is regenerated back from SGA or SGE is still unknown (Dean and Delaney 2008). SA methyltransferase (SAMT) converts SA to MeSA, whereas SABP2/methyl esterase (MES) helps to resynthesize SA from MeSA (Kumar and Klessig 2003).

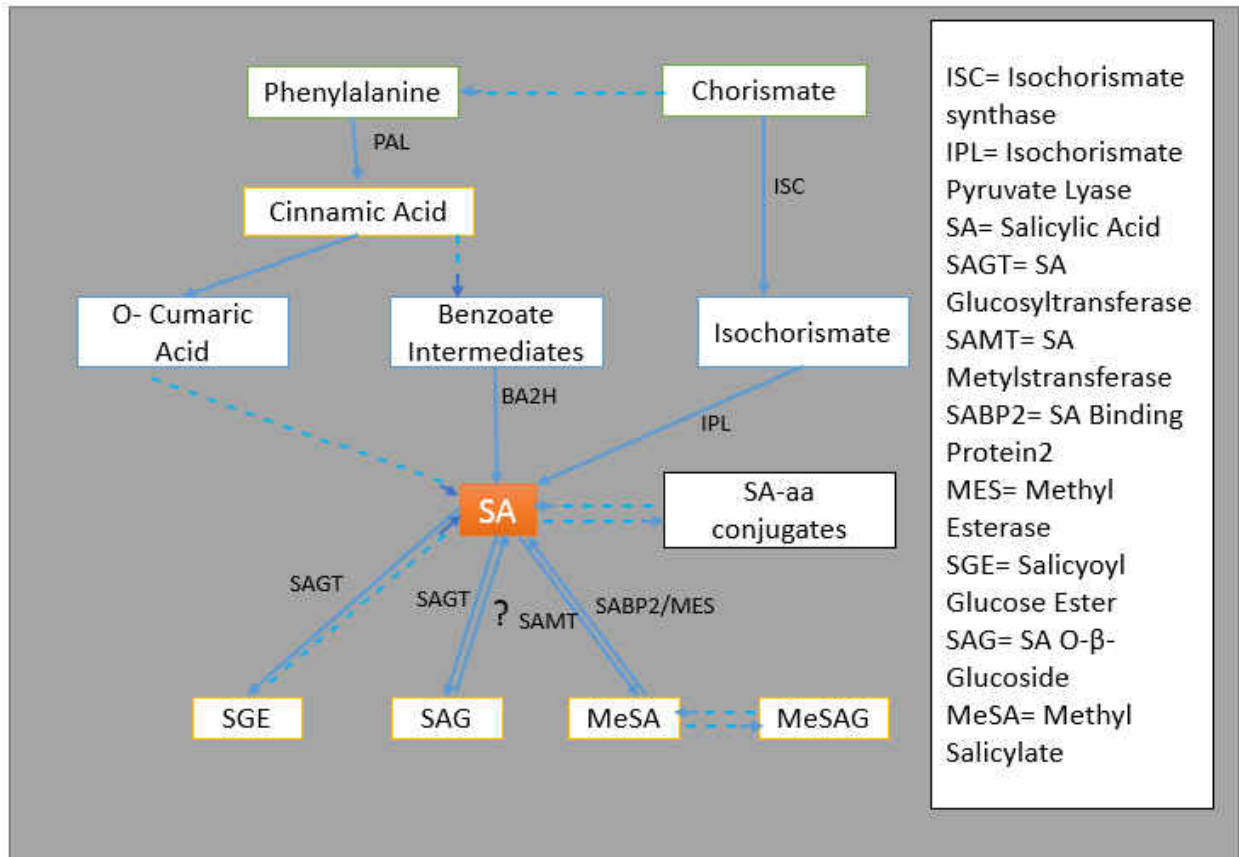


Figure 2: Synthesis of SA from Phenylalanine or Chorismate in Plant (re-drawn with permission from Volt et al. 2009). SA can be converted from SGE, SAG, MeSA. SABP2 helps in conversion of MeSA to SA.

SA plays extensive role in plant defense signaling against pathogen in local disease resistance mechanism, including death of host cell and defense gene expression, and SAR. *PR* genes are expressed by SA during resistance response to bacterial, viral, and fungal pathogen infections in plants.

Salicylic Acid Binding Protein2 (SABP2)

Salicylic acid binding protein_2 (SABP2), a 29kDa enzyme catalyzes the conversion of MeSA to SA (Kumar and Klessig 2003). Abundance of SABP2 is extremely low in tobacco

plants but it binds SA with high affinity. Kumar and Klessig (2003) first reported the role of SABP2 in plant innate immunity. The tobacco *SABP2* silenced plants are more susceptible to TMV and exhibits down regulation of *PR-1* gene expression. In SA signaling pathway, SABP2 plays a significant role in local resistance and SAR. SABP2 likely helps to increase the cytoplasmic SA levels that result in changes in redox potential of cytoplasm. Monomerization of NPR1 oligomers is initiated upon SA mediated changes in redox potential (Beckett and Dorothy 2001). NPR1 monomers migrate to nucleus where TGA class of transcription factors help to induce the expression of SA responsive defense genes resulting in activation of local resistance (Mou et al. 2003). Tripathi et al. (2010) recently reported that SABP2 is required for acibenzolar S-methyl (ASM) (a synthetic analog of SA) mediated activation of SAR in tobacco plants. To better understand the role played by SABP2, a yeast 2-hybrid (Y2H) screen was performed to identify proteins that interact with SABP2.

SABP2 Interacting Proteins

Tobacco leaf proteins were used as prey (Y2H library) and full length SABP2 was used as a bait. Several interactors of SABP2 were identified in this screening. One of the interacting proteins identified is SBIP-428. SBIP-428 shows high homology to Silent Information Regulator 2 (SIR2) family proteins.

Silent Information Regulator2 (SIR2)

SIR2 proteins, also known as sirtuins, are broadly conserved from bacteria to mammals (Frye 2000). In mammals Sirtuins are divided into 7 groups (SIRT1-SIRT7) (Frye 2000). SIRT1 is the closest homologue of SIR2. Deacetylation of acetylated nuclear histones is well known function of SIR2 that is NAD^+ dependent (Northa and Verdin 2004). However, some recent studies show that members of SIR2 protein family are also involved in deacetylation of non

histone proteins in other organelles. Enzymatic activity of SIR2 in yeast is required for the association with the regions distal to the nucleation sites (Moazed 2001). Several chemical compounds have been reported to inhibit or activate the deacetylase activity of SIR2. Splitomicin and sirtinol inhibit the NAD⁺-dependent deacetylase activity of SIR2 in yeast and *Arabidopsis* (Bedalov et al. 2001; Grozinger et al. 2001). Nicotinamide, a product of SIR2 deacetylation reaction also acts as inhibitor of its activity (Bitterman et al. 2002). Quercetin and piceatannol have been shown to increase the activity of SIR1 proteins (Howitz et al. 2003). Hypoacetylation (decreased acetylation) of histone H4 in the rDNA site was shown to be SIR2-dependent (Guarente and Hekimi 2003). Deletion of SIR2 in yeast, resulted in enhanced acetylation in subtelomeric region, mating type loci, and H3 and H4 histone of rDNA (Buck et al. 2002; Robyr et al. 2002). In humans lack of SIR1 (ortholog of SIR2) showed dependency of embryonic development and muscle differentiation (Cheng et al. 2003; Fulco et al. 2003; Lin and Elledge 2003; McBurney et al. 2003).

Drosophila SIR2 (dSIR2) is required for physical interaction with Hairy, a bHLH euchromatic repressor and key regulator of *Drosophila* development (Rosenberg and Parkhurst 2002). dSIR2 is the nuclear protein in adult fly, whereas during embryo stage, prior to nuclear cycle 12, dSIR2 is detected in both nucleus and cytoplasm (Newman et al. 2002; Rosenberg and Parkhurst 2002). Dependency on NAD⁺ for histone deacetylase activity of SIR2 suggested a link between caloric restriction and SIR2 activity that resulted in extension of life span. Short life span of fly resulted as dSIR2 was deleted (McBurney et al. 2003). Free cytoplasmic NAD⁺ is a result of less carbon flow through glycolysis under condition of caloric restriction. In circumstances of caloric restriction, NAD⁺ levels increase that result in SIR2 activation and decrease in the rate of aging. However, Burnett and colleagues (2011) reported that lifespan of

Drosophila and *C. elegans* increased with dietary restriction independently of dSIR2, questioning the effect of sirtuins on the lifespan of metazoan.

SIR2 in Plants

The functions of SIR2 proteins in plants is not well studied. Recently homolog of SIR2 proteins have been reported in rice and *Arabidopsis* (Huang et al. 2007; Wang et al. 2010; Konig et al. 2014). In rice *SIR2*-like gene (*OsSRT1*) is needed as safeguard against genome instability and cell damage to ensure plant cell growth. *OsSRT1* gene is involved in acetylation and dimethylation of histone H3K9. Knock-down of *OsSRT1* resulted in cell death, DNA fragmentation, increased production of H₂O₂ and on the other hand, overexpression showed higher tolerance to oxidative stress (Huang et al. 2007). Wang and colleagues (2010) reported that in *Arabidopsis*, AtSRT2 acted as a negative regulator of basal defense by suppressing SA biosynthesis. AtSRT2 was down-regulated in response to *P. s. pv. tomato* DC3000 infection. Expression of *PR1* was negatively regulated by AtSRT2. HDA19 (histone deacetylase 19), a protein of RPD3/HAD1 superfamily is directly associated with chromatin modification of *PR1* and *PR2* promoter to a repressive state that ensures low basal expression of these genes (Choi et al. 2012). Loss of HDA19 activity increased the level of SA content and expression level of *PR1*, *PR2* (Choi et al. 2012). Zhou et al. (2005) reported that overexpression of *HDA19* increased the expression of JA/ET-regulated genes and resistance to fungal pathogen, *Alternaria brassicicola*, whereas HDA19 knock-down plants were more susceptible. They also reported that HDA19 expression was induced by inoculation with *A. brassicicola*, wounding, and by the treatment with JA and ET. However, Tian et al. (2005) reported that a histone deacetylase (AtHD1) provides positive and negative control of transcription. *AtHD1* gene is involved in ectopic expression of protein synthesis, whereas a negative regulator of SA in leaves and flowers. Microarray analysis

suggested that *AtHDI* is involved in regulation of developmental and environmental gene expression (Tian et al. 2005).

Nonhistone Protein Acetylation and Metabolic Enzymes

Several recent studies suggested that beyond histones, a number of other metabolic enzymes in almost all organisms are regulated by acetylation/deacetylation (Frankemier et al. 2011). Acetyl-CoA and NAD⁺ are most common influencing molecules of protein acetylation that regulates several enzymes activities (Xing and Poirier, 2012). An animal transcription factor, p53, is the other well-known acetylated protein beyond histones (Gu and Roeder 1997). To date, more than 100 other acetylated proteins have been identified in animal, bacteria, and yeast, which include a large number of DNA associated proteins, transcription factors, and nuclear receptors (Kouzarides 2000). Two recent papers have shown that more than 125 different proteins are acetylated in *Arabidopsis*, which are involved in wide range of metabolic pathways (Frankemier et al. 2011; Wu et al. 2011).

Hypotheses

Hypothesis I: SBIP-428, a homologue of Silent Information Regulator 2 (SIR2), is a NAD⁺ dependent deacetylase.

Hypothesis II: SABP2 is acetylated and is regulated by deacetylase activity of SBIP-428.

Hypothesis III: SBIP-428 has an effect on SA mediated defense mechanism in plants.

CHAPTER 2

MATERIALS AND METHODS

Materials

Plant Materials

Three transgenic lines of tobacco plants *Nicotiana tabacum* cv. *Xanthi nc NN* (XNN), NahG (expressing *nahG* gene, that encodes SA hydrosylase that converts SA to catechol), 1-2 (SABP2 silenced) were used for this study. Six mutant lines of *Arabidopsis thaliana* (CS370961, SALK_139443, SALK_131994C, SALK_149295C, SALK_035541, and CS877409) and a wild type (Col-0) also were used for this study. Seeds were grown in autoclaved (for 20min) soil containing peat moss (Fafard Canadian growing mix F-15, Agawam, MA). Tobacco seedlings were transferred to 4 X 4 inch flats after 14 days, 2 in one flats. After 30 days, young plants were transfer to an 8 inch pot. Fertilizer was added to the plants after 3 days of transfer to the pot. Six to 8 weeks old plants were used to perform the experiments. *Arabidopsis* seeds were sown in autoclaved soil with fertilizer. Seeds were kept in the cold dark room for 3 days and then transfer to the growth chamber. The growth chamber (PGW 36, Conviron, Canada) was set at 16-h day cycle with temperature at 22°C.

Chemicals and Reagents

Sodium dodecyl sulfate (SDS), β -mercaptoethanol (β -ME), tetramethylethylenediamine (TEMED), ammonium persulfate (APS), bovine serum albumin (BSA), bovine thrombin, coomassie brilliant blue R-250, coomassie brilliant blue G-250, ponceau-S, ethylenediaminetetraacetic acid (EDTA), TRIS base, phenylmethylsulfonyl fluoride (PMSF), glycine, glycerol, methanol, imidazole, Tween-20, Triton X-100, N,N-Bis(2-

hydroxyethyl)glycine (Bicine), magnesium chloride ($MgCl_2$), sodium chloride (NaCl), sodium phosphate monobasic (NaH_2PO_4), sodium phosphate dibasic (Na_2HPO_4), benzamidine-HCl, ammonium sulfate ($(NH_4)_2SO_4$), sodium citrate ($Na_2HC_6H_5O_7$), and all other standard chemicals were purchased from Fisher Scientific, Pittsburgh, PA. Polyvinylpyrrolidone (PVPP) was purchased from Acros Organics, Audubon Park, NJ. The Mini Protean 3 cell, 30% acrylamide, Bradford's reagent, prestained low molecular weight marker, 10x SDS loading buffer, SDS dye, and Mini trans blot system were purchased from Bio-Rad, Hercules, CA. Polyvinylidene fluoride (PVDF) membranes were purchased from Millipore, Billerica, MA. Mono Q column was purchased from GE Healthcare, Piscataway, NJ. Bicinchoninic acid (BCA) protein assay and Pierce ECL western blotting substrate were purchased from Thermo Scientific, Rockford, IL. Kodak developer and fixer replenisher were purchased from Sigma-Aldrich, St. Louis, MO. 6xHis-tag SBIP-428 protein was expressed in Gateway system. Rabbit polyclonal SABP2 antibodies and monoclonal anti-rabbit, IgG γ chain specific secondary antibodies conjugated to HRPO and tobacco mosaic virus (TMV) were available in-house. Oligo dT-20, Taq DNA polymerase (Invitrogen, CA), dithiothreitol (DTT), DNA ladder (New England Biolabs), MMLV reverse transcriptase, RNase free DNase, recombinant RNasin (Promega), and gel loading dye (Bio-Rad).

Other Materials

One ml syringes (BD syringes, NJ), pestle grinder (Fisher Scientific), cheese cloth and miracloth (Fischer Scientific), Spectrophotometer, high speed centrifuge (Beckman, model J2-21 or Sorvall RC5B), SYNERGY HT Multi-Mode Microplate Reader (Biotek), and AKTA purifier 10 (GE Healthcare) system were used for this research.

Methods

Biochemical Characterization (Hypothesis I)

Bioinformatics Analysis

Sequence Alignments and Database Analysis. The DNA sequence and corresponding amino acid sequence of SBIP-428 were analyzed using BLAST (Basic Local Alignment Search Tool) (Altschul et. al. 1990) at NCBI (<http://blast.ncbi.nlm.nih.gov/Blast.cgi>) and ExPASy Bioinformatics Resource Portal (<http://www.expasy.org/tools/>). To compare it with known tobacco genes, the SBIP428 nucleotide sequence was used to search the tobacco Unigene in solanaceae database (<http://solgenomics.net/tools/blast/index.pl>). Full length protein sequences of *Ricinus communis*, *Populus*, *Arabidopsis thaliana*, and *Oryza sativa* similar to SBIP428 were compared using Multi-sequence alignments of amino acid (ClustalW2; <http://www.ebi.ac.uk/Tools/msa/clustalw2/>).

3D Protein Structure Model of SBIP-428. (PS)²: Protein Structure Prediction Server (<http://ps2.life.nctu.edu.tw/>) was used to generate the 3D protein structure of SBIP-428. A human Sir2 was used as template to generate the 3D structure models.

Subcellular Localization Prediction of SBIP-428. Protein Prowler (http://bioinf.scmb.uq.edu.au/pprowler_webapp_1-2/), MultiLoc (<http://abi.inf.uni-tuebingen.de/Services/MultiLoc/>), and BaCelLo (<http://gpcr.biocomp.unibo.it/bacello/pred.htm>) prediction tools were used to predict the subcellular localization of SBIP-428.

Expression and Purification of SBIP-428

Cloning of SBIP-428. The cloning of full length SBIP-428 in pDONR221 was previously performed (Kumar et al., unpublished). Briefly, the full length coding region of SBIP-428 was

amplified by RT-PCR and cloned into entry plasmid vector pDONR221 (Gateway, Invitrogen). Obtained cDNA was cloned, sequenced, and analyzed. Once a full length SBIP-428 was obtained and verified, it was used for recombinant protein expression. To express recombinant proteins, the full length SBIP-428 was sub-cloned into pDEST17 (Gateway; Invitrogen) with 6XHis tag on its N-terminus. Following verification of sequences, the recombinant SBIP-428 in pDEST 17 was transformed into a suitable *E. coli* host (BL21 (DE3) pLysS and BL21-CodonPlus (DE3)-RIL) for protein expression.

Purification of SBIP-428 Using Ni-NTA Chromatography. Recombinant his-tagged SBIP-428 was first purified by Ni-NTA column chromatography. A modified purification protocol described by Forouhar et al. (2005) was used. The *E. coli* BL21 pLysS cells were grown in the LB agar containing 100 µg/ml ampicillin at 37°C for overnight. The overnight grown single colony was inoculated to 3ml of liquid LB broth (containing 100 µg/ml of ampicillin). The culture was grown for ~12 hour then diluted 100 times in fresh 50 ml LB broth with antibiotics. The overnight grown culture was then diluted to 1.5 L of fresh LB medium (containing antibiotic). Bacterial cultures were grown at 37°C in a shaker maintained at 250 rpm until it reached 0.6-0.7 OD (optical density). At OD= 0.6-0.7, protein expression was induced by adding 0.01 mM of isopropyl β-D-1 thiogalactopyranoside (IPTG) to the culture and was incubated at 17°C in a shaker maintained at 250 rpm for overnight. Overnight culture was centrifuged at 8000 rpm at 4°C for 10 minutes to pellet bacteria. Bacterial pellet was then suspended in 1X Ni-NTA buffer (50 mM Na₂HPO₄, 300 mM NaCl, and 10 mM Imidazole, pH 8.0) containing 0.1 mM protease inhibitors (phenylmethylsulfonyl fluoride (PMSF); 100mM stock in isopropanol) and then lysed using French-press (Thermo Electron Corporation; cell type 20 K, max gauge 1280). Cell lysate was centrifuged at 14000 rpm for 15 min at 4°C to separate soluble (supernatant) and

insoluble (pellet) proteins. Soluble proteins in supernatant were purified by using metal affinity chromatography (Ni-NTA). Ni-NTA resin pre-equilibrated in 1X Ni-NTA buffer (50 mM Na₂HPO₄, 300 mM NaCl, and 10 mM Imidazole, pH 8.0) was added to soluble protein and incubated at 4°C with gentle shaking for overnight. Flow-through containing unbound proteins was collected and loosely bound proteins was washed using 1x Ni-NTA buffer. Bound proteins were eluted using 250 mM of imidazole in 50 mM Na₂HPO₄, 300 mM NaCl, pH 8.0. Purification of SBIP-428 was analyzed by SDS-polyacrylamide gel electrophoresis and western blot was performed using monoclonal Anti-polyHistidine antibody to confirm the presence of SBIP-428.

Purification Using Mono-Q. Fractions containing SBIP-428 from the Ni-NTA chromatography were further purified on a mono-Q anion exchange column. Fractions containing SBIP-428 from Ni-NTA were pooled and desalted using buffer (10 mM Bicine, pH 8.0) in a Hitrap Desalting Column (2x5 ml) (GE Healthcare). Desalted fractions were applied to Mono-Q column (Mono-Q 5/50 GL, GE Healthcare). The bound proteins were eluted with a linear gradient of 0-300 mM ammonium sulfate in buffer (10 mM Bicine, pH 8.0). The presence of SBIP-428 was determined by western blot using monoclonal Anti-polyHistidine antibody (1:3000 dilution in blocking buffer; 1 % BSA, 3 % nonfat milk in 1xPBS), and a 12.5 % SDS-PAGE was run to confirm purification of SBIP-428.

Dialysis of SBIP-428. Mono Q purified proteins (~4 ml) were pooled together in a dialysis bag (Molecular Weight cutoffs: 12000-14000 Da). Samples were dialyzed against deacetylase buffer (50 mM Hepes pH 7.6, 350 mM NaCl, and 20 % glycerol) at 4°C with gentle stirring. Buffer was changed every 8 hours 3 times. Dialyzed proteins were aliquoted (100µl) and stored at -80°C until further use.

Deacetylase Activity of SBIP-428

Deacetylase Enzyme Assay Using Total Leaf Protein as Substrate. A deacetylase enzyme assay was performed as described by Frankemier et al. (2011) with minor modifications. Total acetylated proteins from the tobacco leaves were used as substrate for the enzyme assay. Plant proteins are naturally acetylated and could potentially be used for deacetylation assay. Total leaf proteins were extracted as described below using direct extraction buffer (DEB; 100 mM Tris-HCl pH 8.0, 1.5 M β -mercaptoethanol, 15 % glycerol, 5 mM NaF, 1 mM Na_3VO_4 , and 2 mM EDTA). Proteins were desalted using a spin column prior to the enzyme assay. The SBIP-428 enzyme was purified using mono-Q ion exchange chromatography described as above.

For deacetylase activity assay of recombinant SBIP-428, 12 μg of *N. tabacum* (XNN) leaf protein (naturally acetylated) were incubated with 18 μg , 12 μg , or 8 μg of SBIP-428 for 3 h at 37°C. As a negative control (without SBIP-428), deacetylase buffer (50 mM Hepes, pH 7.6, 350 mM NaCl, 20 % Glycerol) was used instead of SBIP-428. Proteins treated with the enzyme SBIP-428 were then subjected to Western blot analysis using anti Acetylated Lysine Antibody. Experiment details are presented in Table 1 below-

Table 1: Details of SBIP-428 Enzyme Assay Work Flow

	Proteins (substrate)	SBIP-428 (enzyme)	Buffer (5X)	Water	Total Volume	Dye (X)	Loading volume
1	8 μl XNN (12 μg)	11.21 μl (12 μg)	6 μl	4.79 μl	30	5 μl (6X)	33 μl
2		11.21 μl (12 μg)	6 μl	12.79 μl	30	5 μl (6X)	33 μl
3	8 μl XNN (12 μg)	16.82 μl (18 μg)	6 μl	00 μ	30	5 μl (6X)	33 μl
4		16.82 μl (18 μg)	6 μl	7.18 μl	30	5 μl (6X)	33 μl
5	8 μl XNN (12 μg)	5.16 μl (8 μg)	6 μl	10.39 μl	30	5 μl (6X)	33 μl
6		5.16 μl (8 μg)	6 μl	12 μl	30	5 μl (6X)	33 μl
7	8 μl XNN (12 μg)		6 μl	16 μl	30	5 μl (6X)	33 μl
8		16.82 μl (18 μg)				5 μl (6X)	21 μl
9	8 μl					5 μl (6X)	12 μl

XNN; Total leaf protein from *N. tabacum*

SBIP-428 enzyme; Ni-NTA and mono Q purified protein.

Deacetylase Enzyme Assay Using SIRT Glo™ Assay Kit. Mono-Q purified SBIP-428 was used to determine the enzyme activity using SIRT-Glo™ assay kit (Promega). Protein was expressed, purified, and quantified for this assay. SIRT2 deacetylase enzyme activity was determined as described in the manufacturer's protocol. Briefly, SIRT-Glo™ buffer and substrate were equilibrated at room temperature and developer reagent was thawed at room temperature. SIRT-Glo™ buffer (10 ml) was added to SIRT-Glo™ substrate and then mixed gently to form SIRT-Glo™ substrate solution. Developer reagent (10 µl) was added to SIRT-Glo™ substrate solution to form SIRT-Glo™ reagent. SBIP-428 was serially diluted (1 µg to 8 µg) in total 100 µl of SIRT-Glo™ buffer and dispensed in a 96 well plate along with 100 µl of SIRT-Glo™ substrate solution. The final total reaction volume was 200 µl. Three replication of each concentration were used for this enzyme activity. SIRT-Glo™ substrate solution (100 µl) was added with 100 µl of SIRT-Glo™ buffer as negative control for this experiment. Reaction mixture was mixed briefly (~15 sec) at room temperature (RT) using the orbital shaker at 500-700 rpm and incubated at RT for 15 min. Luminescence measurements was taken at steady-state signal.

Deacetylase Enzyme Assay Using HDAC Glo™ Assay Kit. Mono-Q purified SBIP-428 was used to determine the enzyme activity using HDAC-Glo™ assay kit (Promega). Histone deacetylase activity was determined as described in the manufacturer's protocol. SBIP-428 was serially diluted (1 µg to 8 µg) in total 100 µl of HDAC-Glo™ buffer and dispensed in 96 well plate along with 100 µl of HDAC-Glo™ substrate solution. The final total reaction volume was 200µl. Reaction mixture was mixed briefly at room temperature using the orbital shaker at 500-700rpm and further incubated at room temperature for 15min. Luminescence measurements was

detected at signal steady-state. Three replication of each concentration were used for this enzyme activity. HDAC-Glo™ substrate solution (100 µl) was added with 100 µl of HDAC-Glo™ buffer as negative control for this experiment.

Lysine Acetylation of SBIP-428.

Purified SBIP-428 was analyzed for the potential of lysine acetylation. A Western blot was performed to detect the lysine acetylation of SBIP-428.

SABP2 Acetylation (Hypothesis II)

Purification of Recombinant SABP2 Expressed in *E. coli*

A modified protocol was used for SABP2 purification described by Forouhar et al. (2005). *E. coli* cells (MGK cells) containing pET28-SABP2 was grown in the LB agar containing ampicillin 100 µg/ml and kanamycin 10 µg/ml for overnight. The overnight grown single colony was inoculated to 3ml of liquid LB medium (containing 100 µg/ml of ampicillin and 10 µg/ml kanamycin). The culture was grown for 12 hours then diluted 100 times in fresh 200ml LB medium containing antibiotics. Bacterial culture was grown at 37°C in a shaker maintained at 250rpm until reach 0.6-0.7 OD. Once desired OD reaches at 0.6-0.7, protein expression was induced by adding 0.01 mM of isopropyl β-D-1 thiogalactopyranoside (IPTG) to the culture and was incubated at 17°C in a shaker maintained at 250 rpm for overnight. Overnight culture was centrifuged at 8000 rpm for 10 minutes at 4°C to pellet bacteria. Bacterial pellet was then suspended in 1X Ni-NTA buffer (50 mM Na₂HPO₄, 300 mM NaCl, and 10 mM Imidazole, pH 8.0) containing protease inhibitors and then lysed using French-press. Cell lysate was centrifuged at 14000 rpm for 15min at 4°C. Supernatant containing soluble proteins were purified by using metal affinity chromatography using Ni-NTA (Qiagen). Ni-NTA resin (~4 ml)

was equilibrated in 1x Ni-NTA binding buffer by washing at least 4 times. Soluble protein extract was added to the Ni-NTA resin and incubated with gentle shaking for overnight at 4°C. Next morning, Ni-NTA resin with soluble protein extract was brought to room temperature and poured into an empty column. Resin was allowed to settle down before opening stop valve. Flow-through containing unbound proteins was collected and loosely bound proteins were washed using wash buffer (50 mM Na₂HPO₄, 300 mM NaCl, and 10 mM Imidazole, pH 8.0). Bound proteins were eluted using 250 mM of imidazole in 1x Ni-NTA buffer. Purification of 6xHis tagged SABP2 was analyzed by SDS-polyacrylamide gel electrophoresis and western blot was performed using SABP2 polyclonal antibody to confirm the presence of SABP2. SDS-PAGE and Western blot protocol described below.

Purification of Native SABP2 from Tobacco

Native SABP2 was purified from WT (wild type) tobacco *Nicotiana tabacum* cv. Xanthi nc NN (XNN). Fully grown leaves from 6 to 8 week old plants were used for this experiment. Leaves were harvested and then kept frozen in liquid nitrogen. Frozen tissue were ground using a pestle and mortar. Three volumes of protein extraction buffer (20 mM sodium citrate, 5 mM MgSO₄, 1 mM EDTA, 14 mM β-mercaptoethanol, 0.1mM phenylmethylsulfonylflouride (PMSF), 1 mM benzamidine-HCl, and pH-6.3) were added to homogenized tissue sample. All subsequent steps were carried out at 4°C. The homogenate was filtered through 1 layer of miracloth (Calbiochem) and 4 layers of cheesecloth (Electron Microscopy Science). The filtered extract was centrifuged at 10,000 rpm for 20min at 4°C (GS3 rotor, Sorvall). Supernatant were used for further ammonium sulfate fractionation.

Ammonium Sulfate Fractionation. To obtain the 0-50% ammonium sulfate precipitated proteins, 50% ammonium sulfate (313g per liter) was slowly added and stirred into the

supernatant (soluble leaf extract). The saturated supernatant was stirred on ice for additional 20min. After 20 min, the solution was centrifuged at 10,000 rpm for 20min at 4°C (GS3 rotor, Sorvall). The pellet (containing 0-50% precipitated proteins) was stored at -20°C until use. Supernatant containing soluble proteins were precipitated further with 75% ammonium sulfate (176g per liter) by adding powdered ammonium sulfate. Incubation on ice and centrifugation was done as described above. The pellet was collected as 50-75% precipitated proteins and stored at -20°C for future use. The presence of SABP2 and acetylation of SABP2 was determined by Western blot using SABP2 polyclonal antibody and Anti-Acetyl Lysine Antibody, respectively.

Purification of Native SABP2 form Tobacco upon TMV Infection

Six-week-old wild type tobacco plant was infected with tobacco mosaic virus (TMV) with a 10^{-3} dilution of 45µg/ml TMV preparation. Carborundum was dusted evenly on the upper surface of the leaves, and TMV diluted in 0.05 M sodium phosphate buffer was gently rubbed on with a piece of cheesecloth. TMV infected plant was kept separated from uninfected plants and exposed with regular water and light conditions (16h day). SABP2 was purified in the same manner that SABP2 from native tobacco was. SDS-PAGE (12.5%) was done to resolve the 50-75% precipitated proteins and a Western blot was performed using polyclonal SABP2 antibodies to detect native SABP2. The Western Blot was performed with the purified protein with Anti-Acetyl Lysine Antibody to determine the acetylation of native SABP2 upon TMV infection.

SBIP-428 is SA Mediate Defense Pathway (Hypothesis III)

Effect of SA on the Deacetylase Activity in Tobacco Transgenic Plants

Total protein was extracted from tobacco leaves using direct extraction buffer (DEB; 100 mM Tris-HCl pH 8.0, 1.5 M β -mercaptoethanol, 15 % glycerol, 5 mM NaF, 1 mM Na_3VO_4 , and 2 mM EDTA). Plant leaves were ground in 3 times of DEB buffer using a pestle and mortar with acid washed sea sand (Fisher Scientific). Extract was then incubated in boiling water bath for 5 minutes and centrifuged for 10 minutes at 13000 rpm at room temperature. The supernatant was collected as protein sample and quantified using Bradford reagent (Bio-Rad). The Western Blot was performed with the purified protein with Anti-Acetyl Lysine Antibody to determine the effect of SA on deacetylase activity.

Expression of *SBIP-428* in Tobacco Transgenic Plants

To determine the effect of SA on SBIP-428 expression in *Nicotiana tabacum* cv. Xanthi nc (NN), NahG (express *nahG* gene, that encodes SA hydrosylase which convert SA to catechol), 1-2 (*SABP2* silenced) were used. Three leaf disc samples were collected from each plant using a cork borer (size 4).

Expression of *SBIP-428* in Tobacco upon TMV Infection

Six-week-old wild type tobacco plant *Nicotiana tabacum* cv. Xanthi nc (NN) were infected with tobacco mosaic virus (TMV) with a 10^{-3} dilution of 45 $\mu\text{g/ml}$ viral concentration. Carborundum was dusted evenly to the upper surface of the leaves, and TMV diluted in phosphate buffer was gently rubbed on with a piece of cheesecloth. TMV infected plant was kept separate from uninfected plants. Plants were kept under light ($150 \mu\text{Mm}^{-2}\text{s}^{-1}$) and day conditions at $\sim 22^\circ\text{C}$. Three leaf discs were collected at 0, 24, 48, and 72 hpi (hours post inoculation) from

the inoculated leaves of XNN plants. Samples were frozen in liquid nitrogen and stored at -80°C until ready for total RNA isolation.

Complementation Experiment

SIR2 Mutants of *Arabidopsis thaliana*. Six different T-DNA insertion lines were obtained from TAIR (arbidopsis.org). The insertionlines are SALK_131994C, SALK_139443, SALK_149295C, SALK_035541, CS370961, and CS877409. Details of T-DNA insertion lines are presented in Table 2 below.

Table 2: Details of *Arabidopsis SRT2* Mutant

Seed Lines	Back-ground	Clone Name	Insertion site	Gene names	Locus
CS370961	Col-0	pAC161	Intron	<i>Histone deacetylase</i>	AT4G38160
SALK_13944	Col-0	pROk2	Exon	<i>Histone deacetylase</i>	AT4G38160
SALK_131994C	Col-0	pROk2	Intron	<i>SIRTUIN2</i>	AT5G09230
SALK_149295C	Col-0	pROk2	Exon	<i>SIRTUIN2</i>	AT5G09230
SALK_035541	Col-0	pROk2	Intron	<i>SIRTUIN2</i>	AT5G09230
CS877409	Col-0	pDAP101	Intron	<i>SIRTUIN2</i>	AT5G09230

Confirmation of T-DNA Insertion. T-DNA insertion confirmation experiment was carried out following the protocol of the TAIR website. The brief details are as follows: 2 seeds from each seed line were sown in a 3x3 inch flat with autoclaved soil and kept for 3 days in a dark room at 4°C. Seeds were then transferred to a growth chamber with 16h day light (7000 lux). Leaf samples were collected from each mutant line to obtain the DNA and analyze T-DNA insertion.

DNA Extraction Protocol. Three to 4 leaf disks (about 3-5mg) were collected in a 1.5 ml micro-centrifuge tube and weighed. 200µl of Extraction buffer {10 fold dilution of Edward's

solution (200 mM Tris-HCl, pH 7.5, 250 mM NaCl, 25 mM EDTA, 0.5% SDS) in TE buffer (10 mM Tris-HCl, pH 8.0)} was added and homogenized using a hand held tissue grinder. Samples were centrifuged at 14000rpm for 5min at room temperature. Supernatant was collected as a DNA sample. Collected extract (1 µl) was used in total 20 µl of PCR reaction to analyze T-DNA insertion. Primers details of the seed lines are in the Table 3 below.

Table 3: Primer Details of *Arabidopsis SRT2* Mutants

Name of Primers	Sequences
CS370961-LP	GCACTTCTTAGCGTGATGGAG
CS370961-RP	CTTGCCTAGTGCCTACTGCTG
CS877409-LP	TAAGGCCCTCTCTGAGCTTTC
CS877409-RP	GTTATGTGCTTAGAGTGCGGC
SALK_131994C-LP	ATGATCCGGACATTGTGCTAG
SALK_131994C-RP	ATCAGGTGATCTGAAGGCAAG
SALK_149295C-LP	CGCAGAGAGAGAACAAAATCG
SALK_149295C-RP	TTCCACATTCTGTGCTAACCC
SALK_035541-LP	GTTATGTGCTTAGAGTGCGGC
SALK_035541-RP	CAACACCATGTTCTGCAAGTG
SALK_139443-LP	ACTCTTCTCCTTGTCTGCGTG
SALK_139443-RP	ACCAGACAATGAATCAGCACC

Confirmation of Mutant. RT-PCR was used to determine the SIR2 mutant out of these *Arabidopsis* seed lines. Primers were made using the Primer3 software (<http://www.bioinformatics.nl/cgi-bin/primer3plus/primer3plus.cgi/>) to analyze the mutant and listed in Table 4 below.

Table 4: Primer Details of *Arabidopsis SRT2* and *Histone Deacetylase*

Gene Names	Forward Primer	Reverse Primer	Product Size
<i>ATSRT2</i>	TGGGAGCGATCCACTTGAAT	GCATCGCTCTGTTTTGCAAC	354
<i>ATSRT2</i>	GAGTTACGCTGGATGGAGGA	TCAGGCCTTTGTTTCATGCC	324
<i>Histone Deacetylase</i>	TGGAGTGGAGGAGGCATTTT	CCAAGAGCAGTAGGGGAACA	353
<i>Histone Deacetylase</i>	TGTTCCCCTACTGCTCTTGG	GGTACACTTGGAGCATGCTG	265

Growth Phenotype Analysis of Mutant

Arabidopsis SRT2 mutant (SALK_131994C) and *Arabidopsis* wild type (Col-0) were used to analyze the growth phenotype. Fifty seeds were grown from each line to compare the growth phenotype of mutant. Germination rate, number of leaves, leaves size, number of flower, height of flower bolds were measured to compare the growth phenotype of *SRT2* mutant and Col-0. Seeds were sown in autoclaved soil and then kept 4°C in dark and for 3 days before transfer to growth chamber with 700 to 800 $\mu\text{E}/\text{m}^2/\text{sec}$ light at 16 h day period. Germination rate was determined after 7 days of sowing seeds. The number of leaves in each plant was counted, and the length of the leaves was measured after 21 days of germination. Number of flower and height of flower bold were measured between 30 to 35 days.

Bacterial Growth Assay

A recently developed flood-inoculation technique with minor modification described by Ishiga et al. (2011) was used for bacterial pathogenesis assay. Briefly, *Arabidopsis* seeds were surface sterilized by incubating in 70% ethanol for 5min in a microcentrifuge tube followed by 20% (v/v) commercial bleach containing 0.1% Tween 20. Seeds were washed at least 5 times

with sterile milli-Q water. Five seeds were then germinated in half strength MS medium containing Gamborg vitamins solidified with 0.8% Phyto-agar in Petri plates (100 mm X 15 mm). Plates were incubated overnight to remove extra moisture. Seeds were transferred to the MS plates and kept in dark for 2 days at 4°C. Plates with seeds were then transferred to tissue culture room with light intensity of 150-200 $\mu\text{E}/\text{m}^2/\text{sec}$ at 24°C and a 16 hr light period. Two weeks postgerminated seedlings were used for pathogen assay.

Pseudomonas syringae pv. tomato DC3000, and *Pst* DC3000 *AvrRpt2* stains were used for pathogen assay. Bacterial stains were grown in King's B medium containing rifampicin (50 $\mu\text{g}/\text{ml}$) and kanamycin (25 $\mu\text{g}/\text{ml}$) for overnight. Bacteria were suspended in sterile milli-Q water and OD was measured at 600 nm. Two different concentrations (1×10^8 and 5×10^6 CFU) were used for this experiment. Bacterial suspension (40 ml) was added to 2 weeks old postgerminated seedlings and kept in room temperature for 2-3 min. Bacterial suspension was removed by decantation and then plates were sealed with 3 M Micropore 2.5 cm surgical tape. Plates were transferred in growth chamber with a light intensity of 150-200 $\mu\text{E}/\text{m}^2/\text{sec}$ at 24°C with 16h day period. Internal bacterial population was measured at 4dpi. Leaves were collected weight was recorded for each sample. Then leaves were surface sterilized with 3% H_2O_2 for 3min. Samples were then washed with sterile milli-Q water at least 4 times. Washed samples were homogenized in sterile mili-Q water and diluted samples were plated onto King's B medium containing rifampicin (100 $\mu\text{g}/\text{ml}$) and kanamycin (50 $\mu\text{g}/\text{ml}$). Bacterial colony forming units were counted after 2 days using proper diluted samples.

Protocols for RT-PCR (Reverse Transcriptase Polymerase Chain Reaction) and Western Blot

Isolation of Total RNA for Leaves

Leaf discs were ground using a pestle in liquid nitrogen. To the powdered leaf, 1ml of Tri-reagent (Sigma) was added, mixed gently, and incubated for 5 min at room temperature. To the extract, 200 μ l of chloroform was added and mixed by inverting several times. Samples were incubated at room temperature for 3 min. The sample was then centrifuged at 12000 x g for 15 min at 4°C. The aqueous phase was transferred to a new tube, and 0.5ml isopropanol was added. The samples were mixed by inverting several times and incubated for 10min at room temperature. The sample was then centrifuged at 12000 x g for 10 min at 4°C. The supernatant was discarded, and the pellet was collected for further processing. Ice cold 75% ethanol (1ml) was added to the pellet. The sample was gently mixed and centrifuged at 7500 x g for 5 min at 4°C. The supernatant was discarded, and the pellet was air dried for 10-20min. The pellet was then suspended in 43 μ l of 0.1% depc treated water. For DNase treatment, 5 μ l of DNase buffer and 2 μ l of DNase (Promega) was added to the resuspended RNA and incubated at 37°C for 20 min. To remove DNase, the sample was treated with TRI-reagent, chloroform, isopropanol, and chloroform with half of the volume as described above. The pellet was collected after the last step and air-dried for 10-20 min. The air-dried sample was suspended in depc treated water and heated at 55°C for 5-10 min to make sure the pellet was well dissolved in the depc treated water. RNA concentration (ng/ μ l) was measured by using nanodrop spectrophotometer (NanoDrop Technologies ND-1000) at 260 nm. The concentration was maintained at 1 μ g/8 μ l for cDNA synthesis.

cDNA Synthesis

Reverse transcriptase enzyme (Promega) was used to synthesize first strand

complementary DNA (cDNA) from the isolated total RNA. In the first step, 2 μ l of oligo-dT (0.5 μ g/ml) was added to 8 μ l (1 μ g) of total RNA and incubated at 75°C for 10 min in the thermocycler (Effendorf). The sample was then cooled down to 4°C and a 10 μ l mix (1 μ l reverse transcriptase (RT) (MMLV), 4 μ l 5X RT buffer, 1 μ l RNAsin (RNAase inhibitor), 1 μ l 10 mM DNTP, and 3 μ l DEPC treated water) was added to the sample. The sample was vortexed briefly and incubated at 42°C for 60 min and then at 70°C for 10min in the thermocycler. The sample was stored at -20°C for further analysis.

Reverse Transcriptase-Polymerase Chain Reaction (RT-PCR)

The cDNA sample was used to analyze gene expressions. Total 10 μ l of PCR mix was used to amplify each gene. The PCR mix contained 6 μ l depc treated water, 1 μ l 10 X dNTP, 1 μ l 10 X Taq polymerase buffer, 0.2 μ l Taq polymerase, 0.4 μ l of 10 μ M forward primer, 0.4 μ l 10 μ M reverse primer, and 1 μ l of cDNA sample.

Agarose Gel Electrophoresis

Agarose gel electrophoresis was used to analyze the genes using the PCR product. Agarose gel (0.8% to 1.2%) was used according to gene size. Agarose was added to the 1xTAE buffer (40 mM Tris base, 40 mM Acetic Acid, 1 mM EDTA) then heated, and ethidium bromide (10 mg/ml) was added (1 μ l/20ml) before pouring into a gel tray.

SDS-PAGE

Laemmli's protocol (Laemmli, 1970) was followed to perform SDS-PAGE. Unless stated otherwise, each sample was mixed with equal volume 2X SDS sample buffer containing β -ME, boiled for 5minutes, and centrifuged at 13000 rpm for 10minutes at room temperature. Protein separation on SDS-PAGE was performed at 15 mA for one gel or 25 mA for 2 gel at 200

V for 80 to 90 minutes. The buffer composition used is described in the Appendix B.

Western Blot Analysis for SABP2 and His-Tagged Protein

The Western analysis was performed using standard protocol after the electrophoresis gels were incubated in transfer buffer (25 mM Tris, 192 mM Glycine, 10% methanol) for a few minutes (Towbin et al. 1979). Prior to transferring proteins from gel to PVDF membrane, the PVDF membranes were soaked in 100% methanol for 15 seconds following a rinse with milliQ water for 2 minutes and incubated in transfer buffer for 10 minutes. The gel and PVDF membranes were sandwiched between presoaked sponges and Whatman 3mm Chr papers, protein transfers were carried out at a constant 100 V for 1 hour at 4°C. After transfer, the membranes were placed in 100% methanol for 10 seconds and were let dry on Whatman paper. Membranes were soaked again in 100% methanol again for 10seconds and then stained with Ponceau-S and photographed to verify the transfer of proteins. Membranes were washed with PBS buffer until the stains were gone and then probed with rabbit polyclonal SABP2 primary antibody (1:1000) or mouse monoclonal anti PolyHistidine primary antibody (1:3000) in 5ml of blocking buffer (3% BSA, 1% milk in 1 x PBS) overnight at 4°C on a shaker. The blots were washed 3 times for 5 minutes each with 1x PBS, 1x PBST with 3% tween 20, and 1x PBS sequentially. The blot was then probed in either antirabbit secondary antibody or antimouse IgG peroxidase secondary antibody diluted at 1:10000 for 1hour at room temperature and washed sequentially as described earlier. The signals on membranes were developed with ECL substrate (Thermo Scientific) for 1 minute, and protein expression was analyzed by using X-ray films as described by the manufacturer.

Western Blot Analysis for Lysine Acetylated Proteins

Proteins were transferred from gel to PVDF membrane as described above. PVDF

membrane was then subjected to a blocking buffer for 30 minutes at room temperature. PVDF membrane was then washed with PBS and PBST (PBS with 0.5% Tween 20) 2 times each. The blot was then probed in Anti-lysine Antibody diluted in PBST for 16 to 18 hours at 4°C. The blot was then thrice washed with PBST for 5 minutes. Secondary antibody (antirabbit) was added to the blot and kept for 2 hours at room temperature. The signals on membranes were developed with ECL substrate (Thermo Scientific) for 5 minutes, and protein expression was analyzed by using X-ray films as described by the manufacturer.

Spin Column

Syringe (1 ml) was used as column. Fiber glass was added to the bottom of 1 ml syringe and then filled with Sephadex G 25 in citrate buffer (20 mM sodium citrate pH 6.5, 1 mM EDTA, and 5 mM MgSO₄). Column was placed inside 15ml falcon tube and centrifuged with 2000 rpm for 4 min at 4°C using Sorvall RT6000 refrigerated centrifuge and repeated same step until the column was packed with Sephadex G 25. Once column was packed 150 µl of buffer (appropriate to the protein) was added and centrifuged with same condition at least 3 times. Column was ready once 150 µl of buffer was coming out as flow through. Autoclaved 1.5ml microtube was used to collect the desalted protein sample.

CHAPTER 3

RESULTS

Section I: Biochemical Characterization of SBIP-428

Bioinformatics Analysis of SBIP-428

DNA and Corresponding Amino Acid Sequences of SBIP-428. In a yeast 2 hybrid (Y2H) screening using SABP2 as a bait, several positive interactors were detected. SBIP-428 was one of the SABP2 interactors. SBIP-428 was then sequenced and analyzed through BLAST search using Sol genomics network database hosting gene sequences of solanaceae plants (Figure 3). SBIP-428 showed homology to n transcriptional regulator Sir2 family protein.

```
ATGGTTCCTTATTTCGGATCCCCCTAGCATGAAAGATGTGGACAGTTTGTATGAATTCTTTGACAGGAGTACCAAGCT
TGTTGTATTGACGGGAGCTGGCATGAGCACAGAGAGTGGGAATTCGGACTACAGGAGCCCGAATGGAGCTTATAGTA
CTGGTTTCAAACCAATTACCCATCAGGAGTTTCTCAGATCAGTCAAGGCTCGAAGGCGTTATTGGGCACGGAGTTAT
GCTGGCTGGAGACGTTTCACTGCTGCTCAACCTAGTACAGGTCATATAGCTCTATCATCTCTTGAGAAAGCAGGCCA
TATAAGTTTTATGATTACACAGAATGTGGACAGGCTGCATCATCGGGCTGGCAGCAGCCCACTTGAATTGCATGGGA
CTGTCTACATTGTGCGCTGTACAAATTGTGGTTTTACTCTACCTCGAGAACTGTTTCAAGATCAAGTGAAGGCTCAT
AATCCCAAGTGGGCAGCAGCTGTGCGAAAGTTTGGATTATGACAGCCGATCAGACGAGAGCTTTGGTATGAAGCAAAG
GCCTGATGGGGATATTGAGATCGATGAGAAATTCTGGGAGGAGGATTTCTACATTCTGATTGTGAGAGGTGCCAAG
GAGTTCTCAAACCTGACGTTGTCTTCTTTGGGGATAATGTCCCTAAAGCTAGAGCTGATGTTGCCATGGAAGCTGCA
AAGGGATGTGATGCCTTCTTGTACTTGGTTCATCTATGATGACCATGTCTGCTTTCCGGCTTATCAAAGCTGCGCA
CGAGGCAGGCGCTGCGACTGCAATTGTAATATTGGGGTGACACGAGCTGACGATCTTGTACCTTTGAAAATTAATG
CTCGAGTTGGAGAGATACTTCCAAGATTGCTTAATGTTGGATCCTTGAGTATCCCTGCTCTCTAG
```

Figure 3: SBIP-428 DNA Sequence Obtained From Y2H

The sequenced DNA was translated using ExPASy Translate tool

(<http://web.expasy.org/translate/>) to obtain corresponding amino acid sequence (Figure 4).

```
MVPYSDPPSMKDVDSLIEFFDRSTKLVVLTGAGMSTESGIPDYRSPNGAYSTGFKPITHQEFLRSVKARRRYWARSY
AGWRRFTAQPSTGHIALSSLEKAGHISFMITQNVDRLLHHRAGSSPLELHGTVYIVACTNCGFTLPRELFQDQVKAH
NPKWAAAVESLDYDSRSDSEFGMKQRPDGDIEIDEKFWEEEDFYIPDCERCQGVLPDVFVFFGDVNPVKARADVAMEAA
KGCDAFLVLGSSMMTMSAFRLIKAAHEAGAATAIVNIGVTRADDLVPLKINARVGEILPRLNVLGSLSPAL
```

Figure 4: Corresponding Amino Acid Sequence of SBIP-428 Translated Using ExPASy

Bioinformatics Tool.

ExPASy ProtParam tool website was used to predict some other features of SBIP-428.

Based on the analysis, the estimated molecular weight of SBIP-428 is 33470.0 Daltons and theoretical pI of 6.25.

Putative Conserved Domains of SBIP-428. Obtained amino acid sequence was then analyzed in “NCBI Standard Protein BLAST” to identify the putative conserved domains using “Non-redundant protein sequence” database. The BLAST results showed that it has a similarity with SIR2 superfamily and specific hits to SIRT4 NAD-dependent deacetylase (Figure 5). It also predicted substrate binding site, NAD⁺ binding site, and Zn binding site. Internal residues involved in substrate binding site are alanine (101, 227, and 258), arginine (223), aspartic acid (225), valine (226), methionine (228), glutamic acid (229), cysteine (135), histidine (256), and glutamic acid (257). Internal residues involved in NAD⁺ binding site are phenylalanine (20), arginine (22), serine (23), threonine (30), glutamine (31), arginine (81), glutamic acid (81), lysine (82), glycine (84), cysteine (135), phenylalanine (214), lysine (279), glutamic acid (257), and isoleucine (280). Internal residues for Zn binding site are proline (143), leucine (146), aspartic acid (211), and phenylalanine (214).

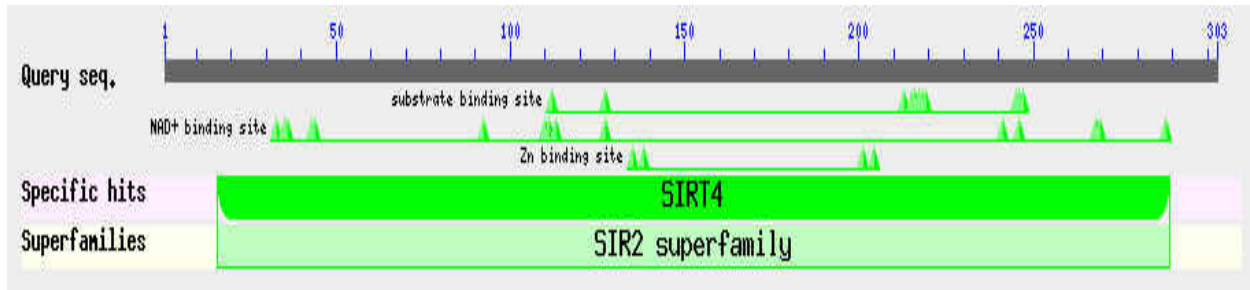


Figure 5: Protein BLAST of SBIP-428. Picture shows the substrate, NAD⁺, and Zn binding sites of SBIP-428 and the putative superfamily protein.

Sequence Alignment with Sirtuin 2 *Arabidopsis thaliana* (AT5G09230) and Human SIR2. ExPASy Bioinformatics Resource Portal ClustalW (<http://embnet.vital-it.ch/software/ClustalW.html>) sequence alignment tool was used to determine the similarities between SBIP-428, SIR2 (*Homo sapiens*) and *Arabidopsis thaliana* SRT2 (AtSRT2). Sequence alignment showed 77% identity with *Arabidopsis thaliana* (locus AT5G09230) and only 29% with human SIR2 (Figure 6).



Figure 6: Sequence Alignment of SBIP-428, AtSRT2, and Human SIR2. Star at the bottom of alignment shows the identity; dot shows conserved substitution; colon shows semiconserved substitution between 2 proteins; and the gaps showing the dissimilarities between them.

Protein Model of SBIP-428. Putative protein model has been created by using the (PS)²: Protein Structure Prediction Server (<http://ps2.life.nctu.edu.tw/>). Protein models were created to analyze the structural similarity between SBIP-428, AtSRT2, and crystallized mammalian SIR2 deacetylase. Human SIR2 was used as template to generate SBIP-428 and AtSRT2 protein models. SIR2 deacetylase crystallized structure was obtained from Protein Data Base (PDB) (Yamagata et al. 2014). Comparison between SBIP-428 and AtSRT2 reveals that there are same number of alpha helices and beta sheets in the 3D structure but folding structure is different from

each other (Figure 7). However, SBIP-428 did not show structural similarities because it has only 29% of identity with the template (Figure 8).

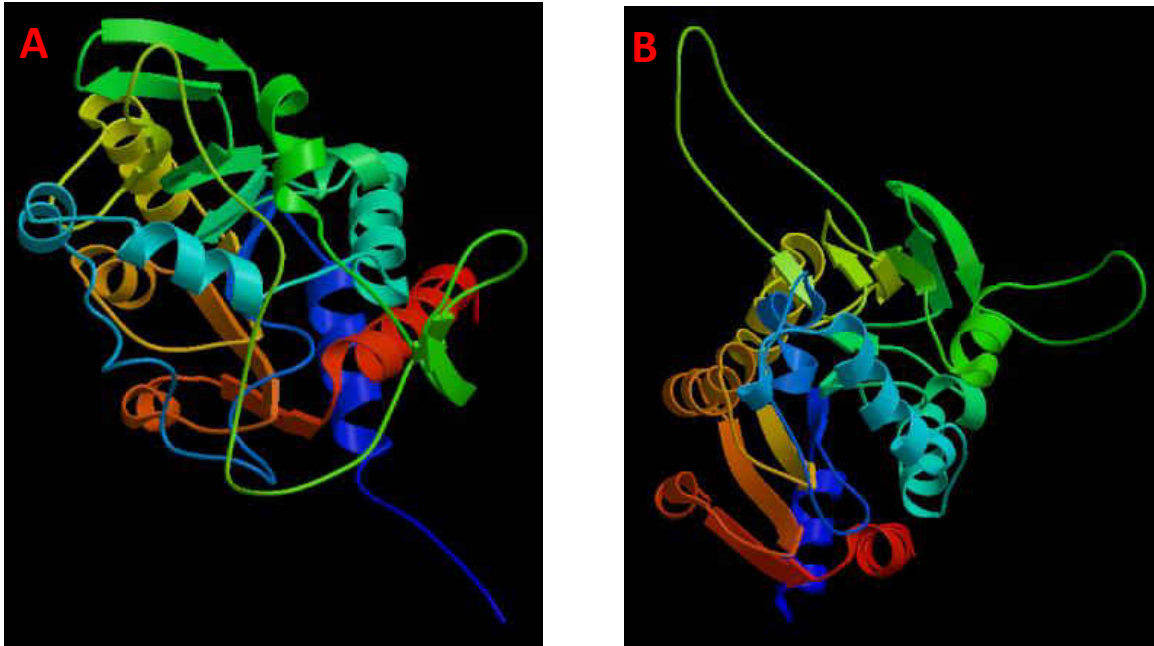


Figure 7: Protein Model of SBIP-428 and AtSRT2. Predicted 3D structures were designed by using MODELLELER 9.13 software. A. 3D structure of SBIP-428 and B. 3D structure of AtSRT2.

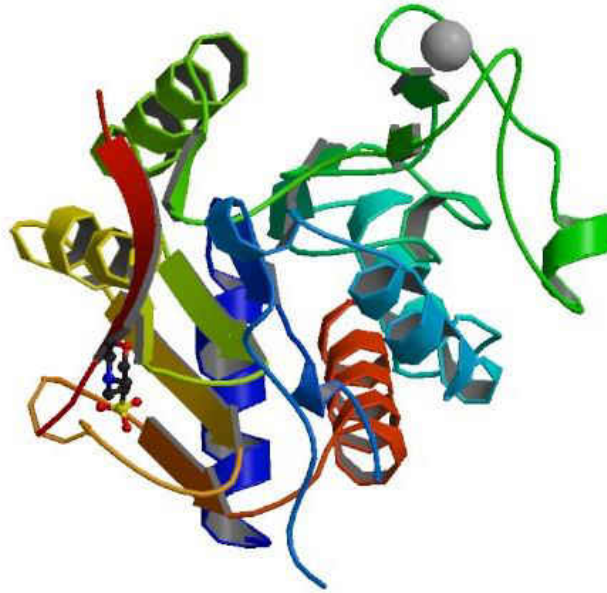


Figure 8: Protein Model of SIR2 Deacetylase. SIR2 deacetylase 3D structure (146346.36) was documented in Protein Data Base (PDB) (Yamagata et al. 2014).

Subcellular Localization Prediction of SBIP-428. There are several prediction sites that were used to determine the putative subcellular localization of SBIP-428. Protein Prowler (http://bioinf.scmb.uq.edu.au/pprowler_webapp_1-2/) and MultiLoc (<http://abi.inf.uni-tuebingen.de/Services/MultiLoc/>) predicted subcellular localization of SBIP-428 in peroxisome whereas BaCellLo (<http://gpcr.biocomp.unibo.it/bacello/pred.htm>) predicted in nucleus (Figure 9). Same prediction sites were used to find putative subcellular localization for AtSRT2. Same results came out from the predicted sites (data not shown).

A

Sequence	PProwler				PTS1Prowler
	SP	MTP	CTP	OTHER	Peroxisome
SBIP-428 [Graph] [Details]	0.04	0.12	0.00	0.84	0.00

B

origin = plant
predictor = MultiLoc

ID	Predicted Location	Score
SBIP-428	peroxisomal	0.57

C

Predictor chosen: **Plants**

Name of the sequence:	Localization:	Localization Steps:
SBIP-428	Nucleus	(Intracellular -> Nucleus or Cytoplasm -> Nucleus)

Figure 9: Predicted Subcellular Localization of SBIP-428. A. prediction using Protein Prowler; B. prediction using MultiLoc; C. prediction using BaCelLo.

Expression and Purification of SBIP-428

Purification of reSBIP-428 Using Ni-NTA Chromatography Expressed in *E. coli*.

Recombinant SBIP-428 (6X his tagged) was expressed in *E. coli* and purified using Ni-NTA affinity chromatography. SDS-PAGE and western blot analysis was performed to confirm the purification of rSBIP-428. Samples were mixed with 2X SDS sample buffer, boiled for 5 min, and centrifuged at 13,000 rpm for 2 min prior to load on gel. SBIP-428 was eluted in fraction #4-11. Most of the other proteins except SBIP-428 did not bind and were removed in wash (lane 3) (Figure 10). Fraction # 3-11 contain highest amount SBIP-428 that was detected by western blot using the monoclonal Anti-polyHistidine antibody (Figure 10B).

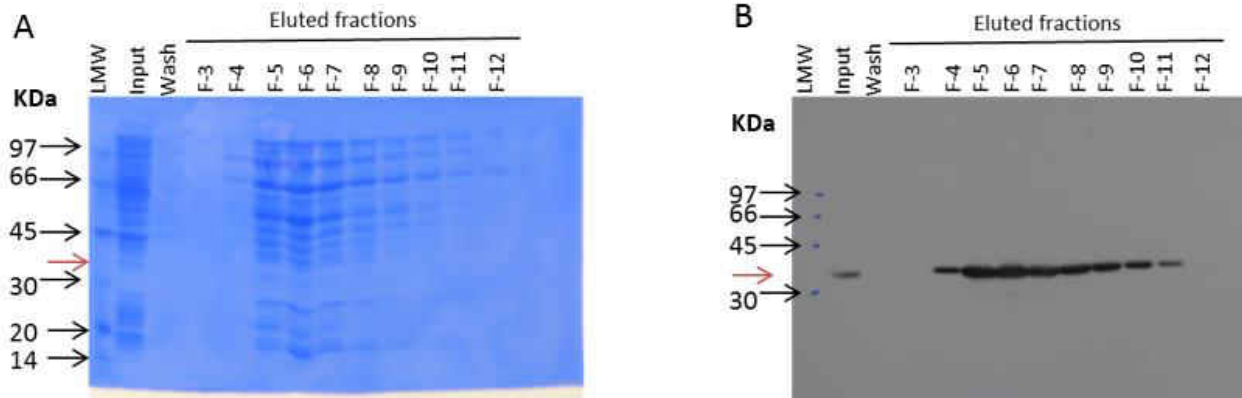


Figure 10: Purification of SBIP-428 Using Ni-NTA Affinity Column. A. SDS-PAGE gel electrophoresis with eluted fractions (F-3 to F-12) and B. Western-blot analysis of purified rSBIP-428. LMW (low molecular weight) protein marker, input, and wash are presented in first 3 lanes in both pictures. Arrow shows the position of recombinant SBIP-428.

Purification of SBIP-428 Using Mono-Q Ion Exchange Chromatography. Ni-NTA purified fractions (#4-11) containing SBIP-428 were pooled and further purified on a Mono Q column. In Mono Q column most proteins eluted as a sharp peak which was collected as fractions #5-18 (Figure 11). The eluted fractions were analyzed by SDS-PAGE and Western blot. SBIP-428 was detected in the fraction #13-16 (Figure 12B).

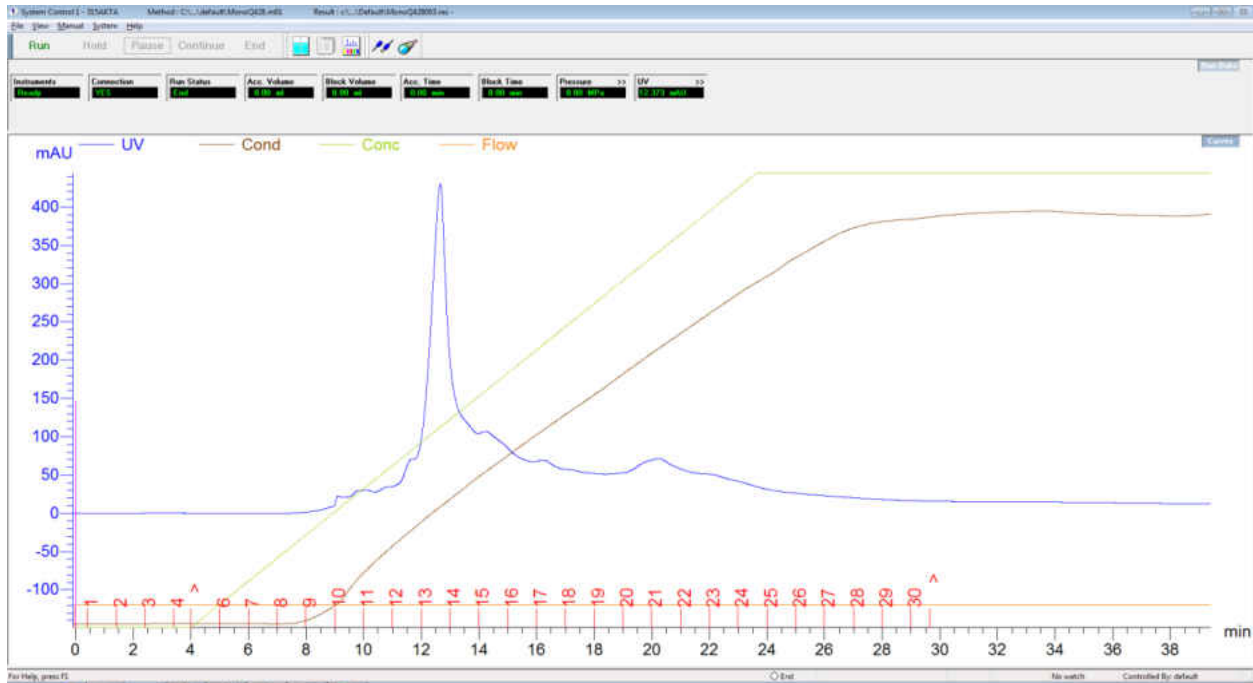


Figure 11: Chromatography Profile of Protein in Mono Q Column. (Blue Line) absorbance of protein at 280nm; (Blue Line) salt conductivity; (brown Line) collected fraction (0.5ml). Fractions #7-16 were used for gel and Western blot analysis.

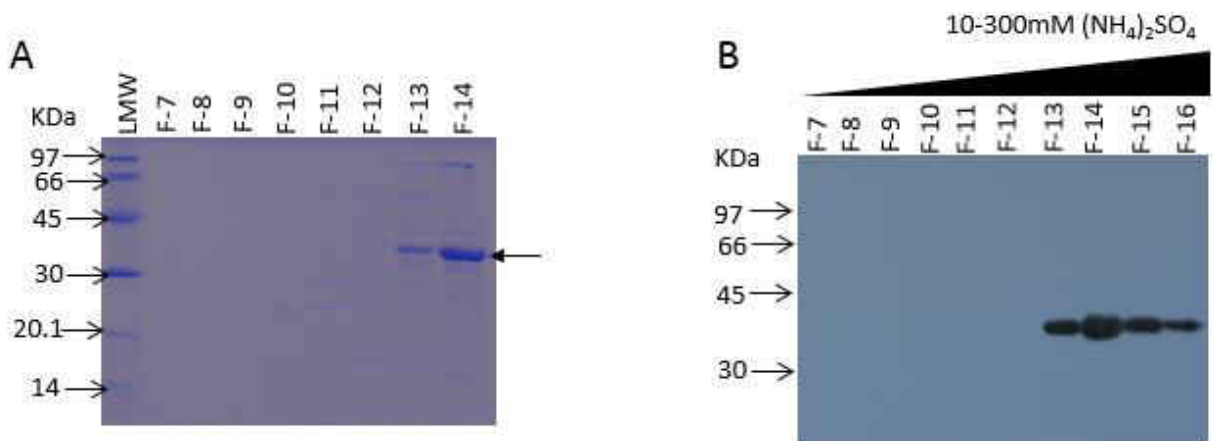


Figure 12: Purification of SBIP-428 in Mono Q Column. Picture A is protein profile of Mono Q eluted fraction #7-14 in SDS-PAGE (coomassie stain); (LMW) low molecular weight marker. (B) SBIP-428 was detected in fractions #13-16 by Monoclonal Anti-PolyHistidine antibody.

Dialysis of Proteins in Deacetylase Buffer. Mono Q purified SBIP-428 fractions were dialyzed against deacetylase enzyme buffer (50 mM Hepes pH 7.6, 350 mM NaCl, and 20% glycerol). Purified SBIP-428 was pooled together and dialyzed against 500ml deacetylase buffer with slow stirring at 4°C. Buffer was changed every 8 hours for a total of 3 changes. Dialyzed protein was analyzed by SDS-PAGE and detected using the monoclonal anti-polyHistidine antibodies (Figure 13). Dialyzed proteins were aliquoted stored at -80°C until further use.

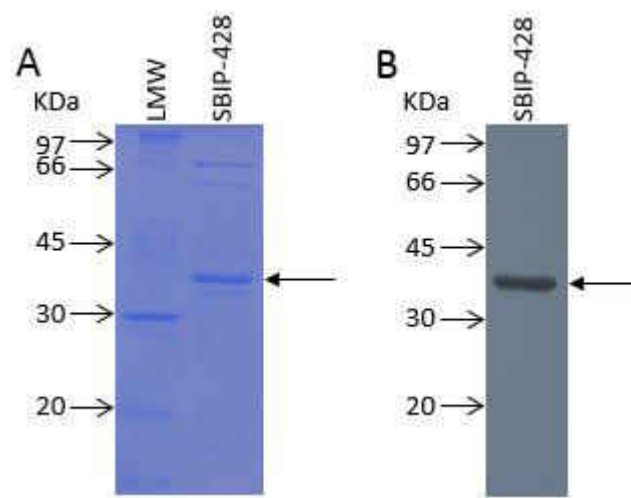


Figure 13: Dialyzed SBIP-428 After Mono-Q Purification. A. 12.5% SDS-PAGE (Coomassie stained) gel picture; B. Western blot analysis with Monoclonal Anti-PolyHistidine antibody. Arrow shows the position of recombinant SBIP-428.

Deacetylase Enzyme Activity of SBIP-428

Deacetylase Activity Using Total Leaf Protein as Substrate. In order to determine the deacetylase activity of SBIP-428, mono-Q purified SBIP-428 was used and total proteins from the leaves of tobacco plant (XNN) were used as the substrate. Western blot was performed to determine the deacetylase activity of SBIP-428. Acetylated Lysine Antibody was used to detect the deacetylation of acetylated tobacco proteins by SBIP-428. Lane #9 was used as positive control with only substrate proteins and lane #7 was used as negative control with substrate proteins and buffer. Lane's #1, #3, and #5 contained both enzyme and substrate proteins; #2, #4, and #6 contained only SBIP-428 and the buffer. There was no significant difference between the enzyme treated samples (#1, 3, and 5) and buffer treated controls (#7) (Figure 14B). Experiment was performed at least 4 times with similar results

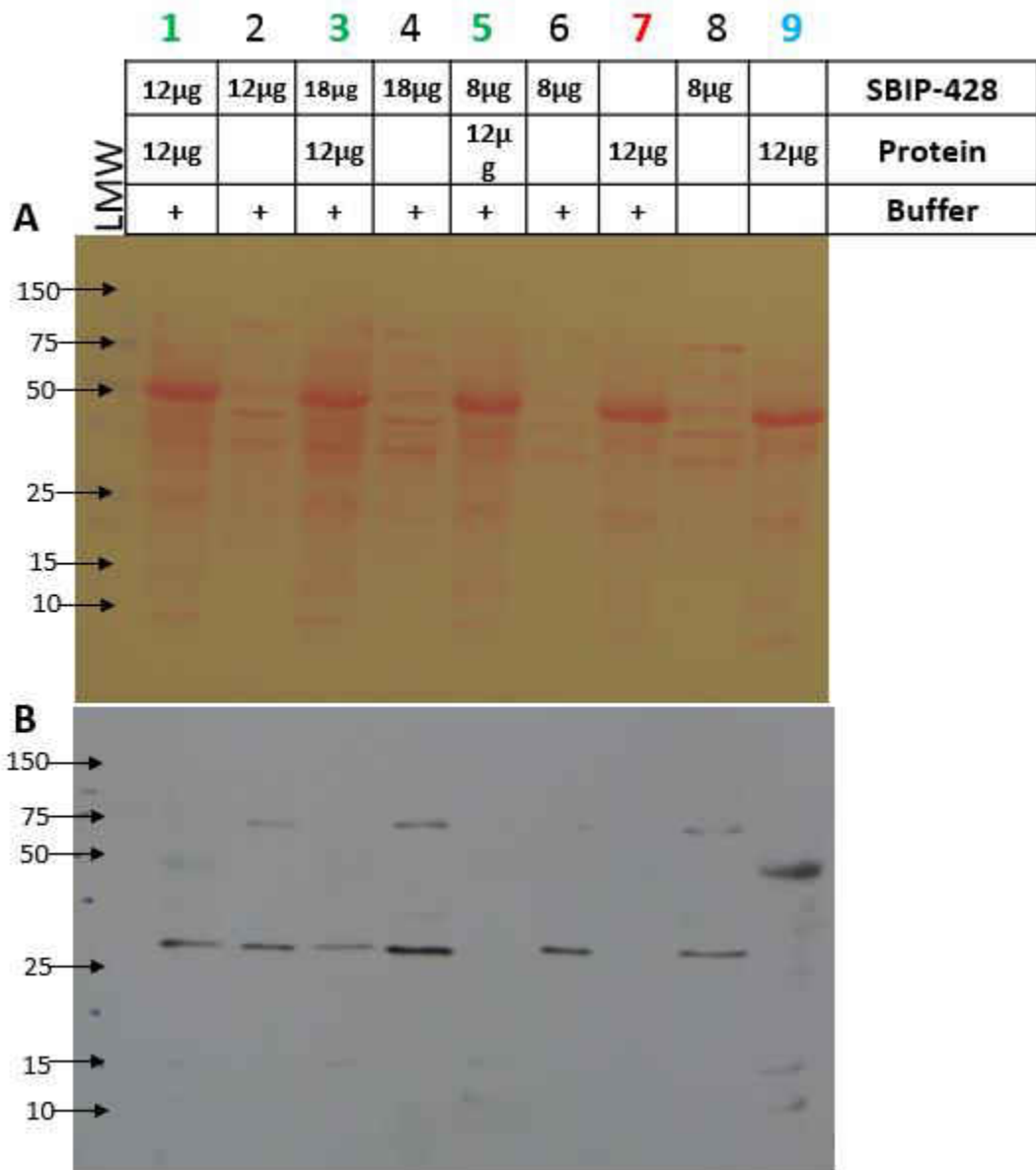


Figure 14: Deacetylase Activity Assay of SBIP-428; A. Ponceau stained blot, and B. Western blot analysis using Acetylated Lysine Antibody. Pre-stained Marker (PSM) was used as marker proteins. Combination and concentration of substrate (Protein), enzyme (SBIP-428), and buffer are presented at the top.

Deacetylase Enzyme Assay Using SIRT Glo™ Assay Kit. Mono-Q purified SBIP-428 (1 µg, 2 µg, 4 µg, and 8 µg) was used to determine the deacetylase activity using SIRT Glo™ assay kit (Promega). SBIP-428 was expressed, purified, and quantified for this experiment. Deacetylase activity was determined as described in the manufacturer’s protocol. An artificial lysine-acetylated peptide of p53 was used as substrate in luminescence based assay. Free aminoluciferin was measured by Ultra-Glo firefly luciferase reaction that produce a persistent, stable emission of light. SBIP-428 was able to deacetylate the acetylated p53 peptide in linear concentration-dependent manner that indicates that SBIP-428 can act as SIRTUIN-type deacetylase (Figure 15). SIRT Glo™ substrate solution without SBIP-428 was used as negative control in this experiment (Table 6; shown as blank). Luminescence reading was detected using plate reader (BioTek). Raw data and statistical analysis shown in Table 5.

Table 5: Luminescence Reading of SBIP-428 Deacetylase Activity and Statistical Analysis

Well ID	Name	Well	Lum	Blank	Blank Lum	Count	Mean	Std Dev	CV (%)
SPL1	8µg	A1	12086	629	11450	3	10929	558	5.1
		A2	11632	609	10996				
		A3	10977	670	10341				
SPL2	4µg	B1	5919	629	5283	3	5405	355	6.58
		B2	6441	609	5805				
		B3	5762	670	5126				
SPL3	2µg	C1	4008	629	3372	3	2774	524	18.9
		C2	3188	609	2552				
		C3	3034	670	2398				
SPL4	1µg	D1	1697	629	1061	3	1288	213	16.5
		D2	1955	609	1319				
		D3	2119	670	1483				

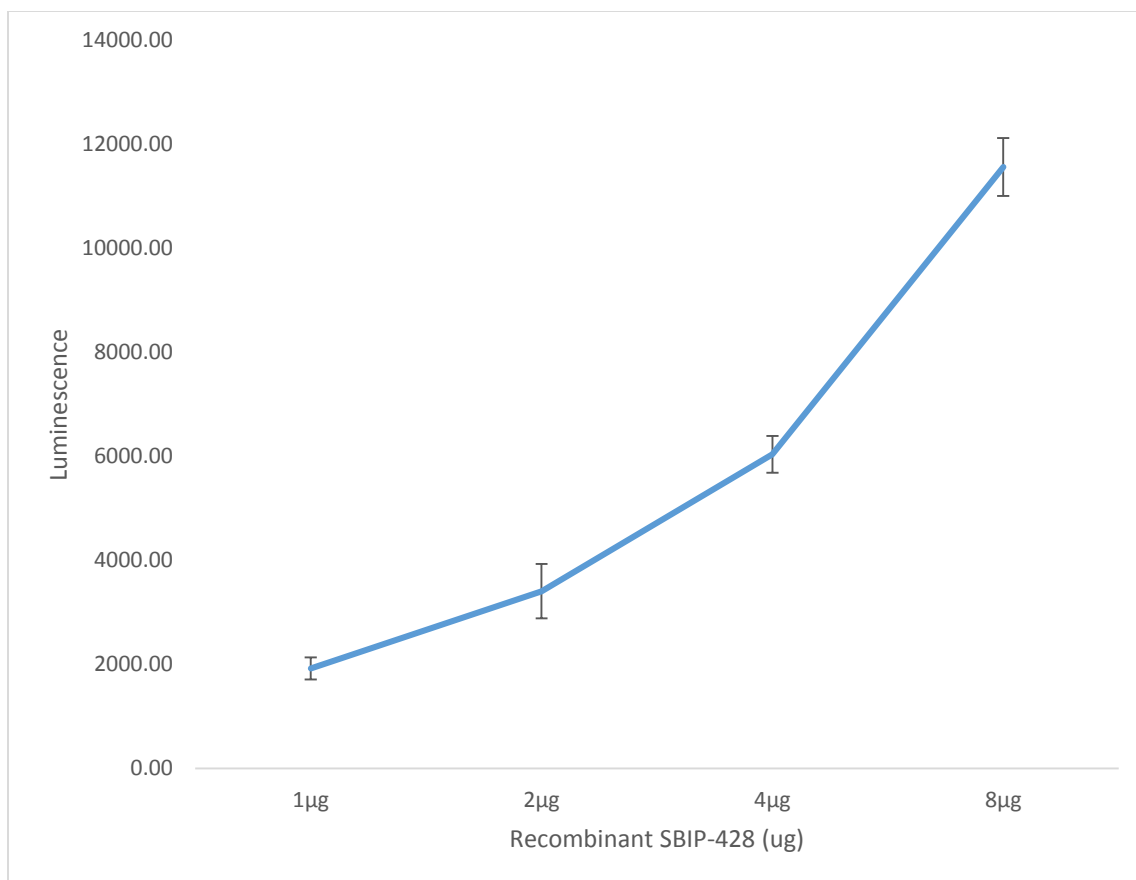


Figure 15: Determination of Linear Range of SBIP-428 Enzyme Activity. Recombinant SBIP-428 was serially diluted in 100 μ l of SIRT-Glo™ buffer and equal volume of SIRT-Glo™ solution reagent was added in 96-well plate; luminescence signal was detected after 2 hr at room temperature.

Deacetylase Enzyme Assay Using HDAC Glo™ Assay Kit. Mono-Q purified SBIP-428 (1 μ g, 2 μ g, 4 μ g, and 8 μ g) was used to determine the deacetylase activity using HDAC Glo™ assay kit (Promega). Artificial histone 4 peptide was used as substrate. Free aminoluciferin was measured by Ultra-Glo firefly luciferase reaction that produce a persistent, stable emission of light. SBIP-428 was not able to deacetylate histone 4 peptide in linear concentration-dependent manner that indicates SBIP-428 is not a histone deacetylase (Figure 16). HDAC Glo™ substrate

solution without SBIP-428 was used as negative control in this experiment (Table 6; shown as blank). Luminescence reading was detected using plate reader (BioTek). Raw data and statistical analysis are shown in Table 6

Table 6: Luminescence Reading of SBIP-428 Deacetylase Activity and Atatistical Analysis

Well ID	Name	Well	Lum	Blank	Blank Lum	Count	Mean	Std Dev
SPL1	8µg	A1	445	317	128	3	-27.33	281
		A2	396	502	-106			
		A3	362	487	-125			
SPL2	4µg	B1	295	317	-22	3	-126.33	27.15
		B2	411	502	-91			
		B3	328	487	-159			
SPL3	2µg	C1	222	317	-95	3	-90.67	68.5
		C2	361	502	-141			
		C3	344	487	-143			
SPL4	1µg	D1	497	317	180	3	-34.33	140.91
		D2	247	502	-255			
		D3	480	487	-7			

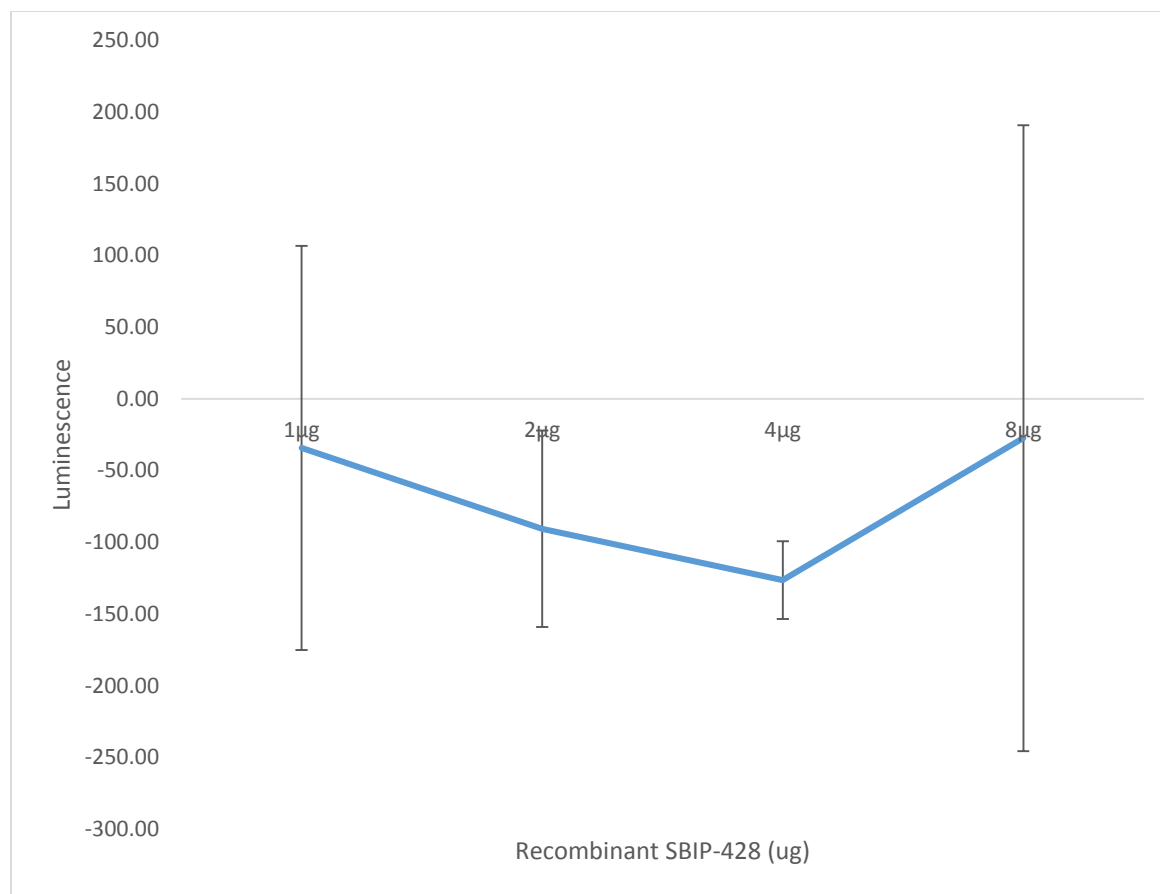


Figure 16: Determination of Linear Range of SBIP-428 Deacetylase Activity. Recombinant SBIP-428 was serially diluted in 100 µl of SIRT-Glo™ buffer and equal volume of HDAC-Glo™ solution reagent was added in 96-well plate; luminescence signal was detected after 2 hr at room temperature.

Lysine Acetylation of SBIP-428

Bioinformatics Analysis of SBIP-428 Acetylation on Internal Lysine. Prediction of Acetylation on Internal Lysine (PAIL) (<http://bdmpail.biocuckoo.org/>) was used to predict the putative internal lysine in SBIP-428 that could potentially to get acetylated. Analysis showed that there are 8 lysine residues that could get acetylated (Table 7).

Table 7: Predicted Internal Lysine Residues in SBIP-428

Peptide	Position	Score	Threshold
SDPPSMKDVDSLY	11	1.00	0.2
FFDRSTKLVVLTG	25	0.26	0.2
AYSTGFKPITHQE	55	0.80	0.2
EFLRSVKARRRYW	67	1.17	0.2
ALSSLEKAGHISF	100	0.58	0.2
DESFGMKQRPDGD	178	0.33	0.2
VAMEAAKGCDAFL	232	0.31	0.2
SAFRLIKAAHEAG	254	0.81	0.2

Acetylation Detection in SBIP-428. In order to determine the lysine acetylation of SBIP-428, mono Q purified SBIP-428 was used. Purification of SBIP-428 was determined by western blot analysis using anti-his antibodies (Figure 17). Acetylated bovine serum albumin (BSA) (Fisher Scientific) and albumin (Sigma) were used as positive control and negative control, respectively for this experiment. To determine the lysine acetylation of SBIP-428, Western blot was performed using Acetylated Lysine Antibody. SBIP-428 resulted acetylation in lysine compared with mono-Q purified SBIP-428 (Figure 18).

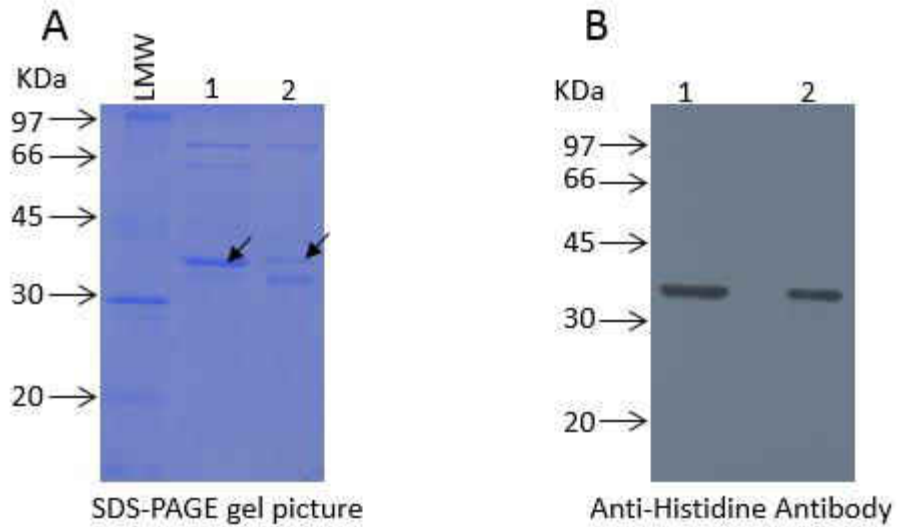


Figure 17: Western Blot Analysis of Mono Q Purified SBIP-428. A. SDS-PAGE gel electrophoresis picture (arrow indicates SBIP-428) and B. Western blot picture using Anti-Histidine antibody; Lane number 1 in the pictures represent SBIP-428 in deacetylase buffer and lane number 2 with SBIP-428 in Bicine buffer.

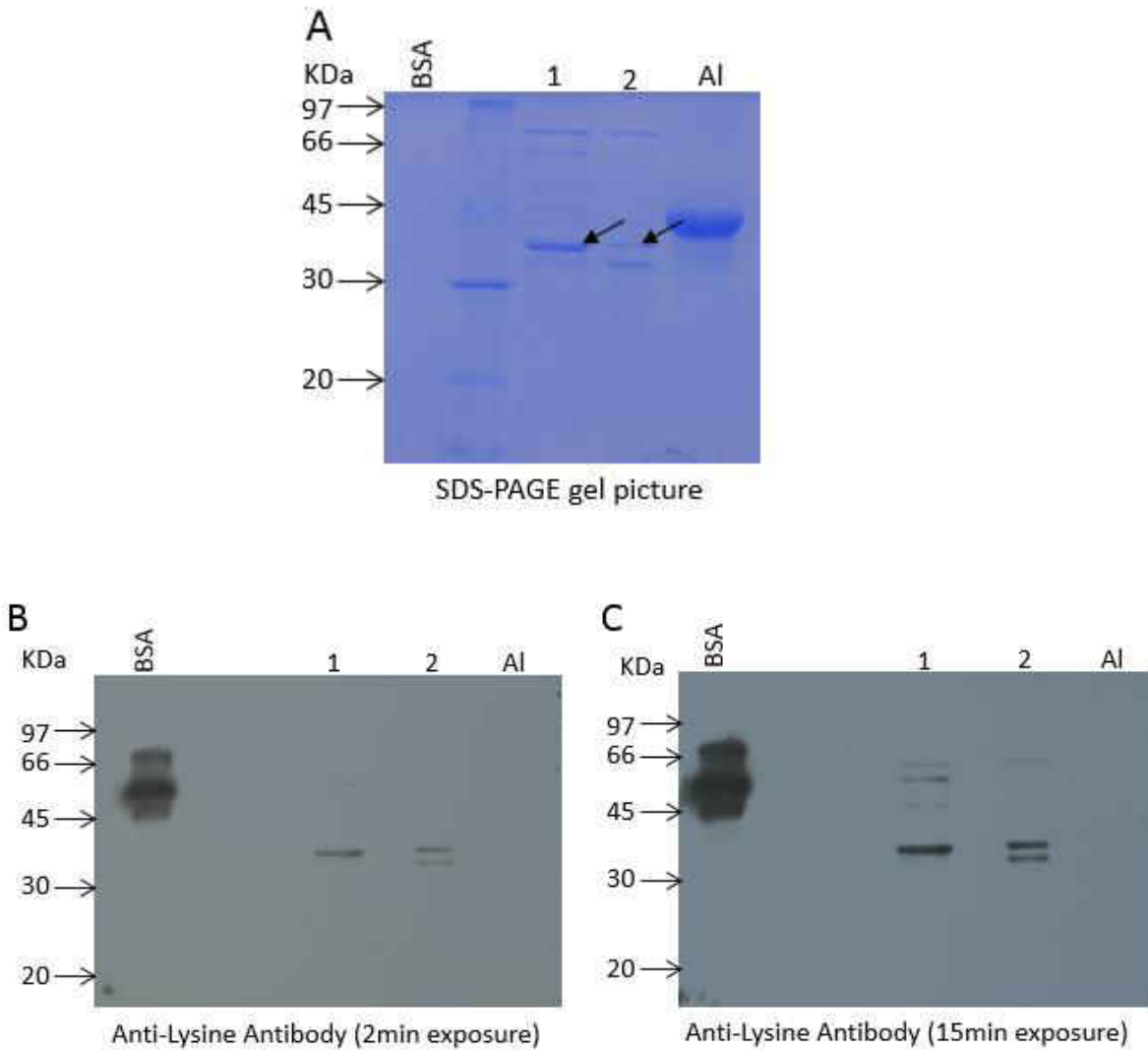


Figure 18: Acetylation of SBIP-428. Acetylated bovine serum albumin (BSA) and Albumin (Al) were loaded as positive and negative control, respectively. A SDS-PAGE gel picture (arrow indicates SBIP-428), B. 2 minutes exposure of film, and C. 15 minutes exposure of film in Western blot; Lane number 1 in the pictures represent SBIP-428 in deacetylase buffer and lane number 2 with SBIP-428 in Bicine buffer. Western blot was performed using Acetyl-Lysine Antibody to detect lysine acetylation.

Section II: Acetylation of Internal Lysine Residues of SABP2

SABP2 Acetylation

To determine the acetylation of SABP2, purified SABP2 expressed in *E. coli*, partially purified native SABP2 from tobacco leaves, and native SABP2 from tobacco leaves upon pathogen infection were used.

Bioinformatics Analysis of SABP2 Acetylation on Internal Lysine. Prediction of Acetylation on Internal Lysine (PAIL) (<http://bdmpail.biocuckoo.org/>) was used to predict the internal lysine in SABP2. Prediction result showed that there are 8 positions where lysine residues have chance to get acetylated (Table 8).

Table 8: Predicted Internal Lysine Residues in SABP2

Peptide	Position	Score	Threshold
MKEG K HFV	2	20.36	0.2
MKEG K HFVLVH	5	6.15	0.2
WSWY K LKPLLEAA	24	0.38	0.2
LEAAGH K VTALDL	33	2.15	0.2
SLSADE K VILVGH	74	0.33	0.2
SMFFGP K FLAHKL	154	0.29	0.2
PKFLAH K LYQLCS	159	1.22	0.2
EDLSKA K YFTDER	190	0.76	0.2

Acetylation of Recombinant SABP2. To determine the acetylation of recombinant SABP2, purified SABP2 was used from *E. coli*. Albumin was used as a negative control, whereas acetylated BSA was used as positive control. Recombinant SABP2 (5.25, 7, and 10 μg); egg albumin (10 and 25 μg); and acetylated BSA (0.02 μg) were used for this experiment (Figure 19A). Western blot was performed to detect the acetylated proteins. Recombinant SABP2 did not show lysine acetylation even after extended (5 min) exposure in Western blot (Figure 19B). After prolonged (30 min) exposure, nonspecific background reaction to anti-acetyl lysine antibodies were visualized (Figure 19C).

A

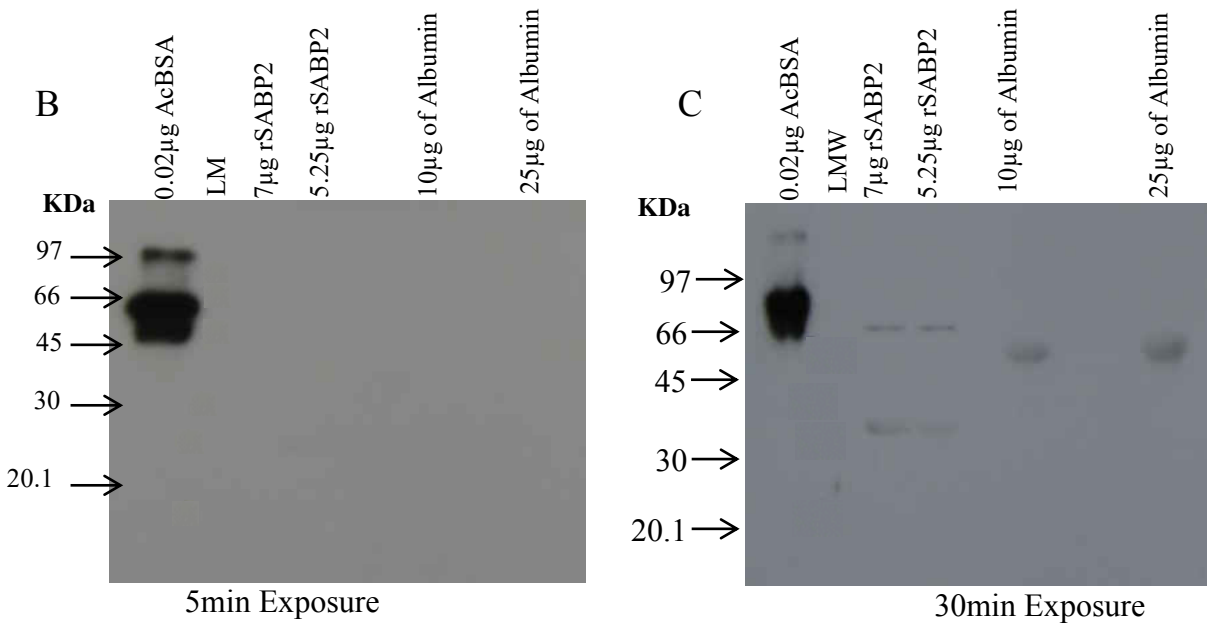
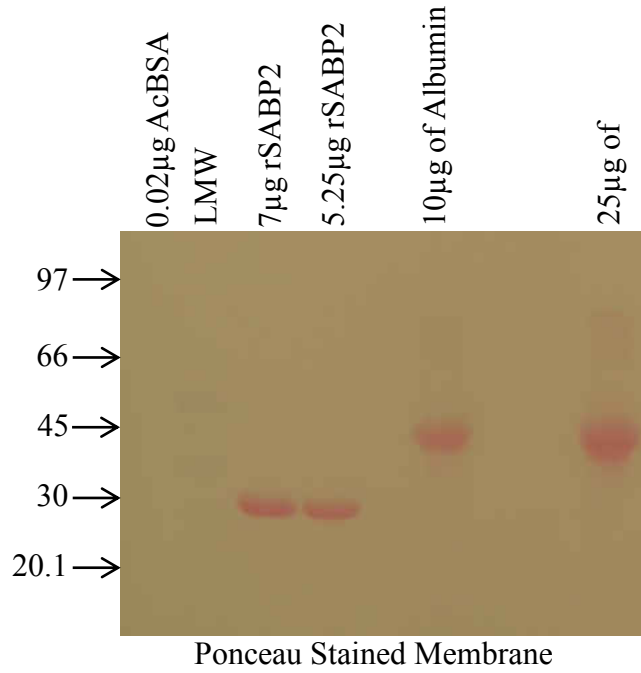


Figure 19: Acetylation of RecombinantSABP2. A. Ponceau stained of blot; B. Western blot analysis using Acetylated Lysine Antibody at 5min; C. Western blot analysis using Acetylated Lysine Antibody at 30 min.

Acetylation of Native SABP2. Native SABP2 was purified using ammonium sulfate precipitation protocol. 50-75% precipitated proteins were used to determine the acetylation of native SABP2. Western blot was performed using Acetylated Lysine Antibody to detect the acetylation of lysine residue in the proteins (Figure 20C). Proteins were extracted, desalted, quantified, and then subjected to Western blot to detect the acetylation of SABP2 (Figure 20A). Partially purified native SABP2 did not show any internal lysine acetylation (Figure 20C).

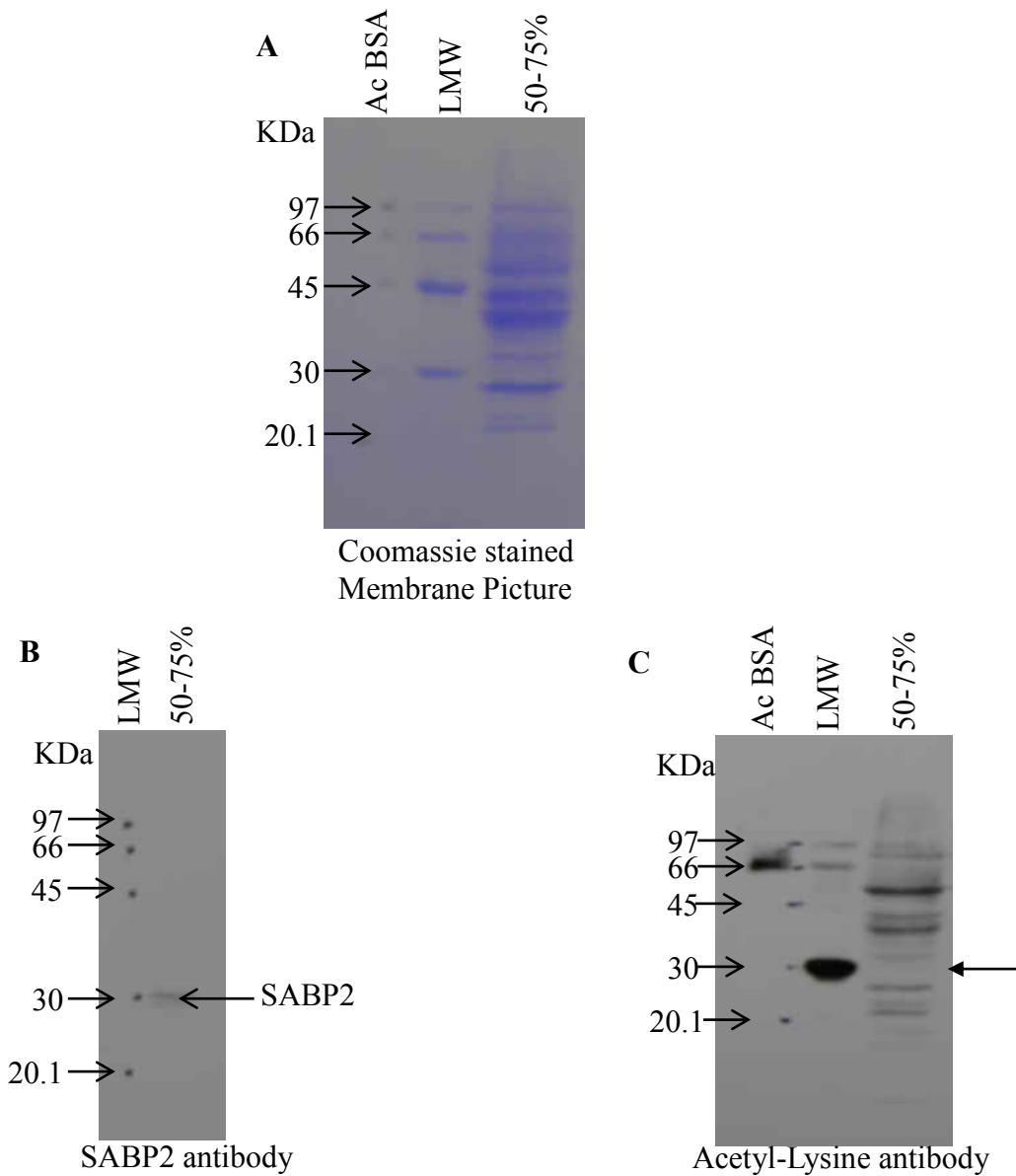


Figure 20: Acetylation of Native SABP2. A. Coomassie blue stained membrane; B. Western blot analysis using polyclonal SABP2 antibody; C. Western blot analysis using Acetylated Lysine antibody.

Acetylation of Native SABP2 upon TMV Infection. *Nicotiana tabacum* cv. Xanthi nc (XNN) tobacco plants were infected with TMV to determine the acetylation of SABP2. Total

soluble protein was extracted and fractionated using ammonium sulfate precipitation. Ammonium sulfate (50-75%) precipitated protein was used to examine SABP2 acetylation (Figure 21). There was no detection of SABP2 acetylation upon TMV infection (Figure 22D). *PR1* gene expression was analyzed to determine successful pathogen infection (Figure 22).

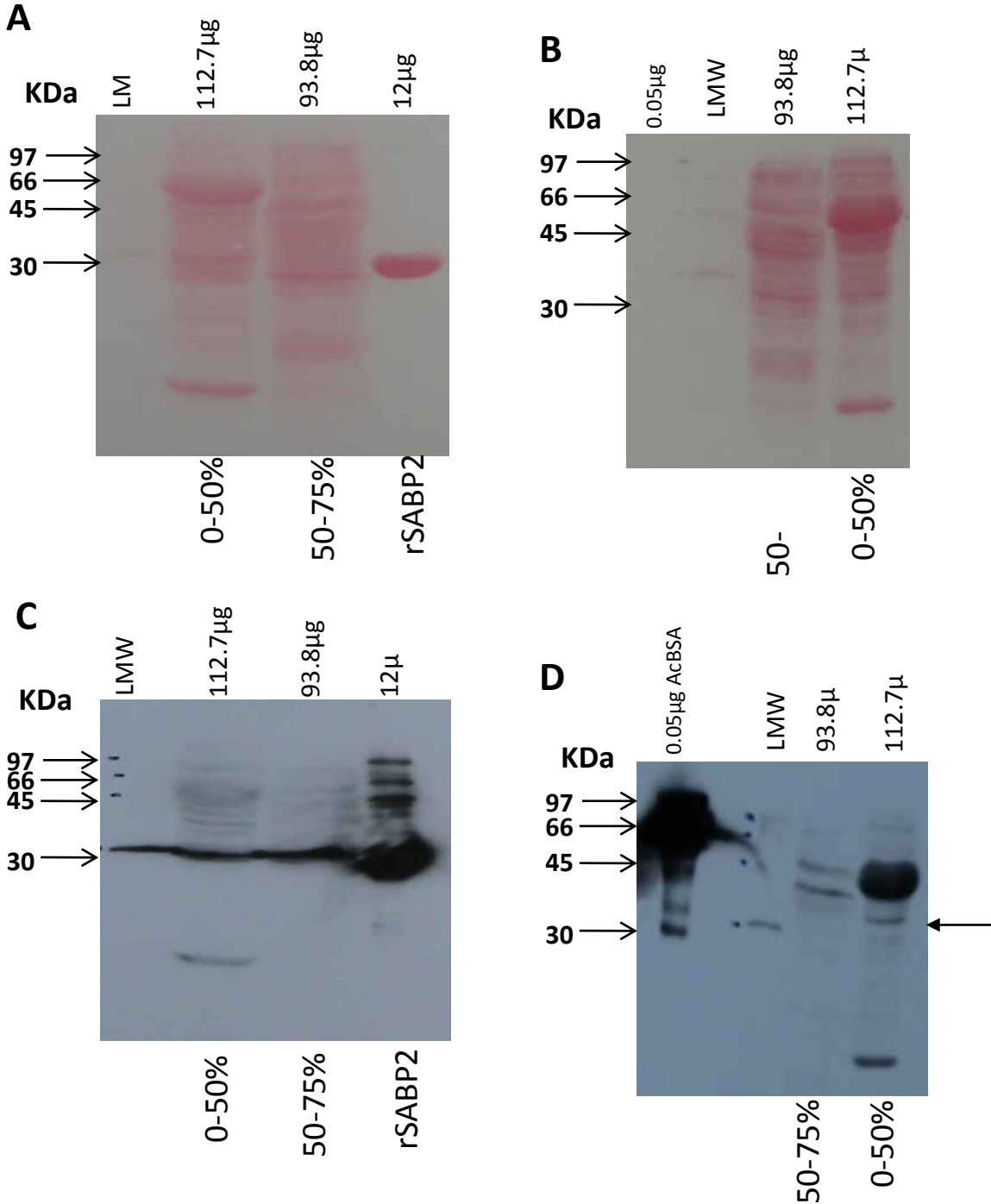


Figure 21: SABP2 Acetylation upon TMV Infection. A. and B. ponceau stained pictures; C. Western blot analysis using polyclonal SABP2 antibody; D. Western blot analysis using Acetylated Lysine Antibody

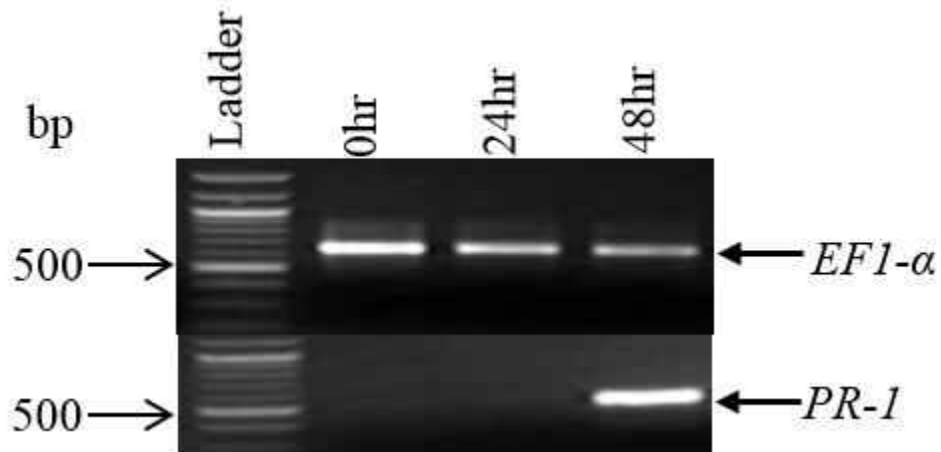


Figure 22: RT-PCR Amplification of *PR1* Gene. Agarose gel represents expression of *PR1* at 35 cycle of PCR amplification. DNA ladder (100 bp) was used on the left most lane.

Section III: SBIP-428 in SA Mediated Defense Mechanism

Effect of SA on the Deacetylase Activity in Tobacco Transgenic Plants

To determine the effect of SA on deacetylase activity in plants, tobacco C3, 1-2 (SABP2-silenced), NahG, and *Arabidopsis* Col-0 were used (Figure 23). Transgenic tobacco 1-2 and NahG plants accumulate lower levels of SA, whereas C3 and *At* Col-0 plants were used as control plants. Both NahG and 1-2 tobacco total leaf proteins showed higher levels of lysine acetylation compared with *At* Col-0 and C3 plant proteins, which implies that deacetylase enzyme is less active in NahG and 1-2 plants (Figure 23C).

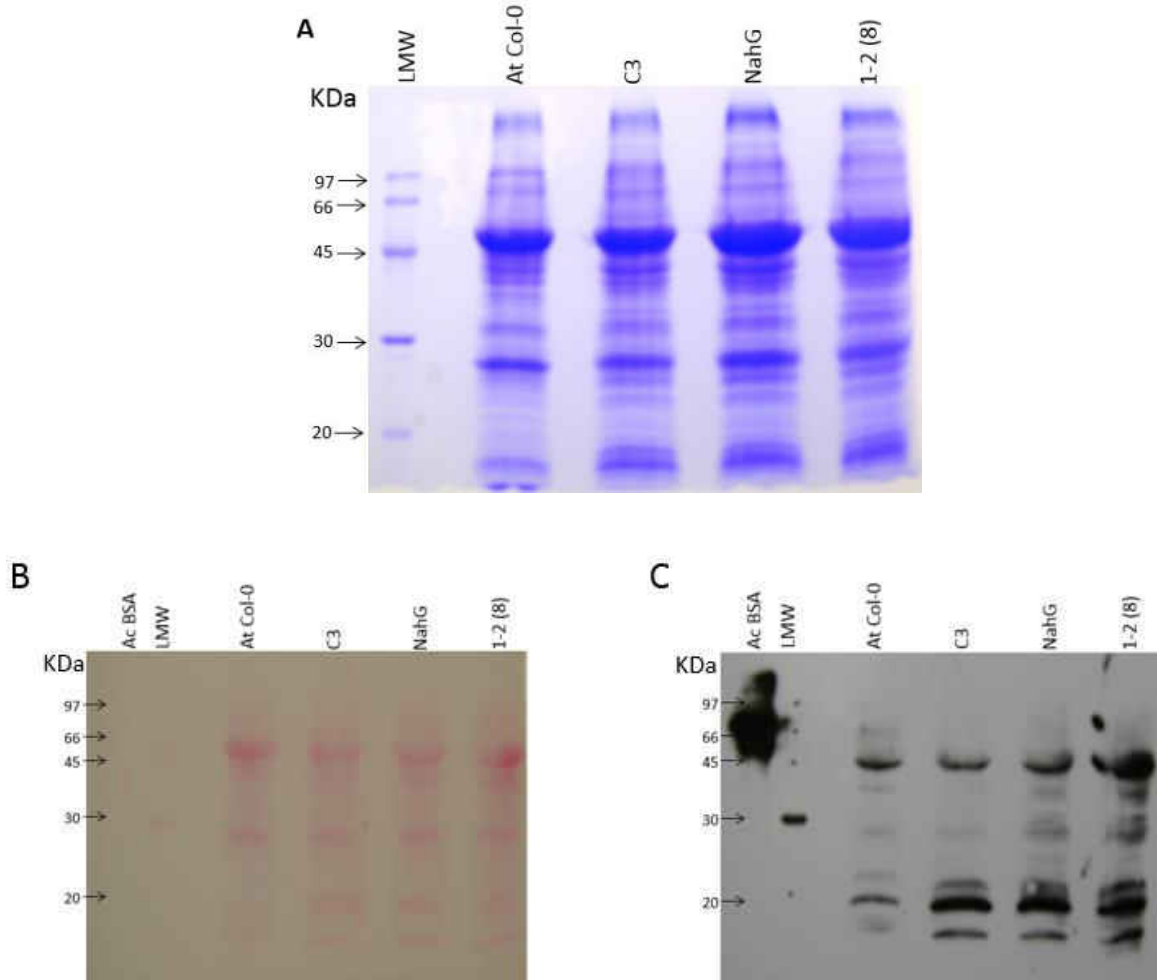


Figure 23: Effect of SA on Lysine Acetylated Protein Profile. (A) SDS-PAGE picture of total proteins from tobacco C3, NahG, 1-2, and Arabidopsis Col-0 plants; (B) Ponceau stained blot; (C) Western blot analysis using Acetylated Lysine Antibody.

Effect of SA in Expression of *SBIP-428*

XNN, NahG, C3, and 1-2 tobacco plants were used for *SBIP-428* expression analysis. NahG and 1-2 plants were used to determine the involvement of SA and SABP2 in *SBIP-428* expression. XNN and C3 plants were used as wild type and control plants, respectively. *EF1 α* was used as loading control for this experiment, whereas *SABP2* gene expression was analyzed to

determine the *SABP2* silencing in 1-2 tobacco plants (Figure 24). *SBIP-428* expression was upregulated in NahG plant compared with XNN and C3 plants (Figure 24).

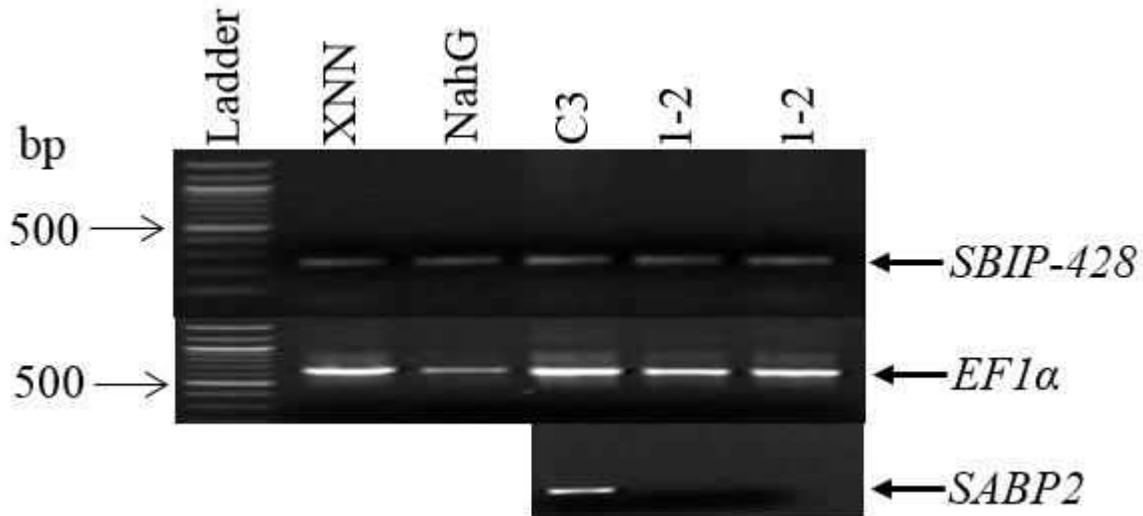


Figure 24: *SBIP-428* Gene Expression in XNN, NahG, C3, and 1-2 Plants. *SBIP-428* gene expression after 35 cycles of PCR amplification; *EF1α* was as loading control; *SABP2* gene expression in C3 and 1-2 plants as confirmation of *SABP2* silencing in 1-2 plant.

SBIP-428 Expression upon TMV Infection

Six-week-old tobacco plant *Nicotiana tabacum* cv. Xanthi nc (NN) were infected with TMV to examine the involvement of *SBIP-428* in plant defense. *PR1* gene expression was analyzed to determine successful pathogen infection and *EF1α* gene was analyzed as loading control (Figure 25). *SBIP-428* gene expression was down regulated at 48 hpi compared with 0, 24, and 78 hpi (Figure 25).

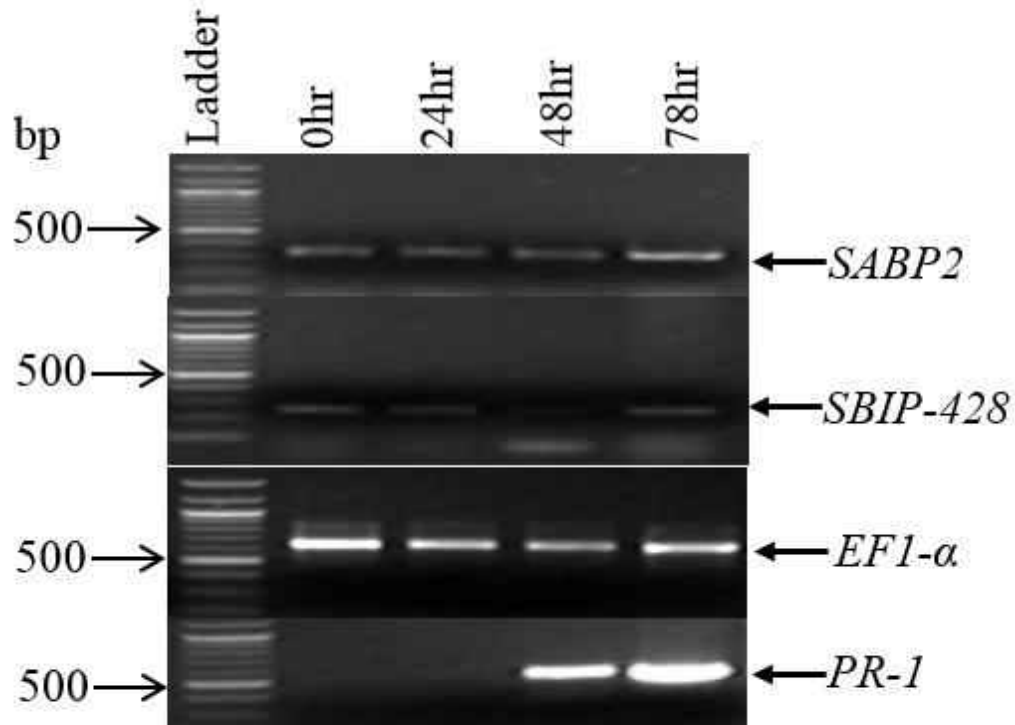


Figure 25: *SBIP-428* Gene Expression in XNN Plant upon TMV Infection. *SBIP-428* and *SABP2* gene expression after 35 cycles of PCR amplification at 0, 24, 48, and 78hpi; *EF1-α* as loading control; *PR1* as confirmation of pathogen infection.

Complementation Assay

Seeds for 6 T-DNA insertion lines of *Arabidopsis thaliana* *SIR2* mutant were obtained from TAIR (arabidopsis.org) to evaluate the role of deacetylase in SA mediate defense signaling. T-DNA insertion lines were SALK_131994C, SALK_149295C, SALK_035541, SALK_139443, CS877409, and CS370961. SALK_139443 and CS370961 mutant lines are histone deacetylase mutant; SALK_131994C, SALK_149295C, SALK_035541, and CS877409 mutant lines are *SIR2* deacetylase mutant.

T-DNA Insertion Confirmation. All T-DNA insertion lines were analyzed for T-DNA insertion. Col-0 plants were used as control because parent line of all mutants was Col-0. For Col-0, RP and LP primer pair and for all the mutants, LB and RP primer pair was used to examine the T-DNA insertion in the genomic DNA. The expected size of PCR amplified product for mutant lines was 410-710 bp and for Col-0 was 900-1100 bp. All the mutant lines showed the T-DNA insertion (Figures 26 and 27).

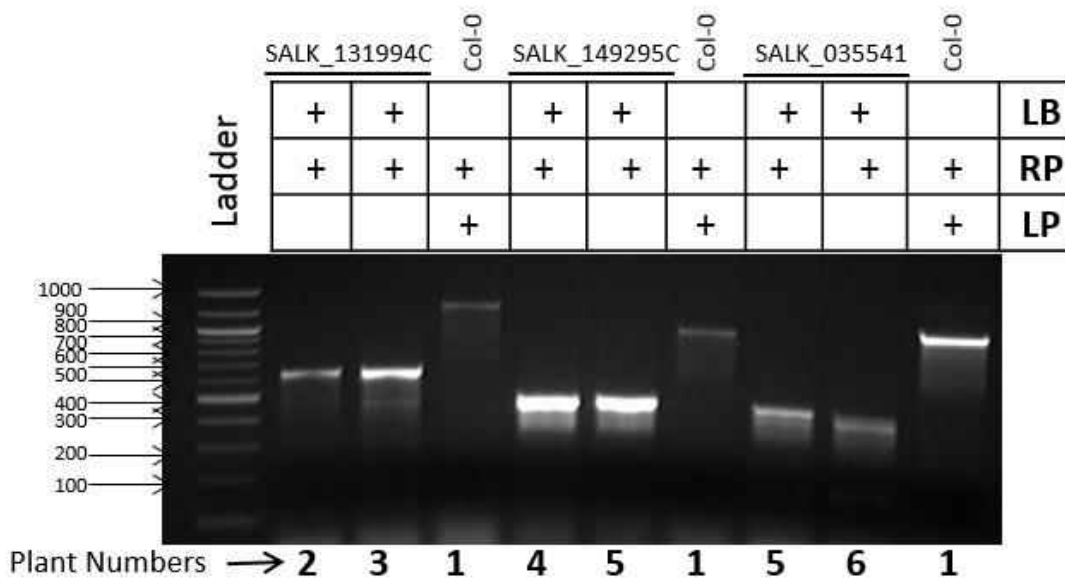


Figure 26: T-DNA insertion Confirmation Analysis of *SRT2* Mutation in *Arabidopsis thaliana*. LB and RP set of primer was used for *Arabidopsis SRT2* mutants and RP and LP set of primer was used for *A. thaliana* Col-0.

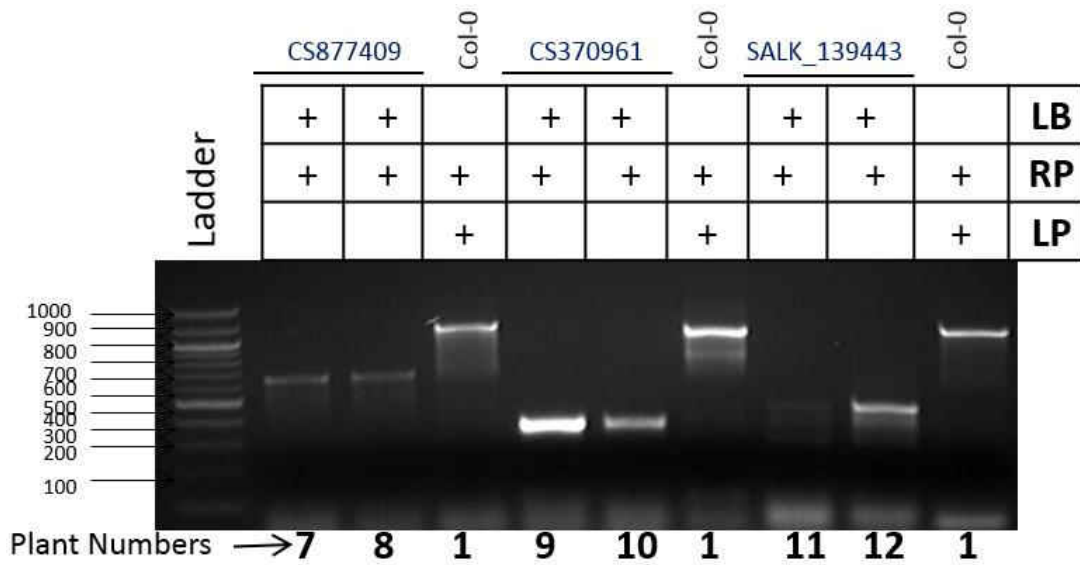


Figure 27: T-DNA Insertion Confirmation Analysis of *Arabidopsis SRT2* Mutant. LB and RP set of primer was used for *Arabidopsis SRT2* mutants and RP and LP set of primer was used for *A. thaliana* Col-0.

SRT2 Expression in *Arabidopsis* Mutants. *SRT2* mRNA expression was analyzed in all *Arabidopsis* mutant along with Col-0. Total RNA was extracted and cDNA was synthesized for RT-PCR amplification of *SRT2* and *Histone Deacetylase*. *EF1 α* was used as loading control for this experiment (Figure 28). Out of 6 seed lines only SALK_131994C line showed altered *SRT2* gene expression (Figure 29A).

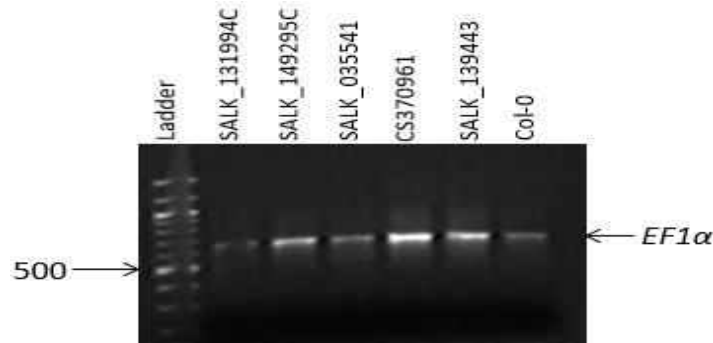


Figure 28: RT-PCR Amplification of *EF1α* Gene in *Arabidopsis*. PCR amplification (35 cycles) was used.

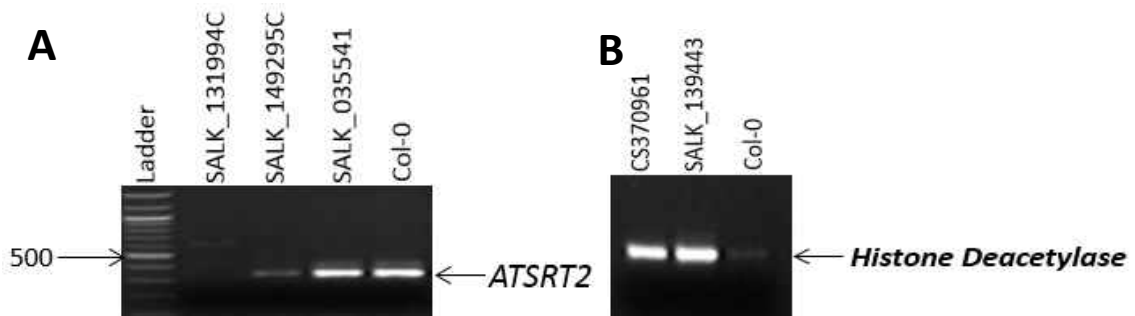


Figure 29: RT-PCR Amplification of *SRT2* and *Histone Deacetylase* Gene in *Arabidopsis* Mutants. A. *SRT2* gene mutation analysis and B. *Histone deacetylase* gene mutation analysis. Col-0 was used as positive control for both mutation analysis.

Confirmation of SRT2 Mutant. To confirm the *SIRT2* mutation in SALK_131994C seed line, total RNA was extracted from mature leaves, cDNA was synthesized, and *AtSRT2* gene analyzed by RT-PCR. SALK_131994C seed line showed *SRT2* mutation (Figure 31). *EF1α* gene was used as loading control (Figure 30).

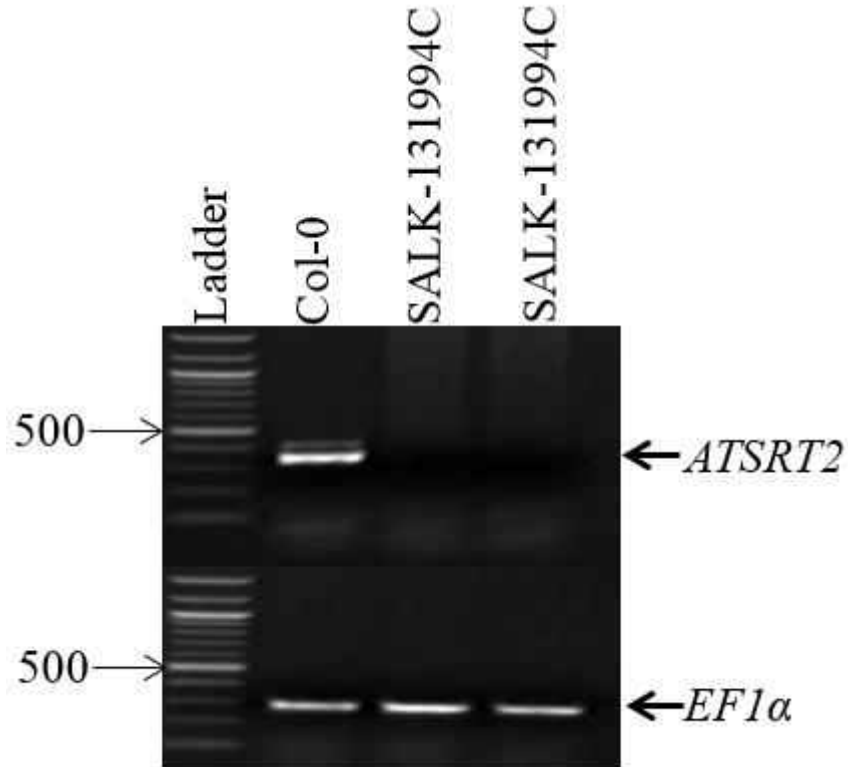


Figure 30: *AtSRT2* Gene Analysis in *SRT2* Mutant. *AtSRT2* gene expression after 30 cycle of PCR amplification; *EF1α* gene was analyzed as loading control.

Growth Phenotype of *Arabidopsis SRT2* Mutant (SALK_131994C)

To determine the morphological difference between *Arabidopsis SRT2* mutant (SALK_131994C) and parent *Arabidopsis thaliana* Col-0, 50 seeds of each mutant and control were grown in autoclaved soil. Sown seeds were kept in dark and cold condition for 3 days and then transferred to the growth chamber with 700 to 800 lux light with 16h day light period. Germination rate was determined after 7 days of sowing seeds. Number of leaves on each plant was counted and length of leaves were measured after 21 days of germination. Number of flowers and length of flowers bolts were measured between 30 to 35 days. For seed germination, 50 seeds were sown for each mutant and control as described above. After 7 days, number of germinated seeds was counted and data analyzed. Germination rate of *Arabidopsis SRT2* mutant

was 98% and Col-0 was 96% (Figure 32A). There was no significant difference in germination rate between *SIR2* mutant and Col-0 seeds.

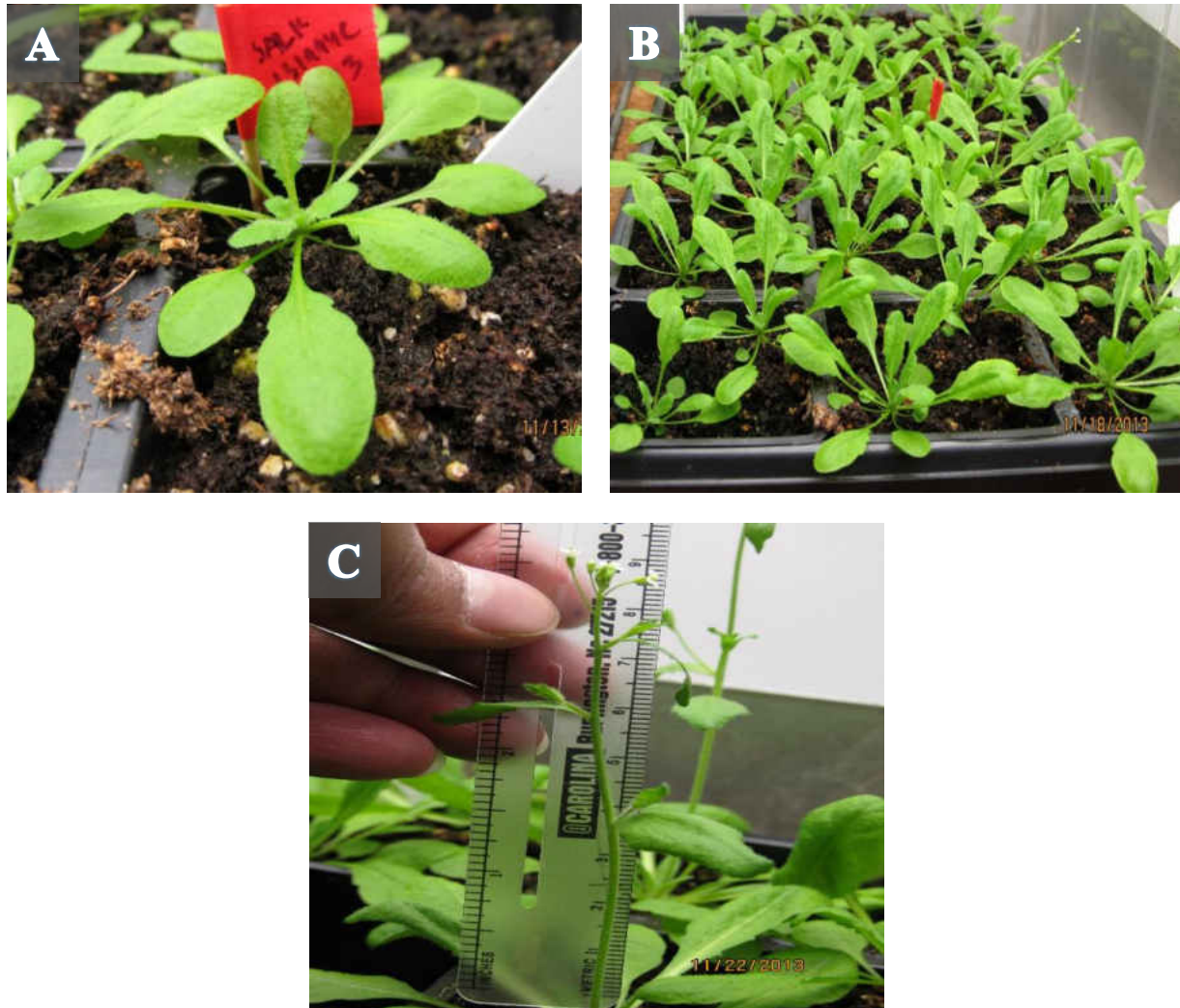
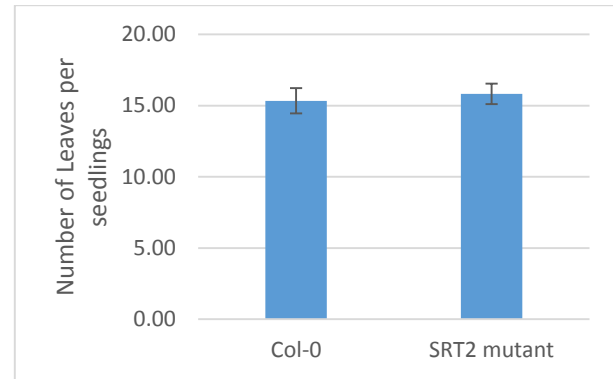
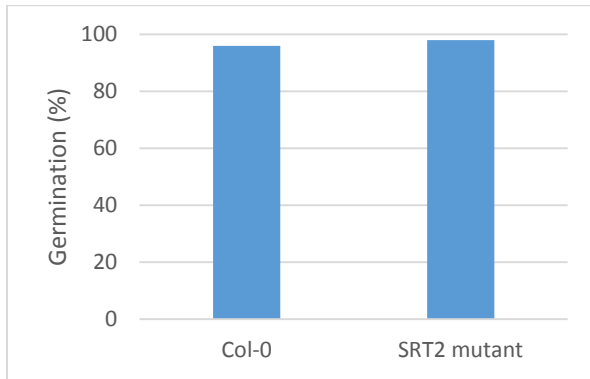


Figure 31: Growth Phenotype of *Arabidopsis SIR2* Mutant. A. Grown seedling of *SIR2* mutant; B. Plants growing in growth chamber; C. Measurement of flower bolts.

To examine the leaf morphology of *Arabidopsis SIR2* mutant, number of leaves was counted as well as length of leaves were measured. Leaf morphology was also examined visually. All 50 plants leaves were measured and counted. The average leaves number of *Arabidopsis SIR2* mutant was 15.8 and Col-0 was 15.3 (Figure 32B). There was no significant

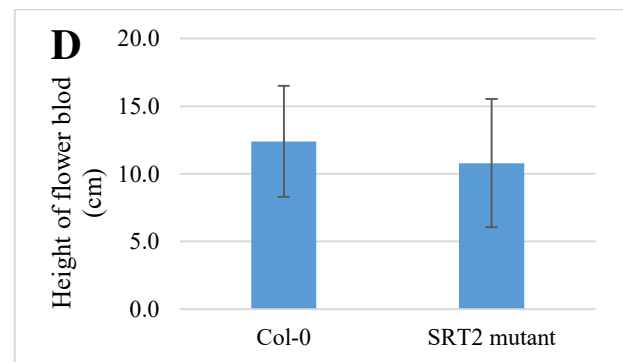
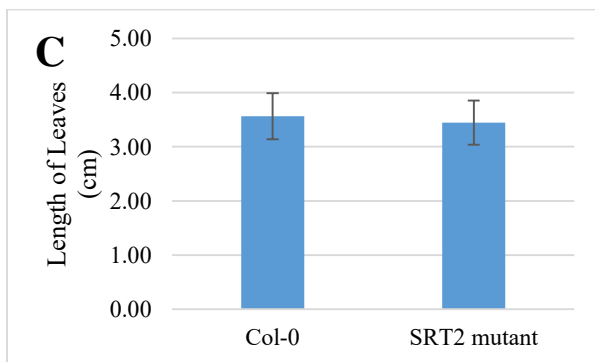
difference in leaves number between Col-0 and *SRT2* mutant. Lengths of leaves were measured using roller scale. The average length of the *Arabidopsis SRT2* mutant leaves was 3.45cm and Col-0 was 3.56cm (Figure 32C). Length of leaves showed no significant difference between *SRT2* mutant and Col-0.

Length of the flower bolts was measured after 35days of germination (Figure 32D). There were no visually distinguishable difference in floral morphology as well as as determined by statistical analysis. Overall growth phenotype study showed no significant difference between Col-0 and *SIR2* mutant.



Germination rate

Leaf morphology: number of leaves



Leaf morphology: length of leaf

Flower morphology: height of flower bolt

Figure 32: Growth Phenotype of *Arabidopsis thaliana* Col-0 and *SRT2* Mutant. A. Germination rate; B. Number of leaves per seedlings; C. length of each leaf; D. Height of flower bolt.

Pathogen Growth Assay

Arabidopsis thaliana wild type Col-0 and *SRT2* mutant seeds were grown in 1/2 strength MS media (Figure 33). Twenty days old plants were used for to pathogen growth assay. Flooding inoculation technique was used to inoculate plants with pathogen. *Pst* DC3000 and *Pst* DC3000 *AvrRpt2* bacterial strains were used for plant inoculations at concentration of 1×10^8 cfu/ml and 5×10^6 cfu/ml. Both Col-0 and *SRT2* mutant plants inoculated with 1×10^8 cfu/ml started to show chlorosis symptoms at 2 dpi and died at 4 dpi (Figure 34). With concentration of 5×10^6 cfu/ml plants started to show chlorosis at 4 dpi (Figure 34). For control, plants were treated with water. Bacterial growth was observed at 4 dpi and colony forming units (cfu/ml) were counted after 2 and 3 days of plating. In Col-0, bacterial population was 6.0×10^7 and 7.1×10^7 cfu/ml when the plans were treated with *Pst* DC3000 and *Pst* DC3000 *AvrRpt2*, respectively (Table 9). Whereas in *SRT2* mutant bacterial population was 2.3×10^7 and 1.18×10^7 cfu/ml when plants were inoculated with *Pst* DC3000 and *Pst* DC3000 *AvrRpt2*, respectively (Table 9). Bacterial growth was more than 3 times higher in Col-0 compared with *SRT2* mutant in plants were treated with *Pst* DC3000 (Figure 35). The bacterial growth was 7 times higher in plants inoculated with *Pst* DC3000 *AvrRpt2* (Figure 36). A comparison growth of *Pst* DC3000 and *Pst* DC3000 *AvrRpt2* bacterial growth in Col-0 and *SRT2* mutant is shown in Figure 37.

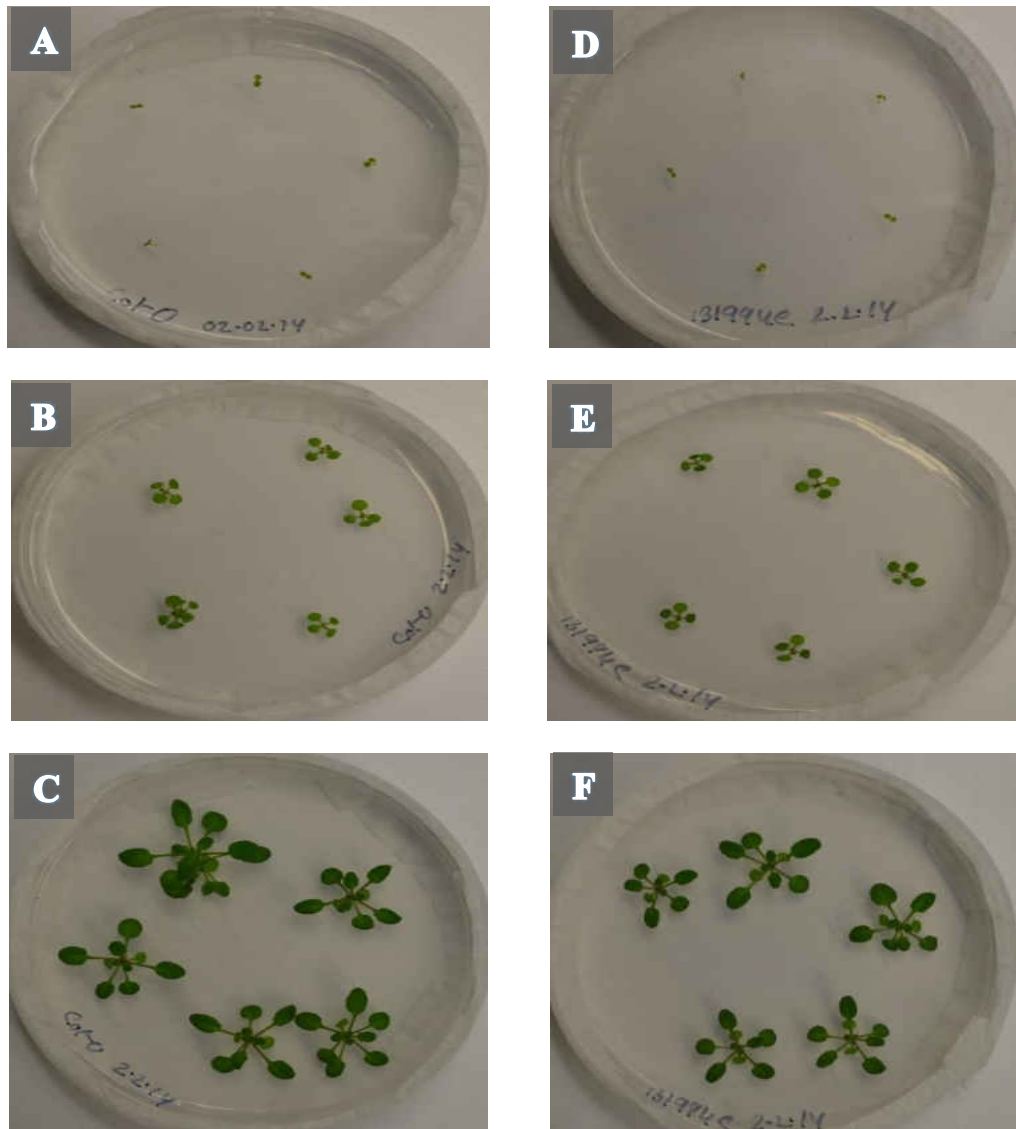


Figure 33: Growth Phenotype of *Arabidopsis SRT2* Mutant in 1/2 MS media. A-C. *Arabidopsis thaliana* Col-0 growth at 7, 14, and 21 days; D-F. *Arabidopsis thaliana SRT2* mutant growth phenotype at 7, 14, and 21 days.

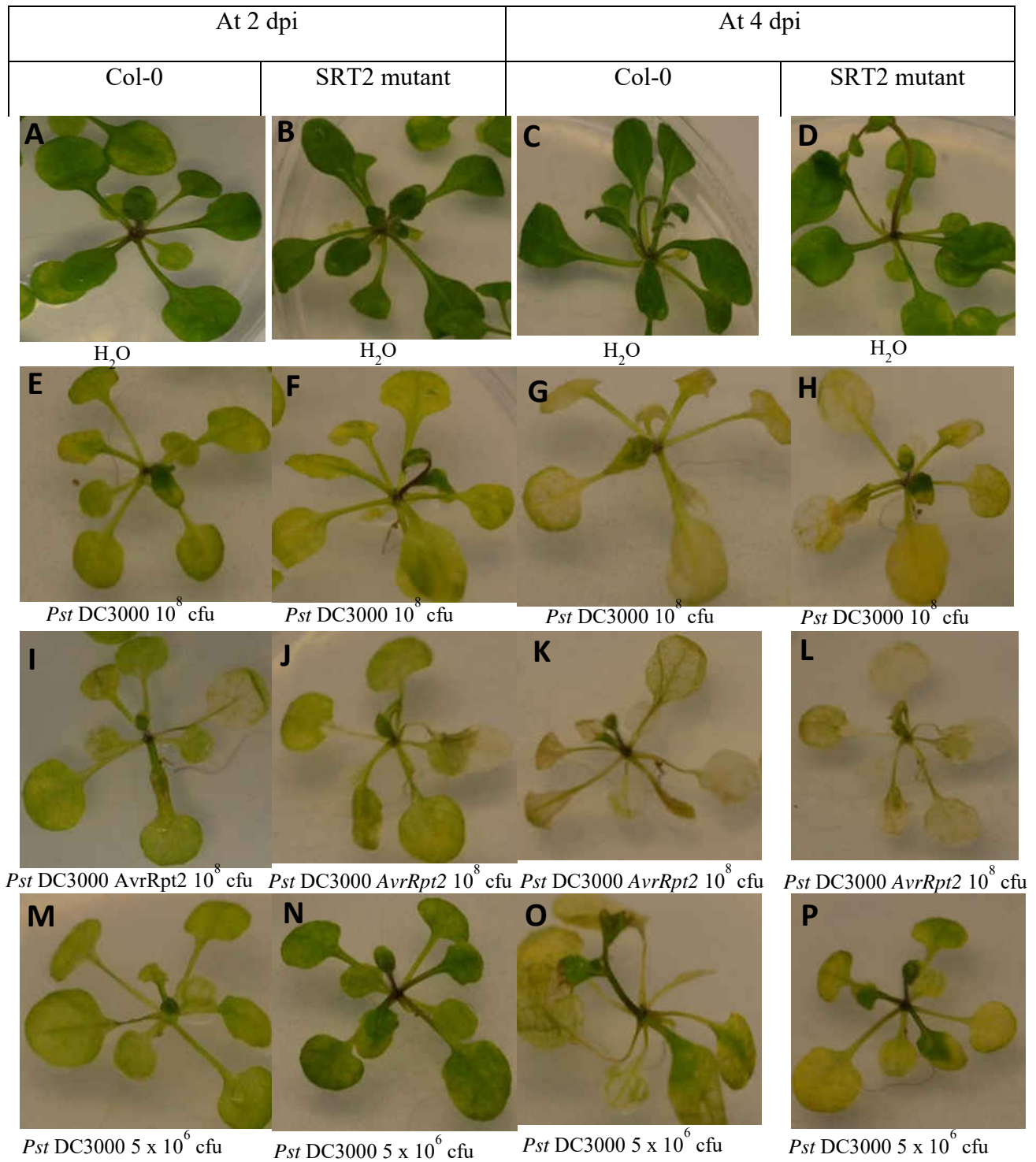


Figure 34 (continued on the next page)

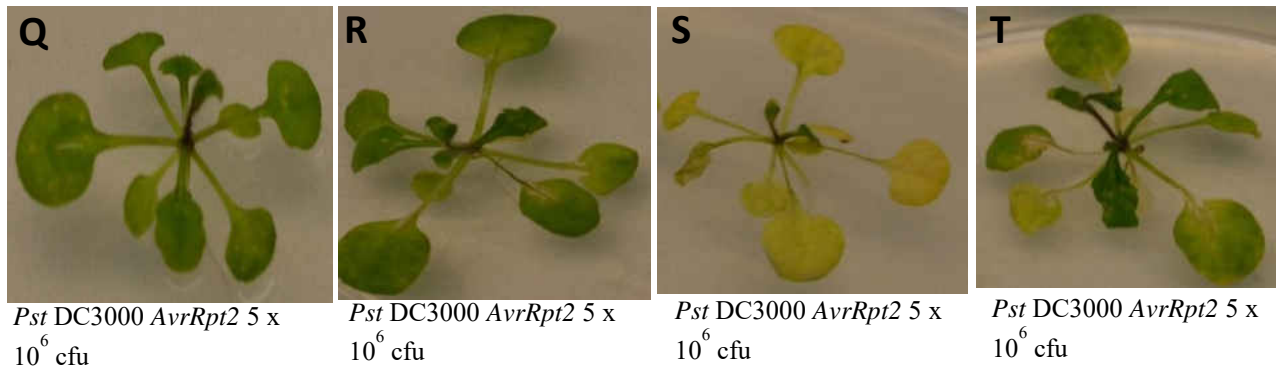


Figure 34: Disease Phenotype of *Arabidopsis thaliana* at 2 dpi and 4 dpi. A-D. H₂O treated *Arabidopsis* Col-0 and *SRT2* mutant; E-H. *Pst* DC3000D 10⁸ cfu/ml inoculated *Arabidopsis* Col-0 and *SRT2* mutant; I-L. *Pst* DC3000D *AvrRpt2* 10⁸ cfu/ml inoculated *Arabidopsis* Col-0 and *SRT2* mutant; M-P. *Pst* DC3000D 5 X 10⁶ cfu/ml inoculated *Arabidopsis* Col-0 and *SRT2* mutant; Q-T. *Pst* DC3000D *AvrRpt2* 5 X 10⁶ cfu/ml inoculated *Arabidopsis* Col-0 and *SRT2* mutant.

Table 9: Bacterial Population (*Pst* DC3000 and *Pst* DC3000 *AvrRpt2*) in Col-0 and *SRT2* Mutant at 4 dpi

	<i>Pst</i> DC3000 (cfu/mg)	<i>Pst</i> DC3000 <i>AvrRpt2</i> (cfu/mg)
Col-0	6.0 x 10 ⁷	7.1x10 ⁷
<i>SRT2</i> mutant	2.3x10 ⁷	1.18x10 ⁷

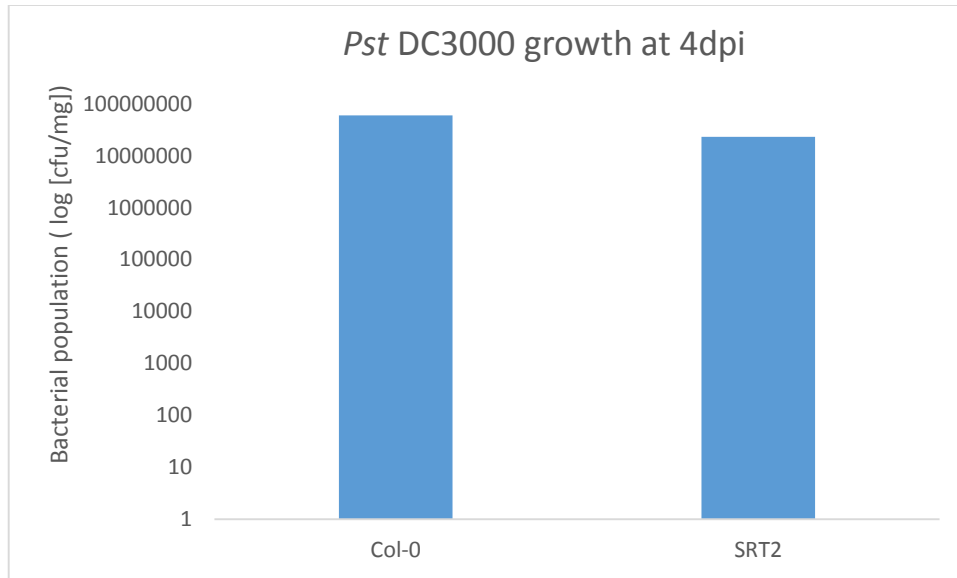


Figure 35: Bacterial Population of *Pst* DC3000 in *A. thaliana* (Col-0) and *A. thaliana* SRT2 Mutant flood-inoculated with a concentration of 5×10^6 cfu of bacterial suspension. Bacterial populations were quantified at 4 dpi.

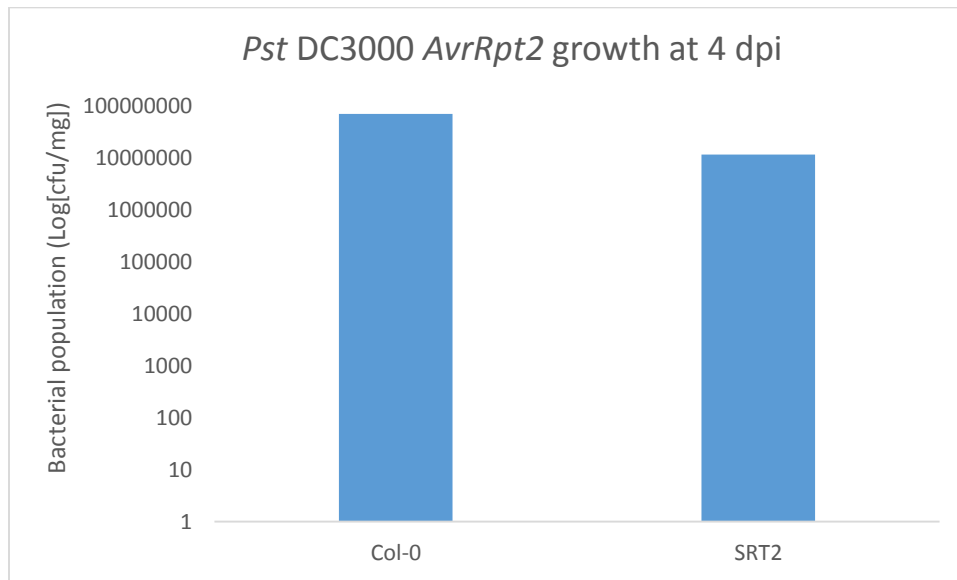


Figure 36: Bacterial population of *Pst* DC3000 *AvrRpt2* in *A. thaliana* (Col-0) and *A. thaliana* SRT2 mutant flood-inoculated with 5×10^6 cfu of bacterial suspension. Bacterial populations were quantified at 4 dpi.

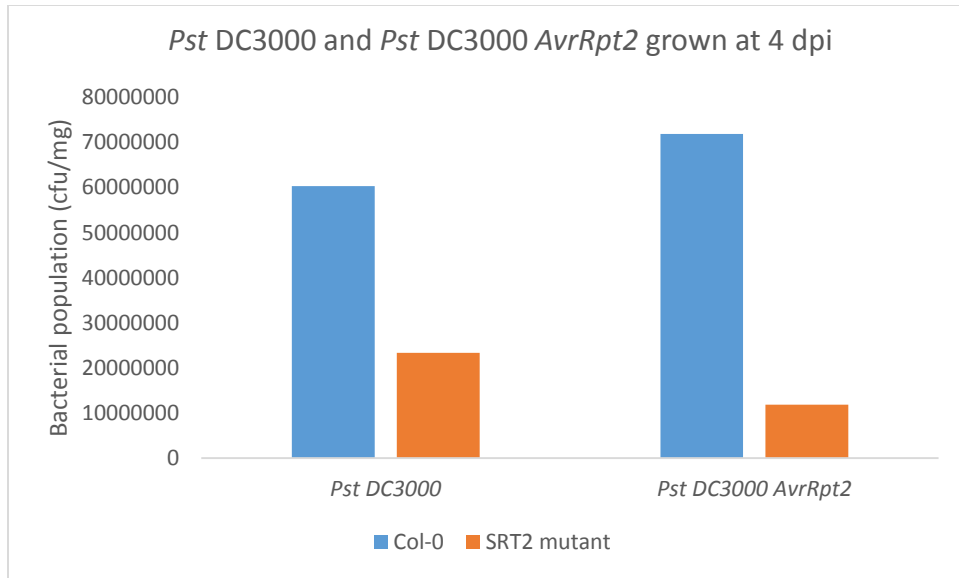


Figure 37: A Comparison Graph between *Pst DC3000* and *Pst DC3000 AvrRpt2* Growth in *Arabidopsis Col-0* and *Arabidopsis SRT2* Mutant at 4 dpi.

CHAPTER 4

DISCUSSION

Understanding the SA signaling pathway in the development of SAR and the involvement of SBIP-428 are the central foci of this project. SABP2 helps to convert lipid soluble MeSA to SA in order to increase the plant's resistance (Kumar and Klessig 2003). SABP2 likely helps to increase the cytoplasmic SA levels that results in changes in the redox potential of the cytoplasm (Tripathi et al. 2010). However, the protein interaction cascade is poorly understood in the SABP2-mediated SA signaling pathway. To understand the interaction cascade in this pathway, a yeast 2 hybrid (Y2H) screening was performed to identify the SABP2 interacting proteins. Several proteins were identified as Salicylic Acid Binding Protein 2 Interacting Proteins (SBIPs). SBIP-428 is one of the interacting proteins. Characterization of SBIP-428 and determining its role in the SABP2 dependent SA signaling pathway has been the main focus of this study. Bioinformatics analysis of SBIP-428 suggested that it belongs to the SIR2 super family of NAD⁺ dependent deacetylases. These group of proteins regulate the acetylation status of proteins. Based on bioinformatics, our first attempt was to determine if SBIP-428 is a true NAD⁺ dependent deacetylase. Interaction of SABP2 with SBIP-428, a deacetylase raises several question: why does SBIP-428 interact with SABP2? Is SABP2 itself acetylated, which may regulate the enzyme activity? Does acetylation/deacetylation play any significant role in the SABP2 mediated SA signaling defense pathway? How does this interaction between SABP2 and SBIP-428 affect the plant defense pathway? To answer some of these questions, we hypothesized that SABP2 is acetylated and is regulated by the deacetylase activity of SBIP-428, and that deacetylase activity of SBIP-428 has an effect on SA mediated defense mechanism.

Biochemical Characterization of SBIP-428

Bioinformatics analysis, protein BLASTS analysis with nonredundant protein sequence, and Protein Data Base (PDB) analysis have shown that SBIP-428 is a potential NAD⁺ dependent SIR2 deacetylase. Translated SBIP-428 protein sequence shows 93% identity with predicted NAD-dependent protein deacetylase SRT2-like (*Solanum lycopersicum*) and 77% identity with sirtuin 2 *Arabidopsis thaliana* (AtSRT2) (AT5G09230). However, BLAST analysis with PDB showed 29% identity with human Sir2 protein that is bound to an acetylated p53 peptide (Avalos et al. 2002).

Few other bioinformatics tools were used to predict the potential localization and signal peptide of SBIP-428. According to “MultiLoc” and “Protein Prowler”, SBIP-428 is potentially localized in peroxisomes. And based on the information obtained from the BaCelLo website, SBIP-428 could potentially be localized in the nucleus (Figure 9). AtSRT2, a negative regulator of SA pathway, was reported in nucleus. However, most recently same AtSRT2 was reported in inner mitochondrial membrane involved in energy metabolism and transportation (Konig et al. 2014). SABP2 is likely localized on the chloroplast outer envelope membranes (Fai and Kumar, unpublished). SBIP-428 was identified as an interactor of SABP2 in yeast 2 hybrid and a physical interaction was determined by pull down assay using a GST-tagged SBIP-428 (Zhao and Kumar unpublished). With respect to SABP2 localization, SBIP-428 may be localized in the nucleus or peroxisomes and it transport to chloroplast outer envelope to interact with and regulate SABP2 activity when is needed. There are reports showed that sirtuin deacetylases can be localized in various subcellular compartments. SIR2 super family proteins can be localized either in nucleus, cytoplasm, or mitochondria (Argmann and Auwerx 2006; Bjoern et al. 2006; Ahuja et al. 2007; Du et al. 2011; Kim et al. 2011; Barber et al. 2012; and Sundaresan et al.

2012). SIRT3 is localized in nucleus and mitochondria (Bunkenborg et al. 2006; Hirschev et al. 2010). SIRT4 that is found in mitochondria in mammals (Ahuja et al. 2007).

Enzyme assay for recombinant purified SBIP-428 was conducted by following the modified deacetylase enzyme activity protocol from Finkemier et al. (2011). Instead of using a specific substrate, total naturally acetylated proteins from tobacco leaf (XNN) was used as a substrate for the deacetylase activity of SBIP-428. There was no significant difference between the deacetylase activity of SBIP-428 and the negative control of buffer (Figure 14), suggesting presence of significant deacetylase activity in tobacco leaves (Figure 14B). Therefore, it was not possible to determine the enzyme activity of SBIP-428 using total acetylated leaf proteins of tobacco.

SIRT-GloTM and HDAC-GloTM assay kits (Promega) were used to test the deacetylase activity of SBIP-428. Lysine-acetylated peptide of p53 as substrate in SIRT-GloTM assay kit whereas histone 4 peptide was used as substrate in HDAC-GloTM assay kit. Mono-Q purified SBIP-428 was used to determine the enzyme activity. Results showed that SBIP-428 was able to deacetylate artificial p53 peptide but not histone 4 peptide in linear concentration-dependent manner (Figures 15 and 16). Ability of p53 peptide deacetylation suggests that SBIP-428 is a sirtuin deacetylase. Sirtuin deacetylase are involved in aging, glucose homeostasis, fatty acid oxidation, control of gene expression, etc. (Argmann and Auwerx 2006; Hirschev et al. 2009; Zhong et al. 2010). Most recently report suggests that Sirtuin deacetylase in *Arabidopsis* plays a role in energy metabolism and metabolic transportation (Konig et al. 2014). Role of sirtuin deacetylases in plant defense yet to be discovered.

Lysine acetylation is a common posttranslational modification that is readily reversible with deacetylation (Finkemier et al. 2011). In certain instance of biological equilibrium, lysine acetylation and deacetylation can occur on the same protein. So far, there are no reports that showed deacetylase enzyme itself is regulated by acetylation/deacetylation. Bioinformatics analysis was performed to predict the potential lysine residues in SBIP-428 (Table 7). Bioinformatics tool for lysine acetylation prediction sites and experimental results were both positive. More than one prediction site was used for lysine acetylation prediction and all of them showed SBIP-428 has potential lysine residues for acetylation. One analysis showed 9 potential acetylation sites and another site showed only 1 site. To biochemically determine if SBIP-428 was itself acetylated, mono Q purified SBIP-428 was subjected to western blot analysis using anti acetyl-lysine antibodies. Results show that SBIP-428 is acetylation (Figure 18). Acetylation of SBIP-428 (sirtuin deacetylase) lead us to believe that a posttranslational modification may be needed for its function and controlled by other regulatory factors. This is similar to another common posttranslational modifications mediated by the MAPK cascades in which MAPK is phosphorylated by MAPKK and MAPKK is by MAPKKK.

Acetylation of SABP2

Interaction of SBIP-428 (a deacetylase) with SABP2 raised the possibility of SABP2 itself being acetylated which could potentially be deacetylated by SBIP-428. Bioinformatics tool for lysine acetylation prediction sites show that SABP2 has potential lysine residues for acetylation (Table 8). Recombinant SABP2 and native SABP2 (partially purified from uninfected or TMV infected tobacco leaves) was used to determine acetylation of SABP2. However, SABP2 (recombinant or native) did not show any acetylation (Figures 19, 20, and 21). Recombinant SABP2 was expressed and purified from *E. coli*. Because acetylation and

deacetylation is a readily reversible reaction, it might be possible that SABP2 becomes acetylated under certain conditions and is deacetylated under another conditions.

SBIP-428 in Plant Defense

Results showed SA has little impact on deacetylase activity in tobacco transgenic plants (Figure 23). Plants known to accumulate or synthesize less SA showed fewer deacetylation of naturally acetylated proteins. Compared with total leaf proteins from C3 tobacco plants (control plant), proteins from NahG and 1-2 plants showed higher lysine acetylation, which suggest that deacetylase enzyme is less active in plants that produce/accumulate less SA. However, proteomics analysis is needed to specify the proteins whose acetylation is affected by SA levels in plants.

The same NahG, 1-2, C3, and XNN plants were used for *SBIP-428* gene expression. NahG transgenic plants always showed higher expression of *SBIP-428* compared with other transgenic and control plants (Figure 24). It suggests that SA and *SBIP-428* regulate each other negatively, which is affirmative to the observation of AtSRT2, a homolog of *SBIP-428* (Wang et al. 2010). Wang et al. (2010) showed that AtSRT2 negatively regulates the SA defense pathway by suppressing defense related genes as well as the genes related to SA synthesis.

To determine the role of *SBIP-428* in host-pathogen interactions, TMV inoculated plants were used. XNN plants were infected with TMV and expression of *SBIP-428* was examined at 0, 24, 48, and 78hpi. Primary observation showed that *SBIP-428* expression was down-regulated and *PR1* expression was up-regulated at the 48hpi (Figure 25). These opposite expression results suggest that expression of *PR1* and *SBIP-428* are inversely correlated. Gene expression is closely related to histone deacetylase and acetyltransferase activity (Choudhary et al. 2009). Less

expression of histone deacetylase facilitate the expression of other genes because more deacetylase activity means more tightly binding of histone to DNA and less genes are allowed to be expressed. Therefore, inverse expression of *SBIP-428* and *PR1* suggests that less expression of putative *sirtuin deacetylase (SBIP-428)* somehow regulates the expression levels of *PR1* gene. As the SIR 2 super family deacetylase is diverse in localization, it is possible that SBIP-428 deacetylase enzyme localized in nucleus and regulates *PR1* gene expression.

The AtSRT2 mutant (SBIP-428 homolog) was studied to understand the effect of deacetylase in the SA defense pathway. Primarily, 6 T-DNA insertion mutants were obtained from TAIR. T-DNA insertion analysis (Figures 26 and 27), AtSIR2 gene expression analysis confirmed that one of the T-DNA insertion line, SALK_131994C line was a true mutant (Figures 28-30). SALK_131994C was used for growth phenotype and bacterial growth assay analysis. Growth phenotype studies showed no significant difference in terms of seed germination, leaf morphology, and flower morphology (Figures 31 and 32).

Wang et al. (2010) have reported the putative deacetylase AtSRT2 function in plant defense. They reported that AtSRT2 deacetylase negatively regulates the plant defense and the expression of *PAD4*, *EDS5*, *SID2*, and *PR1* was down regulated. EDS5 and SID2 are directly related and PAD4 is indirectly responsible for the production of SA. The suppression of these genes indicate that AtSRT2 deacetylase activity is inhibitory to the production of SA and plays a negative role in SA dependent plant defense signaling.

Pathogen growth assay using virulent *Pst* DC3000 showed the similar effect reported by Wang et al. (2010). The *AtSRT2* mutant plants were more resistant compared to Col-0 as observed by Wang et al. (2010). Plants started to show chlorotic symptoms at 2dpi and died at

4dpi with 1×10^8 cfu in both Col-0 and *AtSRT2* mutant, which suggest that high concentration of bacterial inoculation did not make any difference in terms of disease resistance (Figure 33).

However, at low bacterial inoculation (5×10^6 cfu), plants survived till 4 dpi. Chlorosis symptom was observed only in Col-0 plants and bacterial growth was 3-fold higher compared with *AtSRT2* mutants (Figure 34).

To investigate the effector-triggered immunity (ETI), *Pst* DC3000 carrying *AvrRpt2* was used. There was no difference compared with *Pst* DC300 when plants were inoculated with high concentration of 1×10^8 cfu. Plants showed similar chlorosis symptoms at 2 dpi and died at 4 dpi (Figure 34). But when plants were inoculated with 5×10^6 cfu, they showed different response. *AtSRT2* mutant showed better resistance compared with Col-0. *Pst* DC3000 *AvrRpt2* grew 7 times higher in Col-0 (Figure 36). Results suggests that *AtSRT2* mutant showed better resistance against both virulent and avirulent bacterial pathogen. These results demonstrate that *AtSRT2* mutant has a better ETI response compared with wild type, which leads us to believe that *AtSRT2* is a negative regulator of basal defense.

This research was conducted to characterize the SBIP-428 and to determine its role in SA signaling defense pathway. The results presented in this thesis showed that SBIP-428 is a sirtuin decetylase enzyme. Expression of *SBIP-428* revealed that SBIP-428 may have negative correlation with SA. *Arabidopsis SRT2* mutant showed no morphological differences in absence of *SRT2* gene. Mutant study also revealed that mutant plant has better ETI response and *AtSRT2* negatively correlated in basal defense. Absence of *SRT2* make plant more resistant. Another interesting finding was to detect the acetylation of SBIP-428.

Future Direction

Characterization of SBIP-428 is just a beginning of this project. To get better understanding the role of SBIP-428 in plant defense, it will be important to generate transgenic tobacco silenced in SBIP-428 expression or to overexpress it. These transgenic tobacco plants could be used to determine the role of SBIP-428 on the host and nonhost defense responses.

Also, we have shown the first time that deacetylase enzyme itself gets acetylated. It will be important to investigate the deacetylase activity of SBIP-428 by altering the potential lysine residues that are acetylated. Changes in acetylation of SBIP-428 may lead to changes in its catalytic function.

REFERENCES

- Altschul SF, Gish W, Miller W, Myers EW, Lipman DJ. 1990. Basic local alignment search tool. *Journal of Molecular Biology* 215:403-10.
- Alvarez S, Suela J, Valencia A, Fernandez A, Wunderlich M, Agirre X, Prosper F, Martin-Subero JI, Maiques A, Acquadro F, et al. 2010. DNA methylation profiles and their relationship with cytogenetics status in adult acute myeloid leukemia. *Plos One* 5(8).
- Argmann C and Auwerx J. 2006. Insulin secretion: SIRT4 gets in on the act. *Cell* 126(5):837-9.
- Attaran E, Zeier TE, Griebel T, Zeier J. 2009. Methyl salicylate production and jasmonate signaling are not essential for systemic acquired resistance in arabidopsis. *The Plant Cell* 21(3):954-71.
- Avalos JL, Celic I, Muhammad S, Cosgrove MS, Boeke JD, Wolberger C. 2002. Structure of a Sir2 enzyme bound to an acetylated p53 peptide. *Mol Cell* 10(3):523-35.
- Beckett D. 2001. Regulated assembly of transcription factors and control of transcription initiation. *J Mol Biol* 314(3):335-52.
- Bedalov A, Gatbonton T, Irvine WP, Gottschling DE, Simon JA. 2001. Identification of a small molecule inhibitor of Sir2p. *PNAS* 98(26):15113-8.
- Bitterman KJ, Anderson RM, Cohen HY, Latorre-Esteves M, Sinclair DA. 2002. Inhibition of silencing and accelerated aging by nicotinamide, a putative negative regulator of yeast sir2 and human SIRT1. *The Journal of Biological Chemistry* 277(47):45099-106.

- Boller T and Felix G. 2009. A renaissance of elicitor: Perception of microbe-associated molecular patterns and danger signals by pattern-recognition receptors. *Annual Review of Plant Biology* 60:379-406.
- Bruce TJA, Matthes MC, Napier JA, Pickett JA. 2007. Stressful "memories" of plants: Evidence and possible mechanism. *Plant Science* 173(6):603-8.
- Buck SW, Sandmeier JJ, Smith JS. 2002. RNA polymerase I propagates unidirectional spreading of rDNA silent chromatin. *Cell* 111(7):1003-14.
- Burnett C, Valentini S, Cabreiro F, Goss M, Somogyvari M, Piper MD, Hodginott M, Sutphin GL, Leko V, McElwee JJ, et al. 2011. Absence of effects of Sir2 overexpression on lifespan in *C. elegans* and *Drosophila*. *Nature* 477(7365):482-5.
- Cheng H, Mostoslavsky R, Saito S, Manis JP, Gu Y, Patel P, Bronson R, Appella E, Alt FW, Chua KF. 2003. Developmental defects and p53 hyperacetylation in Sir2 homolog (SIRT1)-deficient mice. *PNAS* 100(19):10794-9.
- Chisholm ST, Coaker G, Day B, Staskawicz BJ. 2006. Host-microbe interactions: Shaping the evolution of the plant immune response. *Cell* 124(4):803-14.
- Choi SM, Song HR, Han SK, Han M, Kim CY, Park J, Lee YH, Jeon JS, Noh YS, Noh B. 2012. HAD19 is required for the repression of salicylic acid biosynthesis and salicylic acid-mediated defense responses in *Arabidopsis*. *The Plant Journal* 71(1):135-46.

- Choudhary C, Kumar C, Gnad F, Nielsen ML, Rehman M, Walther TC, Olsen JV, Mann M. 2009. Lysine acetylation targets protein complexes and co-regulates major cellular functions. *Science* 325(5942):834-40.
- Choudhary DK and Johri BN. 2009. Interactions of bacillus spp. and plants – with special reference to induced systemic resistance (ISR). *Microbiol Res* 164(5):493-513.
- Cui J, Bahrami AK, Pringle EG, Hernandez-Guzman G, Bender CL, Pierce N. E., Ausubel FM. 2005. *Pseudomonas syringae* manipulates systemic plant defenses against pathogens and herbivores. *PNAS* 102(5):1791-6.
- Dardick C and Ronald P. 2006. Plant and animal pathogen recognition receptors signal through non-RD kinases. *Plos One* 2(1):0001-15.
- Dean JV and Delaney SP. 2008. Metabolism of salicylic acid in wild-type, *ugt74f1* and *ugt74f2* glucosyltransferase mutants of *arabidopsis thaliana*. *Physiol Plantarum* 132(4):417-25.
- Du J, Zhou Y, Su X, Yu JJ, Khan S, Jiang H, Kim J, Woo J, Kim JH, Choi BH, et al. 2011. Sirt5 is a NAD-dependent protein lysine demalonylase and desuccinylase. *Science* 334(6057):806-9.
- Durrant WE and Dong X. 2004. Systemic acquired resistance. *Annual Review of Phytopathology* 42:185-209.
- Finkemeier I, Laxa M, Miguet L, Howden AJM, Sweetlove LJ. 2011. Proteins of diverse function and subcellular location are lysine acetylated in *arabidopsis*. *Plant Physiology* 155(4):1799-0.

- Fritz-Laylin LK, Krishnamurthy N, Tor M, Sjolander KV, Jones JDG. 2005. Phylogenomic analysis of the receptor-like proteins of rice and arabidopsis. *Plant Physiology* 138(2):611-23.
- Frye RA. 2000. Phylogenetic classification of prokaryotic and eukaryotic Sir2-like proteins. *Biochemical and Biophysical Research Communications* 273(2):793-8.
- Grozinger CM, Chao ED, Blackwell HE, Moazed D, Schreiber SL. 2001. Inhibitor of the sirtuin family of NAD-dependent deacetylases by phenotypic screening. *The Journal of Biological Chemistry* 276:38837-43.
- Gu W and Roeder RG. 1997. Activation of p53 sequence-specific DNA binding by acetylation of the p53 C-terminal domain. *Cell* 90(4):595-606.
- Hekimi S and Guarente L. 2003. Genetics and the specificity of the aging process. *Science* 299(5611):1351-4.
- Howitz KT, Bitterman KJ, Cohen HY, Lamming DW, Lavu S, Wood JG, Zipkin RE, Chung P, Kisielewski A, Zhang LL, et al. 2003. Small molecule activators of sirtuins extend *saccharomyces cerevisiae* lifespan. *Nature* 425(6945):191-6.
- Huang L, Sun Q, Qin F, Li C, Zhao Y, Zhou D. 2007. Down-regulation of a *SILENT INFORMATION REGULATOR2*-related histone deacetylase gene, *OsSRT1*, induces DNA fragmentation and cell death in rice. *Plant Physiology* 144(3):1508-19.
- Jeffery L. Dangl and Jonathan D. G. Jones. 2001. Plant pathogens and integrated defence responses to infection. *Nature* 411(14):826-33.

- Kenichi Tsuda, Masanao Sato, Thomas Stoddard, Jane Glazebrook, Fumiaki Katagiri. 2009. Network properties of robust immunity in plants. *PLoS Genetics* 5(12):1-16.
- Kim H, Patel K, Muldoon-Jacobs K, Bisht KS, Aykin-Burns N, Pennington JD, van der Meer R, Nguyen P, Savage J, Owens KM, et al. 2010. SIRT3 is a mitochondria-localized tumor suppressor required for maintenance of mitochondrial integrity and metabolism during stress. *Cancer Cell* 17(1):41-52.
- Kinkema M, Fan W, Dong X. 2000. Nuclear localization of NPR1 is required for activation of PR gene expression. *The Plant Cell Online* 12(12):2339-50.
- Kloepper JW, Ryu C, Zhang S. 2004. Induced systemic resistance and promotion of plant growth by *bacillus* spp. *Phytopathology* 94:1259-66.
- König A, Hartl M, Pham PA, Laxa M, Boersema PJ, Orwat A, Kalitventseva I, Plöschinger M, Braun H, Leister D, et al. 2014. The arabidopsis class II sirtuin is a lysine deacetylase and interacts with mitochondrial energy metabolism. *Plant Physiology* 164(3):1401-14.
- Kouzarides T. 2000. Acetylation: A regulatory modification of rival phosphorylation? *Nature* 19(6):1176-9.
- Kumar D and Klessig DF. 2003. High-affinity salicylic acid-binding protein 2 is required for plant innate immunity and has salicylic acid-stimulated lipase activity. *PNAS* 100(26):16101-6.
- Leyva-Guerrero E, Narayanan NN, Ihemere U, Sayre RT. 2012. Iron and protein biofortification of cassava: Lessons learned. *Curr Opin Biotechnol* 23(2):257-64.

- Lin S and Elledge SJ. 2003. Multiple tumor suppressor pathways negatively regulate telomerase. *Cell* 113(7):881-9.
- Liu, Po-Pu, Dahl, Caroline C. von, and Klessig, Daniel F. 2011. The extent to which methyl salicylic is required for signaling system acquired resistance is dependent on exposure to light after infection. *Plant Physiology* 157(4):2216-26.
- Loake G and Grant M. 2007. Salicylic acid in plant defence--the players and protagonists. *Current Opinion in Plant Biology* 10(5):466-72.
- Ma K, Flores C, Ma W. 2011. Chromatin configuration as a battlefield in plant-bacteria interaction. *Plant Physiology* 157(2):535-43.
- McBurney MW, Yang X, Jardine K, Hixon M, Boekelheide K, Webb JR, Lansdorp PM, Lemieux M. 2003. The mammalian SIR2alpha protein has a role in embryogenesis and gametogenesis. *Molecular and Cellular Biology* 23(1):38-54.
- Moazed D. 2001. Enzymatic activities of Sir2 and chromatin silencing. *Curr Opin Cell Biol* 13(2):232-8.
- Mou Z, Fan W, Dong X. 2003. Inducers of plant systemic acquired resistance regulate NPR1 function through redox changes. *Cell* 113(7):935-44.
- Newman BL, Lundblad JR, Chen Y, Smolik SM. 2002. A drosophila homologue of Sir2 modifies position-effect variegation but does not affect life span. *Genetics* 162(4):1675-85.

- North, Brian J. Verdin, Eric. 2004. Sirtuins: Sir2-related NAD-dependent protein deacetylases. *Genome Biol* 5(5):224.1,224.12.
- Pieterse CMJ, Wees SCM, Pelt JAv, Knoester M, Laan R, Gerrits H, Weisbeek PJ, Van Loon LC. 1998. A novel signaling pathway controlling induced systemic resistance in arabidopsis. *The Plant Cell* 10(9):1571-80.
- Ritter C and Dangl JL. 1996. Interference between two specific pathogen recognition events mediated by distinct plant disease resistance genes. *The Plant Cell* 8(2):251-7.
- Robyr D, Suka Y, Xenarios I, Kurdistani SK, Wang A, Suka N, Grunstein M. 2002. Microarray deacetylation maps determine genome-wide function for yeast histone deacetylases. *Cell* 109(4):437-46.
- Rosenberg MI and Parkhurst SM. 2002. Drosophila Sir2 is required for heterochromatic silencing and by euchromatic Hairy/E (spl) bHLH repressors in segmentation and sex determination. *Cell* 109(4):447-58.
- Schwer B, Bunkenborg J, Verdin RO, Andersen JS, Verdin E. 2006. Reversible lysine acetylation controls the activity of the mitochondrial enzyme acetyl-CoA synthetase 2. *Proceedings of the National Academy of Sciences* 103(27):10224-9.
- Strawn, Marcus A. Marr, Sharon K. Inoue, Kentaro. Inada, Noriko. Zubieta, Chloe. Wildermuth, Mary C. 2007. Arabidopsis isochorismate synthase functional in pathogen-induced salicylate biosynthesis exhibits properties consistent with a role in diverse stress responses. *Journal of Biological Chemistry* 282(8):5919-33.

- Tao YZ, Drenth H, J., Henzell RG, Franzmann BA, Jordan DR, Butler, D. G. McIntyre, C. L. 2003. Identifications of two different mechanisms for sorghum midge resistance through QTL mapping. *TAG Theoretical and Applied Genetics* 107(1):116-22.
- Tian L, Fong PM, Wang JJ, Wei NE, Jiang H, Doerge RW, Chen JZ. 2005. Reversible histone acetylation and deacetylation mediate genome-wide promoter-dependent and locus-specific changes in gene expression during plant development. *Genetics* 169(1):337-45.
- Ton J, De Vos M, Robben C, Buchala A, Metraux JP, Van Loon LC, Pieterse CM. 2002. Characterization of arabidopsis enhanced disease susceptibility mutants that are affected in systemically induced resistance. *The Plant Journal* 29(1):11-21.
- Towbin, H. Staehelin, T. Gordon, J. 1979. Electrophoretic transfer of proteins from polyacrylamide gels to nitrocellulose sheets: Procedure and some applications. *Proc Natl Acad Sci U S A* 76(9):4350-4.
- Tripathi D, Jiang YL, Kumar D. 2010. SABP2, a methyl salicylate esterase is required for the systemic acquired resistance induced by acibenzolar-S-methyl in plants. *FEBS Letters* 584(15):3456-63.
- Truman W, Bennett MH, Kubigsteltig I, Trunbull C, Grant M. 2007. Arabidopsis systemic immunity uses conserved defense signaling pathways and is mediated by jasmonates. *PNAS* 104(3):1075-80.
- Tsuda K and Katagiri F. 2010. Comparing signaling mechanisms engaged in pattern-triggered and effector-triggered immunity. *Current Opinion in Plant Biology* 13(4):459-65.

- Tsuda K, Sato M, Stoddard T, Glazebrook J, Katagiri F. 2009. Network properties of robust immunity in plants. *PLoS Genetics* 5(12).
- Van den Burg, H. A. and Takken FL. 2009. Does chromatin remodeling mark systemic acquired resistance? *Trends in Plant Science* 14(5):286-94.
- Van Loon LC and Bakker, P. A. H. M. 2006. Induced systemic resistance as a mechanism of disease suppression by rhizobacteria. *PGPR: Biocontrol and Biofertilization* (36):39-66.
- Van Loon LC, Rep M, Pieterse CM. 2006. Significance of inducible defense-related proteins in infected plants. *Annual Review of Phytopathology* 44:135-62.
- Van Loon LC, Bakker, P. A. H. M., Pieterse CMJ. 1998. Systemic resistance induced by rhizosphere bacteria. *Annual Review of Phytopathology* 36:453-83.
- Verberne, Marianne C. Verpoorte, Rob. Bol, John F. Mercado-Blanco, Jesus. Linthorst, Huub J.M. 2000. Overproduction of salicylic acid in plants by bacterial transgenes enhances pathogen resistance. *Nat Biotech* 18(7):779-83.
- Volt CA, Dempsey DA, Klessig DF. 2009. Salicylic acid, a multifaceted hormone to combat disease. *Annual Review of Phytopathology* 47:177-206.
- Wang C, Gao F, Wu J, Dai J, Wei C, Li Y. 2010. Arabidopsis putative deacetylase AtSRT2 regulates basal defense by suppressing PAD4, EDS5 and SID2 expression. *Plant and Cell Physiology* 51(8):2191-9.

- Wildermuth, Mary C. Dewney, Julia. Wu, Gang. Ausubel, Frederick M. 2001. Isochorismate synthase is required to synthesize salicylic acid for plant defence. *Nature* 414(6863):562-5.
- Wu X, Oh M, Schwarz EM, Larue CT, Sivaguru M, Imai BS, Yau PM, Ort DR, Huber SC. 2011. Lysine acetylation is a widespread protein modification for diverse proteins in arabidopsis. *Plant Physiology* 155(4):1769-78.
- Xing S and Poirier Y. 2012. The protein acetylome and the regulation of metabolism. *Trends Plant Sci* 17(7):423-30.
- Yamagata K, Goto Y, Nishimasu H, Morimoto J, Ishitani R, Dohmae N, Takeda N, Nagai R, Komuro I, Suga H, et al. 2014. Structural basis for potent inhibition of SIRT2 deacetylase by a macrocyclic peptide inducing dynamic structural change. *Structure* 22(2):345-52.
- Zhou C, Zhang L, Duan J, Miki B, Wu K. 2005. Histone deacetylase19 is involved in jasmonic acid and ethylene signaling of pathogen response in arabidopsis. *The Plant Cell* 17(4):1196-206.

APPENDICES

Appendix A – Abbreviations

SABP2 - Salicylic acid binding protein 2

SBIP-428 – SABP2 Interacting Protein-428

C3 - Control plants (*Nicotiana tabacum* cv Xanthi nc, a local lesion host of Tobacco Mosaic Virus and contains empty silencing vector.

NahG - Plants expressing salicylate hydroxylase which converts SA to catechol.

1-2 - SABP2 - silenced plants (transgenic *N.t.* cv Xanthi nc in which *SABP2* gene expression is silenced by RNA interference.

PRRs - Pattern recognition receptors

PAMPs - Pathogen-associated molecular patterns

R protein - Resistance protein

Avr - Avirulence

ICS 1 - Isochorismate synthase 1

BA2H - Benzoic-2-hydroxylase

HR - Hypersensitive response

PCD - Program cell death

SA - Salicylic acid

JA - Jasmonic acid

ET - Ethylene

ISR - Induced systemic resistance

SAR - Systemic acquired resistance

SAMT - Salicylic acid methyl transferase

MeSA - Methyl salicylate

NO - Nitric oxide

SDS PAGE - Sodium dodecyl sulphate-polyacrylamide gel electrophoresis

TMV - Tobacco mosaic virus

PR - Pathogenesis-related

BTH - Benzo-(1, 2, 3)-thiadiazole-7-carbothioic acid S-methyl ester

INA - 2, 6-dichloro-isonicotinic acid

ROI - Reactive oxygen intermediates

NPR1 - Non-expresser of pathogenesis-related protein 1

IPL - Isopyruvate lyase

NFAT - Nuclear factor of activated T-cells 87

cfu - colony forming units

β ME - β mercaptoethanol

Pst - *Pseudomonas syringae*

EFalpha1 - *Elongation Factor alpha 1*

PAD4 - *Phytoalexin Deficient 4*

R-genes - *Resistance genes*

RLK - Receptor-like kinase

RLP - Receptor-like proteins

TAE - Tris-Acetate EDTA

KBM - King's B Medium

KDa - Kilo Dalton

OD - Optical Density

UV - Ultra violet

μg - micro gram

μl - micro litre

ml - milli litre

mM - milli Molar

Appendix B – Buffers and Reagents

Protein Extraction Buffer (buffer A) (1L)

Sodium Citrate (7.44g), M.W. = 372.24g/L, final concentration = 20mM

MgSO₄ (1.23g), M.W. = 246.48g/L, final concentration = 5mM

EDTA (0.42g), M.W. = 416.20g/L, final concentration = 1mM

Adjust pH to 6.3

Stored at 4°C until use.

Prior to grinding plant tissue add 1ml of β-ME (14.4mM final concentration), 1ml of PMSF (100mM) (0.1mM final concentration), 0.15g of benzamidine HCl (156.61g/mol, final concentration 1mM) and 15g of 100% PVPP (1.5% wt/vol) to 1L of buffer.

KING'S B Medium

Protease peptone # 3 = 20 g

Potassium phosphate dibasic = 1.50 g

Magnesium sulfate = 1.50 g

Glycerol = 10 ml

Adjust the volume to 1 liter with distilled water

Adjust the pH to 7.0

Agar = 17.50 g (for solid medium)

Autoclave for 30 minutes before use

10 mM Magnesium Chloride

MgCl₂ = 0.952 g

Adjust the volume to 1 liter with distilled water 88

1M Magnesium Sulfate

MgSO₄ = 246.48 g

Adjust the volume to 1 liter with distilled water

0.1M Sucrose Solution

Sucrose = 34.2 g

Adjust the volume to 1 liter with distilled water.

Filter sterilize the solution and store at -20°C

0.1% Diethyl Pyrocarbonate Treated Water

Diethyl pyrocarbonate = 0.1 ml

Add to 100 ml distilled water

Incubate for ~12 hours at 37°C

Autoclave for 15 minutes

RIFAMPICIN (14 mg/ml)

Rifampicin (powder) = 0.14 g

Add to 10 ml of Methanol

Add to King's B media at 25 µg/ml

Bicine buffer (buffer B) (1L)

Bicine (1.63g), M.W. = 163.2g/mol, final concentration = 10Mm

Adjust pH to 8.0 with 1 N NaOH

10x Phosphate Buffer Saline (10x PBS)

Sodium Chloride (76g), M.W. = 58.44g/mol, final concentration = 1.3M

Sodium Phosphate dibasic (10g), M.W. = 141.96g/mol, final concentration = 70mM

Sodium Phosphate monobasic (4.1g), M.W. = 119.96g/mol, final concentration = 30mM

For 1x PBS (1 L), dilute 100mL of 10x PBS in 900mL of water. 88

For 1x PBS (1 L) with 3% Tween 20, dilute 100mL of 10x PBS in 870mL, then add 30mL of tween 20.

Western Blotting Blocking Buffer (100mL)

1x PBS buffer, 100mL

Dry Milk (1g), final concentration = 1%

BSA (3g), final concentration = 3%

4x SDS-PAGE Stacking gel Buffer (500mL)

Tris base (30.28), M.W. = 121.1g/mol, final concentration = 0.5M

Adjust pH to 6.8

Add SDS (0.2g), final concentration = 0.04%

SDS Gel Loading Buffer (2 X):

50mM Tris-HCl (pH 6.8)

100mM DTT

2% (wt/vol) SDS

0.1% (wt/vol) bromphenol blue

10% (vol/vol) glycerol

10x SDS-PAGE Running Buffer (1 L)

Tris base (30g), M.W. = 121.1g/mol

Glycine (144g), M.W. 75.07g/mol

SDS (10g) 89

10x Western Blotting Transfer Buffer (1L)

Tris base (30.3g), M.W. = 121.1g/mol, final concentration = 125mM

Glycine (72.06g), M.W. = 75.07g/mol, final concentration 960mM

For western, 1x transfer buffer is prepared by mixing 100mL of 10x transfer buffer, 100mL of 100% methanol, and 800mL of cold water.

Ammonium Persulfate (20% in 1mL)

Dissolve Ammonium persulfate (20mg) in 1mL of water

2x SDS-PAGE Loading Dye (100mL)

1M Tris-Cl, pH 6.8 (10mL), final concentration = 100mM

SDS (0.4g), final concentration = 0.4%

Glycerol (20mL), final concentration, 20%

Bromophenol blue (0.2g), final concentration = 0.2%

Add 5mL of ME before use.

Ponceau S Stain (100mL)

Ponceau S (0.1g), final concentration = 0.1%

Acetic acid (5mL), final concentration = 5%

MS media with Gamborg's Vitamins

MS media (4.4g/L)

Myo-Inositol (100mg/L)

Nicotinic Acid (1mg/L)

Pyridoxine. HCl (1mg/ml)

Thiamine. HCl (10mg/ml)

VITA

MD IMDADUL HAQ

- Education: Master of Science in Biology, 2014
East Tennessee State University, Johnson City, TN
Master of Science in Biotechnology, 2012
University of Malaya, Kuala Lumpur, Malaysia
Bachelor of Science in Botany, 2007
University of Dhaka, Dhaka, Bangladesh
- Professional Experience: Graduate Student, East Tennessee State University, Tennessee,
Department of Biological Sciences, 2012-2014.
Research Assistant, University of Malaya, Malaysia,
Department of Biological Sciences, 2009-2011.
- Research Award: Marcia Davis Research Award, 2013,
East Tennessee State University
- Publications: Imdadul Haq and Dharendra Kumar. A SABP2 interactor, tobacco
SRT2 deacetylase play an important role in SA mediated plant
defense. (In preparation)
- Imdadul Haq, A.B.M. Sharif Hossain, Mohammad Moneruzzaman
Khandaker, Amir Feisal Merican¹, Golam Faruq, A. Nasrulhaq
Boyce, and M. Sofian Azirun. 2014. Antioxidant and antimicrobial
activities of different extracts and fractions from the in vivo and in
vitro explants of mangrove plant *Sonneratia alba*. *International
Journal of Agriculture & Biology*. 14. Pages 707-714.
- Imdadul Haq, Sani Wirakarnain, Hossain A.B.M. Shariff and Taha
Rosna Mat (2011). Total phenolic contents, antioxidant and
antimicrobial activities of *Bruguiera gymnorrhiza*. *Journal of
Medicinal Plant Research*. 5(17), Page 4112-4118.
- Imdadul Haq, Sani Wirakarnain, Koshy Philip, Rafat Arash,
Hossain A.B.M. Shariff, and Taha Rosna Mat (2010). Valuable
Antioxidant and Antimicrobial Extracts from *Rhizophora
mucronata* of Asiatic Mangrove Forests. *Research journal of
biotechnology*. 6(1), Page 10-14.
- B. Banisalam, W. Sani, K. Philip, H. Imdadul and A. Khorasani,
(2011). Comparison Between *In Vitro* and *In Vivo* Antibacterial

Activity of *Curcuma zedoaria* from Malaysia. *African Journal of Biotechnology*. 10(55), Page 11676-11681.

Moneruzzaman KM, Amru NB, Hossain ABMS, Saifudin M, H. Imdadul, and Wirakarnain S. (2010). Effect of sucrose and kinetin on the quality and vase life of *Bougainvillea glabra* var. Elizabeth Angus Bracts at different temperatures. *Australian Journal of Crop Science*. 4(7). Pages 474-479.

Conferences:

Imdadul Haq and Dharendra Kumar. SBIP-428, a SIR2 like deacetylase, and its role in SABP2 dependent SA mediated pathway. Oral presentation at *Appalachian Student Research Forum 2014*, East Tennessee State University, Johnson City, Tennessee.

Imdadul Haq and Dharendra Kumar. Does Lysine Acetylation Have Any Role in the SABP2-Mediated Salicylic Acid Signaling Pathway? Poster presentation at *52nd Annual Meeting of the Phytochemical Society of North America (PSNA)*, 2013, Oregon State University, Corvallis, Oregon.

Imdadul Haq and Dharendra Kumar. Lysine Acetylation, a Posttranslational Modification of Proteins is involved in Salicylic Acid Mediated Signaling Pathway. Oral presentation at *Appalachian Student Research Forum 2013*, East Tennessee State University, Johnson City, Tennessee.

Imdadul Haq, Hira Chowdhury, Nkongho Binda, Amukta Mayakoti, and Dharendra Kumar. Cloning and Characterization of Tomato Homolog of Tobacco Methyl salicylate Esterase. Poster Presentation at *Appalachian Student Research Forum 2012*, East Tennessee State University, Johnson City, Tennessee.

Imdadul Haq, Sani Wirakarnain, Rafat Arash, Hossain A.B.M. Shariff, Taha Rosna Mat. Antioxidant activity and total phenolic content of leaf extract of *Rhizophora mucronata*. Poster Presentation at *3rd ICYC International Conference*, 2011, Penang, Malaysia.